INL RPT-24-80854

# Technoeconomic Analysis of Kraft Pulp Mill Integration with an Advanced Nuclear Reactor

September 2024

## *Decarbonization with Carbon Capture, Oxy-Fuel Combustion, and Thermal Substitution*

Elizabeth K. Worsham, Eliezer A. Reyes Molina, Nahuel Guaita, Samuel Root, Kathleen Sweeney, Virginia Garcia, Rami Saeed, L. Todd Knighton, Richard Boardman

***Idaho National Laboratory***

Edgar Carrejo, Sunkyu Park

***North Carolina State University***

IES
Integrated Energy Systems

*INL is a U.S. Department of Energy National Laboratory operated by Battelle Energy Alliance, LLC*

INL RPT-24-80854

# Technoeconomic Analysis of Kraft Pulp Mill Integration with an Advanced Nuclear Reactor

## Decarbonization with Carbon Capture, Oxy-Fuel Combustion, and Thermal Substitution

**Elizabeth K. Worsham, Eliezer A. Reyes Molina, Nahuel Guaita, Samuel Root, Kathleen Sweeney, Virginia Garcia, Rami Saeed, L. Todd Knighton, Richard Boardman**
**Idaho National Laboratory**
**Edgar Carrejo, Sunkyu Park**
**North Carolina State University**

**September 2024**

**Idaho National Laboratory**
**Integrated Energy Systems**
**Idaho Falls, Idaho 83415**

**http://www.ies.inl.gov**

**Prepared for the**
**U.S. Department of Energy**
**Office of Nuclear Energy**
**Under DOE Idaho Operations Office**
**Contract DE-AC07-05ID14517**

*Page intentionally left blank*

# EXECUTIVE SUMMARY

Nuclear power presents a highly efficient and clean energy solution that could meet the energy needs of the pulp and paper industry. In this sense, the U.S. Department of Energy's (DOE) Integrated Energy Systems (IES) program is actively engaged in research, development, design, economic siting, and risk analysis to demonstrate how advanced nuclear reactors can be integrated with existing industrial operations to provide clean energy, thereby reducing $CO_2$ and other emissions. An IES initiative aims to facilitate the first on-site demonstrations and commercial deployments of advanced high-temperature gas-cooled reactors (HTGRs) within industries such as chemical production, refining, iron and steel manufacturing, and more. The DOE IES program seeks to prove that advanced nuclear reactors can sustainably and cost-effectively meet the heat, steam, and power demands of different industries while significantly cutting $CO_2$ emissions and improving decarbonization.

This study focuses on post-combustion capture and oxy-fuel combustion for the boilers at the mill, as well as steam integration with the nuclear power plant (NPP). The primary goal of the research outlined in this report is to design, analyze, and document the integration of an industrial-scale HTGR with a reference kraft pulp mill. The purpose is to deliver reliable, cost-effective, and sustainable clean energy alternatives while reducing $CO_2$ emissions. Specifically, this study focuses on six different scenarios that include carbon capture equipment, and some of them use nuclear power to meet the heat and electricity needs of the reference plant. Two of these scenarios are created while also producing clean hydrogen through integrated high-temperature steam electrolysis (HTSE). This report offers a detailed techno-economic assessment of different scenarios for a kraft pulp mill, including an analysis of tax credits (sections 45V, 45Q, and 48E) provided by the Inflation Reduction Act (IRA) of 2022. The evaluation explores the potential economic benefits and challenges of incorporating different configurations, including nuclear energy, into kraft pulp mill operations, with particular attention to energy efficiency, economic implications, and environmental impact. By assessing both technical feasibility and economic viability, this analysis aims to identify existing gaps and propose solutions for the successful implementation of nuclear integration. The findings are intended to provide valuable insights for stakeholders considering the adoption of advanced nuclear reactors in the pulp and paper industries.

Chemical wood pulping is essential for extracting cellulose from wood, but it contributes significantly to $CO_2$ emissions, particularly through the kraft, sulfite, and neutral sulfite semichemical processes. The kraft process, which dominates U.S. production with over 80% of chemical pulp output, is heavily impactful due to its energy-intensive nature and reliance on fossil fuels for additional steam generation. The kraft process involves the high pressure, medium temperature digestion of wood chips in a solution of sodium sulfide and sodium hydroxide. After the pulping process, the spent cooking liquor is concentrated and combusted in a recovery furnace, which generates process steam and recovers chemicals. However, the steam generated is often insufficient, necessitating the use of conventional boilers fueled by coal, oil, natural gas, or biomass, thereby increasing $CO_2$ emissions. In addition, the lime used in the chemical recovery cycle requires high temperature to be produced, and the technology used to provide the heat required relies mostly on fossil fuels.

Decarbonization potential in the chemical wood pulping sector lies in reducing reliance on fossil fuels, enhancing energy efficiency, and adopting cleaner technologies. Transitioning to renewable energy sources for process heating and steam generation, optimizing the chemical recovery process, and exploring innovative pulping methods could significantly lower the sector's carbon footprint. Prioritizing these strategies is critical for reducing the environmental impact of the kraft process and advancing the industry's contribution to global decarbonization efforts. Nuclear integration to pulp and paper operations offers significant benefits, such as cogeneration of heat and power, carbon neutrality, and power source reliability and stability.

Hydrogen generation from the integration of nuclear power in the conventional kraft process for producing pulp and paper products can lead to new opportunities that include: (1) using nuclear hydrogen as a fuel source for the lime kiln, or in combination with natural gas or other fuels to decrease its carbon intensity, and (2) assessing alternatives to convert woody biomass (e.g., lignin, bark) to biofuels. Scenarios 4 and 5, when an oxy-fuel combustion retrofit in the boilers is considered, show a potential capacity of more than 200 metric tons of hydrogen production per day.

The decarbonization pathways for kraft mills fall into two categories: reduction of fossil fuel use and carbon capture.

- Nuclear integration: coupling NPPs with the pulp and paper industry has been happening for decades around the globe. For instance, the Gösgen NPP in Switzerland has supplied process steam to nearby heat users, and district heating for nearby municipalities.
- Black liquor gasification: black liquor gasification allows harvesting black liquor solids, using the energy released from the gasification process in the form of syngas, to be burned in other applications or processed into fuels and chemicals. Some studies show that over the next two decades, a significant number of recovery boilers will be replaced, and a significant quantity of new recovery capacity will be added. The total new recovery capacity is estimated to be 12 million pounds. Benefits of this pathway are described in section 2.1.2.
- Lignin precipitation: studies show that lignin recovery processes are only profitable for kraft pulp plants if the precipitation increases pulp yields, however, higher lignin market prices and government subsidies can increase the internal rate of return.
- Hydrogen blend with natural gas: there is a well-established precedent of utility companies blending hydrogen into natural gas through specialized equipment to combust high hydrogen fuel gas blends at a manufacturing plant scale. More recently, some new projects are targeting hydrogen content up to 100%, relying on specialized materials.
- Carbon-neutral and clean fuels: opportunities exist for fuel switching in the lime kiln unit, which is the only unit in a pulp plant that relies mainly on fossil fuels for normal operation. Co-firing or complete fuel substitution in the lime kiln are technologically feasible with alternative fuels such as tall oil and tall oil pitch, producer gases, hydrogen, bark powder, lignin, and torrefied biomass.
- Electric lime kilns: electrification offers an alternative to reduce the carbon footprint of lime kilns in the paper industry, however, large-scale demonstrations of this technology are still needed.

A reference kraft pulp mill for the small modular nuclear reactor (SMNR)-based integration was partially modeled in Aspen Plus V12 to serve as a base case for comparison with various nuclear integration options. The baseline plant is a 400,000 ADt/yr pulp plant generating unbleached softwood (southern) kraft pulp. The plant is assumed to be purely a market pulp plant, so there is no paper production line. The baseline plant uses 188.1 MWth of natural gas to power the auxiliary boiler, and the rest of the fuels are biogenic. In total, the mill emits 0.81 MMT $CO_2$ per year.

We evaluated six scenarios for the decarbonization of the reference unbleached softwood kraft mill. The net present value (NPV) of the total profits from the reactor coupling and tax credits are estimated for each. The cases are separated into three decarbonization phases to reflect the technical readiness of each scenario. Phase 1 consists of conventional carbon capture at the plant using monoethanolamine (MEA) and nuclear steam as a drop-in fuel. Phase 2 includes oxy-fuel combustion of the boilers. Phase 3 is not quantified here but would consist of converting the biomass feedstock that would usually be burned for fuel into bioproducts, synthetic fuels, or chemicals. Phase 0 is the business as usual (BAU) case, in which no changes are considered. Case 1 in Phase 0 is used to compare to the following cases. A description of the five cases across three decarbonization phases is presented in Table ES-1.

Table ES-1. Summary of each nuclear integration and TEA case with the required SMR size, total $CO_2$ emitted, and the reduction from the baseline plant.

| Phase Number | Case Number | Description | SMNR size Required (MWth) | $CO_2$ emitted (% Reduction from Baseline) |
|---|---|---|---|---|
| 0 | 1 | BAU | 0 | 0.81 MMT/yr |
| 1 – Carbon Capture with MEA | 2 | Carbon Capture with MEA technology, powered by an auxiliary NG boiler. | 0 | 0.10 MMT/yr (-88%) |
| | 3a | Carbon capture with MEA technology, powered by nuclear steam and electricity. Nuclear steam integrated to replace multi-fuel boilers. | 400 | 0.07 MMT/yr (-93%) |
| | 3b | Alternative configuration for nuclear integration with carbon capture. | 200 | 0.07 MMT/yr (-93%) |
| 2 – Oxy-Fuel Combustion | 4 | Oxy-Fuel combustion of all boilers and lime kiln with carbon capture. Oxygen steam from nuclear-powered HTSE unit. | 1200 | 0 (-100%) |
| | 5 | Case 4 with nuclear steam integration to eliminate multi-fuel boilers. | 1000 | 0 (-100%) |
| 3 – Biomass Conversion | Future Work | Waste biomass and lignin are extracted and converted to bioproducts or biofuels. | Not Quantified | Not Quantified |

All the decarbonization pathways effectively use carbon capture to reduce the $CO_2$ emissions from the baseline plant. The highest decarbonization is in Case 4 and 5, where the $CO_2$ sweep in the oxy-fuel combustion process allows for eliminating effectively 100% of emissions. The lowest $CO_2$ reduction is seen in Case 2, the natural gas fired MEA capture case, because additional $CO_2$ emissions must be captured from natural gas combustion. However, the nuclear MEA case, Case 3, reduces 5% more $CO_2$ emissions, because the emissions from the hog boiler and natural gas combined heat and power (CHP) boilers from the baseline plant are eliminated, and the energy to power the capture system is non-carbon emitting. In future work, more pathways will be explored to replace the biomass fuel from the plant with nuclear energy and upgrade the biomass to bioproducts or liquid fuels.

A technoeconomic analysis (TEA) was performed to compare the financial performance of each decarbonization case and compare cost drivers. Because most of the emissions are biogenic, the main motivation for decarbonizing a pulp mill is to harvest the production tax credit (PTC) 45Q tax credit for carbon capture, which does not distinguish between the source of the $CO_2$ that is captured (e.g., biomass - vs. fossil). The credit is up to \$60/metric-ton-$CO_2$ captured and sequestered. Therefore, we expect a pulp mill to improve its year-over-year financials by adding a carbon capture system, assuming the investment and fuel costs for the system are not more than the credits gained. When a NPP is used in the decarbonization pathway, additional credits can be earned. The investment tax credit (ITC) 48E can be earned for investment in facilities that generate clean electricity. In the oxy-fuel combustion scenarios,

oxygen is generated through HTSE, with hydrogen as a byproduct. In these cases, the PTC 45V tax credit is earned for the clean hydrogen generated from nuclear.

Table ES-2 shows the results of Case 2-Case 5 at different capital costs of the SMR. The SMR costs do not affect Case 2, because nuclear is not integrated. In each case, the NPV is shown as a delta from the baseline case (Case 1), which illustrates the change in the total cash flow based on the decarbonization pathway. Positive delta NPVs indicate that the case was more profitable than the baseline, and negative deltas indicate that the case was less profitable than the baseline.
Definite conclusions cannot be made from this data because these scenarios are specific to the reference pulp mill, however, the observations can be summarized as follows:

- The highest NPV of cashflows scenario evaluated was Case 3a with tax credits (ITC-48E and PTC-45Q) and low capital costs. As capital costs rise, the NPV of cashflows for the capture system powered by nuclear in Case 3a is lower than that for natural gas (Case 2). This suggests that a carbon capture system powered by natural gas may be equally cost-effective or more cost-effective than one powered by nuclear. However, these results would have to be confirmed by comparing Case 2 with several other integration scenarios.
- The tax credits reduce the net investment costs and make all the nuclear integration scenarios (Cases 3, 4, and 5) more cost-competitive than the BAU scenario when the capital costs are low ($3,000 per kWe). With high capital costs and without tax credits, there are no scenarios that have a higher net present value than the BAU.
- There is an important balace between the investment costs of the reactor and the profits from selling excess electricity. In case 3a a 400 MWth reactor is used, and in Case 3b a 200 MWth reactor is used. The tradeoff is that the 200 MWth has less excess electricity available to sell to the grid (about 80% less than case 3a). When captial costs are only $3,000 per kWe, the 400 MWth scenario has a higher NPV of cashflows. As capital costs rise, the 200 MWth scenario has a higher NPV. The only difference between these two cases is the reactor capital cost as the revenue from exported electricity. This suggests that in addition to the capital cost, the electricity revenue is also a major cost driver.
- In the high capital cost scenario, Case 3b (200 MWth) is more competitive than Case 3a (400 MWth) because it requires less initial capital investment. This result, however, is specific to the high electricity prices in the region, and may change in a different location.
- Between the two oxy-fuel combustion configurations, Case 5 always has a higher NPV than Case 4. Case 5 is likely more profitable because similar tax credits can be harvested with a smaller capital investment in the SMR (1000 for Case 5, compared to 1200 for Case 4). Case 4, however, has a larger demand for oxygen and therefore produces more hydrogen as a byproduct. In this configuration, the capital cost of the reactor is driving the NPV more than the hydrogen production credit. However, Case 5 is extremely sensitive to the capital cost of the SMR and the availability of tax credits.
- In all capital cost scenarios, Cases 4 and 5 have the lowest NPV.
- With tax credits,Case 2 always has a higher NPV of cashflows than Case 1.

The avoided cost of carbon (ACC) is the ratio between the total cost (without revenues) and the amount of carbon avoided over the lifetime of the project. The net cost is the same ratio, but the total cost is decreased by the value of credits that are harvested. A negative net ACC indicates that the value of tax credits earned is higher than the investment costs of the decarbonization pathway. The important observations from these results are as follows:

- Case 2 has a negative ACC. This confirms the important assumption of this study that biogenic and non-biogenic $CO_2$ emissions be treated and captured equally. This result suggests that even without nuclear integration, implementing carbon capture at existing kraft pulp mills by 2030 may be a profitable business decision. These results should be confirmed on an individual basis for each mill.
- Case 3a has a higher NPV than case 3b, but the avoided net cost of carbon (ANCC) is more positive for case 3a than case 3b. This confirms that the revenue from electricity in Case 3a is driving the higher NPV. In terms of investment costs, the ANCC is more favorable for Case 3b.
- At low reactor capital costs, the ANCC is negative for all cases. This indicates that the credits earned are a greater value than the investment costs.
- The ANCC for case 5 is more negative than for Case 4. Case 4 harvests more H2 credits, but Case 5 requires a smaller reactor. This indicates that scaling up the reactor to harvest more H2 credits may not be the most competitive option.

The integration method chosen is not the most thermally efficient, and different integration scenarios could change the competitiveness between nuclear-powered carbon capture and natural gas powered carbon capture. Additionally, if the multi-fuel boilers were re-included into the thermal systems, more total $CO_2$ would be captured, increasing the share of positive NPV of cashflows from harvested tax credit 45Q. In future work, these cases will be explored thoroughly.

Table ES-2. Technoeconomic analysis (TEA) results summary of advanced nuclear reactor integrations in methanol synthesis Case 1 (BAU is not listed).

| 40-Year Project Lifetime | | | | | |
|---|---|---|---|---|---|
| Case Study | Case 2 | Case 3a | Case 3b | Case 4 | Case 5 |
| Tax Credits | TC 45Q | ITC 48E + TC 45Q | ITC 48E + TC 45Q | ITC 48E + PTC 45V + TC 45Q | ITC 48E + PTC 45V + TC 45Q |
| High Level Reactor Cost | CAPEX HTGR = $8,000/kilowatt electrical (kWe) | | | | |
| Delta Net Present Value (NPV) from BAU | +$229M (+8%) | -$159M (-6%) | -$54M (-2%) | -$1987M (-72%) | -$1422M (-51%) |
| Avoided Cost of Carbon (ACC) ($/metric-ton-CO2) w/o credits | $9.30 | $30.60 | $15.60 | $111.70 | $90.50 |
| Avoided Net Cost of Carbon (ANCC) ($/metric-ton-CO2) w/credits | -$7.20 | $7.50 | -$2.90 | $21.60 | $13.30 |
| Internal Rate of Return (IRR) | 962.0% | 73.0% | 123.0% | 22.0% | 30.0% |
| Medium Level Reactor Cost | CAPEX HTGR = $5,500/kWe | | | | |
| Delta NPV from BAU | +$229M (+8%) | +$138M (+5%) | +$97M (+3%) | -$454M (-16%) | -$392M (-14%) |
| ACC ($/metric-ton-CO2) w/o credits | $9.30 | $21.80 | $11.20 | $87.60 | $70.40 |
| ANCC ($/metric-ton-CO2) w/credits | -7.20 | $2.40 | -$5.50 | $7.60 | $1.60 |
| IRR | 962.0% | 103.0% | 168.0% | 43.0% | 49.0% |
| Low Level Reactor Cost | CAPEX HTGR = $3,000/kWe | | | | |
| Delta NPV from BAU | +$229M (+8%) | +$378M (+14%) | +$243M (+9%) | +$149M (+5%) | $164M (+6%) |
| ACC ($/metric-ton-CO2) w/o credits | $9.30 | $13.50 | $6.30 | $64.80 | $51.90 |
| ANCC ($/metric-ton-CO2) w/credits | -7.20 | -$2.30 | -$8.60 | -$5.20 | -$8.70 |
| IRR | 962.0% | 170.0% | 326.0% | 68.0% | 76.0% |

**ITC 48E:** clean electricity investment tax credit, **PTC 45V:** clean hydrogen production tax credit, **TC 45Q:** carbon sequestration tax credit.

The three main conclusions that can be drawn from this report are:

Carbon capture through conventional methods, powered by natural gas, is likely going to be a cost-effective solution for pulp mills for as long as the tax credits are in place. Because the tax credit 45Q for carbon sequestration does not distinguish between the source of the $CO_2$, capturing biogenic $CO_2$ can provide a new revenue stream for pulp mills and potentially drive their life cycle carbon accounting into the net-negative.

Depending on the cost of electricity in a region, it may be advantageous to oversize the reactor in order to sell excess electricity generation. Pulp and paper mills, in general, will likely only require a small portion of a reactor to meet their low-pressure steam demand needs. In Case 3b, only a 200 MWth reactor module was used, and there was still excess electricity to sell. This result is important because (1) it suggests that investing in more capacity spread across several markets and commodities can help recoup initial investments, and (2) it strengthens the argument for utilities to own and operate reactors for the grid and contract a portion of their capacity to industrial customers.

In this study, the hydrogen tax credit was not a better revenue driver than the investment costs of the reactor. In Case 5, generating less hydrogen and using a smaller reactor was more cost-effective than Case 4. Oxy-fuel combustion, in general, was not a cost-effective solution compared to MEA. More decarbonization pathways should be explored to confirm if this is the case. Also, using the hydrogen generated from HTSE in these cases to upgrade biomass to new products could significantly increase the NPVs of both Case 4 and Case 5.

Overall, the results of this study were too specific to a single case to make any overarching claims about the prospects of nuclear to be cost-effective for the pulp and paper industry. However, the findings illuminate the cost and revenue drivers for decarbonization and nuclear integration. Future work will assess the results for a variety of mill configurations and include deeper decarbonization pathways.

*Page intentionally left blank*

# CONTENTS

# FIGURES

# TABLES

*Page intentionally left blank*

# ACRONYMS

| | |
|---|---|
| ACC | avoided cost of carbon |
| ADt | air dry ton |
| ASU | air separation units |
| APEA | Aspen Process Economic Analyzer |
| ANCC | avoided net cost of carbon |
| BFD | block-flow diagram |
| BLRB | black liquor recovery boiler |
| BAU | business as usual |
| BOAK | between-of-a-kind |
| CAPEX | capital expenditures |
| CCUS | carbon capture use and sequestration |
| CHP | combined heat and power |
| DCCs | direct capital costs |
| EBITDA | earnings before interest, taxes, depreciation, and amortization |
| FOAK | first-of-a-kind |
| GAIN | Gateway for Accelerated Innovation in Nuclear |
| GHG | greenhouse gas |
| HTGR | high-temperature gas-cooled reactor |
| HTSE | high-temperature steam electrolysis |
| ICC | indirect capital costs |
| ITC | Investment Tax Credit |
| IRA | Inflation Reduction Act |
| KANI | Kartonfbrik Niedergosgen |
| MEA | monoethanolamine |
| NPV | net present value |
| NIHPA | Nuclear Integrated Hydrogen Production Analysis |
| NPP | nuclear power plant |
| OCC | overnight capital cost |
| O&M | operation and maintenance |
| PEM | polymer electrolyte membrane |
| PSA | pressure swing adsorption |
| PFD | Process-flow diagram |
| PTC | Production Tax Credit |

| | |
|---|---|
| RISE | Research Institutes of Sweden |
| RWGS | reverse water gas shift |
| SLRP | sequential liquid-lignin recovery and purification |
| SMNR | small modular nuclear reactor |
| SET | Standardized Economic Tool |
| TEA | technical and economic assessment |
| TRL | technology readiness level |

*Page intentionally left blank*

# Technoeconomic Analysis of Kraft Pulp Mill Integration with an Advanced Nuclear Reactor

## 1. INTRODUCTION

Despite significant efforts to reduce carbon dioxide ($CO_2$) emissions focused on electricity generation, electric power generation accounts for 25% of the total greenhouse gas (GHG) emissions across the United States (U.S.) (U.S. Environmental Protection Agency 2021). As of 2021, the industrial sector was ranked as the third-largest contributor of direct GHG emissions in the U.S., producing around 23% of total national emissions, trailing closely behind the transportation sector at 28% (U.S. Environmental Protection Agency 2021). Furthermore, when considering electric power emissions by end use, the industrial sector owns approximately 30% of lifecycle emissions (U.S. Environmental Protection Agency 2023). In 2022, the industrial sector's GHG emissions totaled about 1,393 million metric tons (MMT) per year, with forecasts predicting a 7% reduction to 1,282 MMT/yr. by 2050 (Intergovernmental Panel on Climate Change 2023).

According to the Greenhouse Gas Reporting Program, the pulp and paper industry emitted a total of 135 MMT CO2e, of which 74% was from biogenic sources. Because of its high utilization of biofuels—almost entirely from internal energy generation— the pulp and paper industry has not historically been targeted for decarbonization projects. However, the sector accounted for 6.2% of U.S. (U.S. Energy Information Administration 2021) industrial energy and 4% of industrial energy-related $CO_2$ emissions in 2020 (including biogenic emissions).

There are an estimated 290 pulp mill sites in the U.S. that produce over 81 million air dried metric tons per year (ADt)/yr of pulp or paper product. 95 sites are kraft pulp mills and another 50 are a combination of kraft and another pulping process, making up 65.7% of total U.S. pulping capacity. 26.6% of U.S. pulping capacity is mechanical recycle mills, which in contrast to the kraft mills must purchase all their energy needs from external sources. Based on the Environmental Protection Agency's Facility Level Information on Greenhouse Gases Tool (FLIGHT), wood pulp production is concentrated in the southeast U.S., particularly Georgia, Alabama, and Louisiana (U.S. Environmental Protection Agency Office of Atmospheric Protection 2023).

Kraft pulping constitutes 80% of the total chemical pulping industry, making it the predominant method employed worldwide (Food and Agricultural Organization of the United Nations n.d.). It involves digesting wood chips at elevated temperatures and pressures in "white liquor" (an aqueous solution composed of sodium sulfide and sodium hydroxide). The chemical dissolution of lignin, which binds cellulose fibers in wood, occurs through this white liquor. The physical pulping of wood chips is conducted in digester systems, via either a batch or a continuous process. Though most kraft pulping occurs in batch digesters, continuous digesters are becoming more prevalent.

After digesting, the contents are transferred to an atmospheric tank commonly known as a blow tank. The entirety of the blow tank contents is sent to pulp washers, where the pulp is separated from the spent cooking liquid. The pulp then undergoes a series of defibrating, washing, and bleaching stages (if needed) (Oliveira, Mateus, and Santos 2019). One advantage of the kraft process design is the recovery and recycling of cooking chemicals and heat. Spent cooking liquor and pulp wash water combine to form a weak black liquor that contains about 15% solids and is later concentrated to about 40%–55% solids in a multi-effect evaporator system. The liquor is further concentrated to approximately 65%–75% solids (strong black liquor) by using flue gases in a direct-contact evaporator or in an indirect-contact condenser. The strong black liquor is fired in a recovery furnace, providing energy for the pulping process and the conversion of sodium sulfate into sodium sulfide. (Cheremisinoff, Rosenfeld, and Davletshin 2008)

Inorganic chemicals in the black liquor collect as molten smelt at the furnace's base and are later dissolved in water to form green liquor. The green liquor is transferred to a causticizing tank, where quicklime (calcium oxide) is added to convert the solution back into white liquor for return to the digester system. Lime mud precipitates from the tank and undergoes calcination in a lime kiln to regenerate quicklime. (Cheremisinoff, Rosenfeld, and Davletshin 2008) This quicklime is added to the green liquor to return it to white liquor for reuse in the digester. A simplified diagram of the kraft pulping process is shown in Figure 1. In 1994, recovery boilers represented 35% of total boiler capacity in the pulp and paper industry. Including other waste fuels, about 50% of boiler capacity is fueled by the chemical recovery process and its byproducts (National Renewable Energy Laboratory 2002). The recovery furnace provides up to 100% of the total energy requirement for market pulp mills, whereas the percentage for integrated mills widely varies based on the pulp and paper production capacities. The remaining energy requirements are met by conventional fossil fuels such as natural gas, fuel oil, or wood boilers. The wood boiler fuel commonly consists of solid wood waste stemming from log cutting and debarking conducted as part of woodyard processing, enabling a self-sufficient energy cycle at the mill. Additionally, the lime kiln is typically fired with natural gas or fuel oil because of the process sensitivity to high temperature levels and contaminants. (Kuparinen and Vakkilainen 2017)

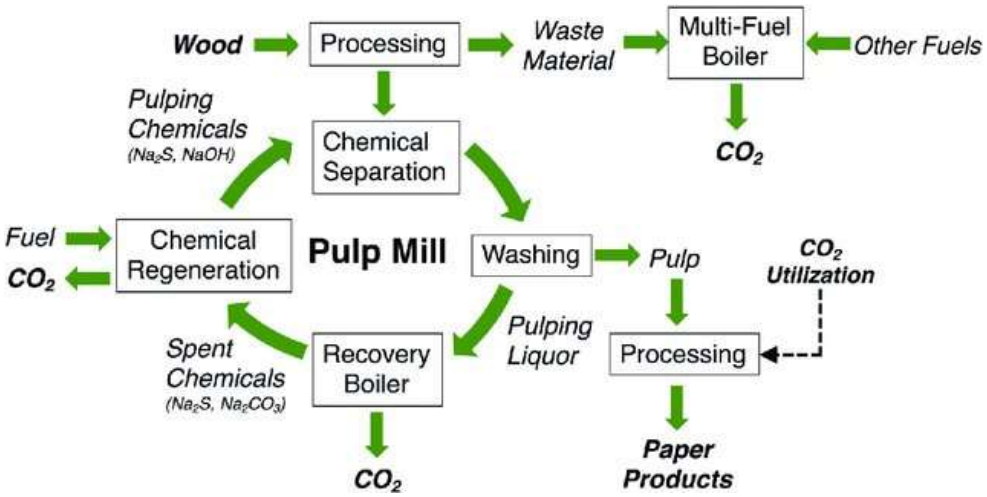


Figure 1. Flow diagram of a kraft pulp mill (Sagues et. al 2020).

The kraft pulping process is unique to other industrial processes in that it generates a large portion of its energy (up to 100%, depending on plant size and configuration) from its own internal byproducts. The main fuel is black liquor, which is a slurry of pulping chemicals and lignin, the remaining portion of the woody biomass after cellulose fibers are separated as the pulp product. Other biomass waste products—mainly separated wood bark and wood chips rejected due to quality control—can be burned in multi-fuel boilers to supply heat throughout the plant. Fossil fuels are typically deployed to meet the plant requirements that are not met from the combustion of byproducts.

Even though the kraft process uses mainly biogenic fuels, it should not be overlooked when considering carbon capture and other improved pollutant capture. The main sources of carbon emissions are the recovery boiler, power boilers, and lime kiln. The recovery boiler, typically the main source of steam for the mill, burns lignin fuel with pulping chemicals, and therefore is also responsible for emission of particulate matter, total reduced sulfur compounds (TRS), NOx, Opacity, $SO_2$, CO, and hazardous air pollutants (HAPs) emissions. Modifications to decarbonize the recovery furnace, or the complete replacement of the furnace with a nuclear steam source, would reduce these controlled emissions in addition to $CO_2$.

Also, while the recovery boiler produces most of the steam at pulp mills, most of that steam is consumed in the multi-effect evaporators used to concentrate black liquor to be combusted in the recovery boiler. More effective evaporation methods or alternatives to black liquor combustion have the potential to drastically reduce heat demands at the mill, reducing overall fuel use, and in the case of nuclear integration, a cost savings due to reduced thermal demands.

Another target for decarbonization and carbon capture is the lime kiln. The energy required for the lime kiln must be supplied at high temperatures (>1000˚C) and is therefore typically supplied by the combustion of fossil fuels. Combustion flue gas from the lime kiln contains fuel combustion residuals and the $CO_2$ released when heat splits CaCO3 into CaO (quicklime) and $CO_2$. The average $CO_2$ concentration of lime kiln flue gases is 21mol% (Sagues et al. 2020), although it only consists of about 10% of the total $CO_2$ released by the mill. By reducing combustion flue gases in the lime kiln, the kiln would produce a high purity stream of $CO_2$ to be captured and potentially utilized. There are several options for decarbonizing the lime kiln through nuclear integration, including hydrogen, oxy-firing, or electric heating. There are also options for recirculating captured $CO_2$ and oxygen through the lime kiln to reclaim carbon for the pulping process.

Therefore, there are three unit operations at a kraft mill that can be targeted for decarbonization: the lime kiln, the multi-fuel boiler, and the recovery boiler. Sagues et al. completed a technoeconomic analysis for capturing the $CO_2$ output at pulp and paper mills through conventional amine scrubbing (Sagues et al. 2020). They tested two scenarios for the biomass boiler (steam provided by the boiler with purchased electricity, and steam and power provided by the boiler) and two conditions for carbon capture (capture from combined emissions of all plant sources and capture only from the lime kiln). As seen in Table 1, the lime kiln contributes the smallest amount of $CO_2$ emissions to the total and has the highest $CO_2$ concentration, which requires less energy per mol of $CO_2$ captured. Combining all flue gas streams decreases the average $CO_2$ concentration but increases the volume of flue gas. However, for three out of four mills studied, the cost of $CO_2$ capture on a mass basis was lower in scenarios when all flue gas streams were combined than in scenarios where only the lime kiln stream was captured. This was due to the benefits of economy of scale for larger capture systems. In addition to the cost of the capture system being lowered as it increased in size, it allows the mill to obtain more tax credits for $CO_2$ capture because more $CO_2$ is captured overall. The results from this study indicate that the cost of capture will be the lowest when $CO_2$ output from all units is combined into one capture system and average $CO_2$ concentration is maximized.

Table 1. Emissions characteristics of the average U.S. pulp and paper mills (Sagues et al. 2020).

| Operation | $CO_2$ emissions (metric-ton-CO2/yr) | Contribution to total emissions (%) | Avg. $CO_2$ concentration (mol%) | Energy to separate $CO_2$ (kJ/mol-$CO_2$) |
|---|---|---|---|---|
| Lime Kiln | 13.7 | 9 | 21 | 13.1 |
| Multi-Fuel Boiler | 64.1 | 43 | 9 | 40.7 |
| Recovery Boiler | 71.4 | 48 | 13 | 24.9 |
| Combined | 149.2 | 100 | 10 | 37.4 |

This study presents a technoeconomic analysis of a paper mill decarbonized through integration with a nuclear power plant (NPP) or small modular nuclear reactor (SMNR). This study is motivated by the desire of the pulp and paper industry to decarbonize, along with directives from the DOE through the Industrial Heat Shot program and the opportunity for the industry to take advantage of tax credits for capturing $CO_2$. Many previous efforts to reduce $CO_2$ emissions at pulp mills have been focused on the black liquor boiler, as detailed in Section 2, specifically removing lignin from the chemical slurry and transforming it into fuels that burn cleaner and have a higher heating rate. In this study, no modifications were made to the pulping process or the black liquor itself.

The decarbonization is done in three phases, to reflect the technology readiness for each decarbonization measure. Phase 0 presents the business as usual (BAU) case for the reference pulp mill, which includes no carbon capture or decarbonization measures. Phase 1 incorporates conventional carbon capture methods using amine scrubbing, with steam and power provided to the capture system from either natural gas or a SMNR. Phase 2 introduces carbon capture through oxy-fuel combustion in all boilers and the lime kiln, and steam integration with the SMNR to eliminate steam production from the multi-fuel boilers. In this phase, the oxygen would be supplied to the boilers from a high temperature steam electrolysis (HTSE) unit powered by the SMNR. Phase 3, while not quantified in the technoeconomic analysis, requires altering the pulping process and converting the biogenic fuels typically used by the mills to biofuels or other bioproducts that can be utilized at the plant or sold to displace fossil-based products.

This work supports the U.S. DOE Office of Nuclear Energy's Integrated Energy Systems (IES) Program by providing a preliminary technical and economic assessment (TEA) and gap analysis of advanced nuclear reactor integration in kraft pulp mills. To thoroughly understand the potential for decarbonization and nuclear integration in process economics, this report compiles comprehensive information from previous studies and original assessments for the pulp and paper industry, including:

- Process-flow diagrams (PFDs) and block-flow diagrams (BFDs) of the reference kraft mill and corresponding nuclear-integrated configurations, detailing main process unit operations and conditions, including energy and material flows.
- Overall balance datasheets for each main process unit operation, including electric power consumption, heat demand from fuel combustion, steam consumption, steam generation, steam quality, heat loss, $H_2$ demand, heating value of byproducts, and $CO_2$ emissions.
- Evaluation of advanced nuclear reactor integration opportunities considering overall process requirements.
- Consideration of each nuclear integration case and its own variations, to conduct a TEA with a reference kraft pulp mill by using the standard economic tool, including:
  - Substitution of nuclear energy for conventional energy supply
  - Avoided cost of carbon (ACC) dioxide emissions reduction
  - Schedule for advanced reactor construction and implementation
  - Capital costs, engineering costs, etc.
  - Gaps in technology development and demonstration
  - Concepts of operations (including labor).

# 2. DECARBONIZATION PATHWAYS FOR THE PULP AND PAPER SECTOR

There have been many efforts over the decades to improve energy efficiency at pulp and paper mills, and to reduce controlled air emissions, but few have been focused primarily on reducing carbon emissions. Carbon output from the kraft process comes from the generation of process steam via the black liquor recovery boiler (BLRB), biomass waste and fossil fuel boilers, combustion of fossil fuels to provide high-temperature heat in the lime kiln, and emissions from the chemical reduction of lime. Therefore, the decarbonization pathways for kraft mills fall into two categories: reduction of fossil fuel use and carbon capture.

## Reduction of Fossil Fuel Use

Although 72% of the emissions from the pulp and paper industry are biogenic, its main fuel—lignin dissolved in pulping chemicals—is not the most efficient option. 30% to 36% of the energy output of the recovery boiler is used in the evaporator, which concentrates the black liquor solids to be used as fuel. Still, reducing combustion in the recovery boiler is an industry priority because black liquor has a high water content, and therefore a lower higher heating value (HHV) than other fuel options. Additionally, the recovery boiler heating capacity is limited by the pulp production capacity. Increased pulp production leads to increased lignin production but installed BLRBs do not have the capacity to handle extra caloric value from lignin. Therefore, much of the decarbonization work in the pulp and paper industry has focused on the black liquor boiler, specifically to convert black liquor into higher-value fuels that can be used within the plant. Black liquor gasification (Section 2.1.2) and lignin precipitation (Section 2.1.3) are two major pathways for this method. Steam can also be provided by alternative fuels, including nuclear power.

The lime kiln gets less attention for decarbonization because it is only responsible for about 10% of plant emissions. However, the lime kiln technology at a pulp mill is nearly identical to what is used in the cement and lime industry, which, when both the process emissions and fuel emissions of the cement and lime industry are considered, amounted to 68.8 MMT of $CO_2$ in 2021, and is one of five industries targeted by the DOE's industrial decarbonization roadmap (United States Department of Energy 2022). However, the high temperature requirements mean that the main decarbonization pathways are electrification and carbon capture use and sequestration (CCUS). (United States Department of Energy 2022) Development of these technologies for the cement industry will likely improve prospects for lime kiln decarbonization in pulp mills.

### 2.1.1 Nuclear Integration

Nuclear power has been used in the pulp and paper industry for decades. Experience in NPP and process heat applications began with the Halden reactor project in Norway, which operated from 1964 to 2018. The research reactor delivered steam to a nearby paper factory only when the reactor was producing heat (Institutt for Energiteknikk - Halden Reactor Project 2008).

One current example of an industrial plant and NPP coupling is the Gösgen NPP in Switzerland. Since it began operation in 1979, the plant has been supplying process steam to a nearby cardboard production plant, Kartonfbrik Niedergosgen (KANI), and other heat users. In 1996, the system was extended into district heating for nearby municipalities. An additional cardboard recycle mill was connected in 2009.

The steam from the NPP replaced heavy oil burning for steam production at KANI, avoiding the emission of several thousand metric tons of carbon dioxide per year, along with emissions of sulfur dioxide, nitrous oxides, and other air pollutants (Alpiq Group 2010). The two heavy oil fired boilers are now operated on standby status and can take over the steam supply within 15 to 30 minutes (International Atomic Energy Agency 2007). The motivation for this coupling was both environmental and economical, considering that even in 1979, the cost of steam produced by the NPP was much less than the cost of steam produced from heavy oil (Blum 1982). Steam from the NPP replaces almost 59,000 kg of heavy oil daily (International Atomic Energy Agency 2007).

Process steam generation is separated from the steam required for electricity generation by the NPP through a special evaporator that uses extracted steam from the live steam pipe leading from the reactor to the turbine. The steam generated is 14 bar, 222˚C, and superheated by 27˚C to keep the steam line dry. In 1982, the steam total capacity to KANI was 80 metric-tons/hour, less than 1% of total NPP steam production, with plans to expand the capacity for future expansions of the mill (Blum 1982). The amount of steam can fluctuate between 0 and 22.2 kg/s while maintaining constant pressure (International Atomic Energy Agency 2007). After steam is condensed, it returns to the NPP to be reheated and transported back to the mill (Blum 1982). The system was designed so malfunction of the evaporator plant would not affect the normal operation of the nuclear power station. When the second paper facility was connected in 2009, a 2 km pipeline was installed to deliver steam at 15 bar pressure (Alpiq Group n.d.). The pipeline from the power plant to the cardboard plant was built partially above ground to allow for line checks and maintenance. The steam is used for the paper machine for heating the drying cylinders at the end of the manufacturing process (International Atomic Energy Agency 2019).

These couplings show an optimistic outlook for using nuclear power to decarbonize across the paper industry. The configuration and steam of the kraft pulp mill is different than KANI, which does not have internal steam generation from pulping processes, and the challenges for integration are described in more detail in this chapter. However, the design of the Gösgen evaporator system could be a useful starting point for more sophisticated steam integration systems.

### 2.1.2 Black Liquor Gasification

One commercially ready alternative to BLRBs is black liquor gasification. In conventional boilers, the liquor solids are combusted in the BLRB to produce steam. The benefit of gasification over combustion is that the energy harvested from black liquor solids can be harvested through the energy released from the gasification process, and in the form of syngas, a CO and $H_2$ rich gas that burned in other applications or processed into fuels and chemicals.

Two black liquor gasification plants have been successfully demonstrated by ThermoChem Recovery International (TRI) and Chemrec (National Energy Technology Laboratory n.d.-b).

Although these processes were successfully demonstrated by 2008 and studies have quantified significant savings for gasification, there has not been widespread adoption of the process. This is likely due to the capital intensity, technical challenges to the gasifier itself, and the impact of gasification on the causticizing load.

The first BLRB was put into operation in 1929, and quickly expanded to 700 in the world by 1980 (Vakkilainen 2005). The initial motivation for the recovery process was to recycle the expensive pulping chemicals used in the pulping process; without it, the kraft process would not be economically viable (Parrish 1998). Later developments to the boilers focused on increasing heat recovery and preventing corrosion (Vakkilainen 2005).

At the time that black liquor gasification was being conceptualized in the 1980s, the industry had little interest in investing in a new technology. In 1997, Babcock and Wilcox Company surveyed 25 industry executives and technical personnel regarding the future of black liquor gasification. The response was uniform interest in gasification, but confidence in the future viability of the technology was varied (Southards 1997). However, the B&W study also includes an insight relevant to the market of today:

“Our internal studies show that over the next two decades a significant number of recovery boilers will be replaced and a significant quantity of new recovery capacity will be added. The total is estimated to be 12 million lbs. dry solids / day liquor processing capacity installation on average within the next two decades. This will include a mix of incremental capacity, replacement units, and new units” (Southards 1997).

A barrier to implementing gasifiers has been the capital investments required, which is especially disinteresting if the current boilers are operating adequately. If P&P facilities are anticipating that current boiler equipment will be replaced soon, this, along with emerging regulations for $CO_2$ emissions, could explain the resurging interest in black liquor gasification technology.

There are still some technology barriers to the full-scale adoption of gasification technology. Material corrosion issues limit the service life of gasifiers. The Norampac TRI plant in Ontario operated at least 18,000 hours before the plant's closure in 2012. The Chemrec process plant at the Weyerhauser mill in New Bern, North Carolina operated for about 50,000 hours as of 2008, although it is unclear if it is still operating (National Energy Technology Laboratory n.d.-b).

Black liquor gasification also impacts the recovery process. The combustion of black liquor facilitates the reduction Na2SO4 to form Na2S, a main component of white liquor. Gasification causes a sulfur-sodium split, and addition sulfur recovery must be added to maintain proper liquor chemistry. This also results in a higher causticizing capacity requirement and higher fuel consumption in the lime kiln per unit of black liquor solids compared to a conventional BLRB.

In 2003, Larson quantified the benefits of black liquor gasification on a U.S. scale (Larson, Consonni, and Katofsky 2003). The highlights include:

- Higher pulp yields, reducing pulpwood requirements by 7% per unit paper output
- Up to $6.5 billion ($2002) in cumulative energy cost savings over 25 years
- Reduced cooling water and makeup water requirements at the mill scale
- Annual displacement of up to 32 million metric tons (35 million short tons) net $CO_2$, 15 minioon metric tons (160,000 short tons) net $SO_2$, and 91,000 metric tons (100,000 short tons) net $NO_X$, with additional reductions of particulates, volatile organic compounds (VOCs), and total TRS
- Up to 156 billion kWh more electricity produced than with Tomlinson boilers over 25 years, about 28% of which is considered renewable
- Up to 360 trillion BTU/yr of fossil savings within 25 years of introduction
- Potential for displacement of petroleum through fuel and chemical production from black liquor and biomass feedstocks.

Although the quantified benefits may be different today, this study indicates the economic and environmental benefits that make gasification so attractive.

### 2.1.3 Lignin Precipitation

Burning lignin as fuel in the BLRB produces steam and energy. This is beneficial to pulp plants, as energy is produced onsite. However, it is a hinderance to productivity, as pulp production is limited by the BLRB heating capacity. Increased pulp production leads to increased lignin production but installed BLRBs do not have the capacity to handle extra caloric value from lignin. Rather than spending millions of dollars to replace boilers with higher-capacity equipment, lignin can be separated from black liquor and redirected for other purposes. According to Valmet, "If 25% of the lignin in the black liquor is removed, boiler capacity can be increased to enable 20-25% more pulp production" (Valmet 2015). The isolated lignin can be used as fuel within the plant or as a feedstock for other bioproducts such as fuels, materials, and chemicals.

The first commercial lignin precipitation process was patented by the West Virginia Pulp and Paper Company (Westvaco) in the 1940s. Since lignin is soluble in black liquor at pH>10, Westvaco added $CO_2$ as an acidifying agent to lower the pH to 8-10, where the lignin would precipitate. Since then, lignin precipitation processes have improved. Now, commercial pulp and paper plants utilize the patented LignoBoost and LignoForce systems. These systems utilize the same principles as the Westvaco process while increasing lignin yield, lowering chemical requirements, and improving filterability (Kienberger et al. 2021).

In the LignoBoost process, the black liquor is acidified using $CO_2$, filtered with a chamber press, then re-slurried using sulfuric acid (H2SO4). The addition of sulfuric acid improves the filterability of the mixture. The slurry is then refiltered, washed with H2SO4 and water, and dried (Tomani 2010). LignoBoost was first commercialized by Valmet in 2013 in Domtar's Plymouth, North Carolina pulp plant. Since then, it has been implemented in Stora Enso's Finland plant, Klabin's Brazil plant, and Mercer's Germany plant (Valmet n.d.). The ANDRITZ Group developed a similar lignin precipitation process called LignaRec. They announced a partnership to implement LignaRec in the Sodra pulp plant, with lignin production scheduled to begin in 2027 (Andritz 2024). LignoForce differs from LignoBoost and LignaRec by adding an oxidation step before acidification. The exothermic oxidation reaction increases the temperature of the mixture, which decreases dissociation of the charged groups in lignin and allows for larger lignin particles to form. LignoForce boasts decreased acid requirements for precipitation and washing compared to LignoBoost (Kouisni et al. 2012). FPInnovations demonstrated the LignoForce system at the Resolute Thunder Bay mill in 2014 (Noram 2014), and commercially implemented it at West Fraser's Hinton mill in 2016 (FPInnovations n.d.).

Sequential liquid-lignin recovery and purification (SLRP) is a lignin recovery process that operates continuously and separates lignin as a dense liquid. Funded by the DOE, The Liquid-Lignin Company began developing SLRP in 2009 with the goal of developing an energy-efficient lignin recovery process. In SLRP, $CO_2$ and black liquor are fed counter-currently through a column reactor. As the fluids contact one another, the pH of the black liquor decreases to 9-10, where the lignin can precipitate. Since the column is operated at elevated temperature and pressure, the lignin separates in a liquid phase. The dense liquid-lignin is then reacted continuously with sulfuric acid and filtered. Because SLRP is a continuous process, it has lower capital and operating costs, and smaller space requirements. The Liquid-Lignin Company operated a pilot plant in Clemson, South Carolina, but has not yet commercialized the process (Lake and Blackburn 2014).

Adding a lignin recovery system to a kraft pulp plant affects the rest of the process. In the conventional kraft process, the steam produced by burning lignin in the BLRB is integrated with the rest of the plant, but removing lignin from the BLRB reduces steam production. Benali et. al. analyzed a reference mill with a pulp production capacity of 400 metric-tons/day and found that when 100 metric-tons/day of lignin were removed from the BLRB, steam production decreased by 6.13%. Additionally, due to higher pulp yield and extra drying processes, the steam demand in the plant increased. Using advanced process integration, Benali et. al. decreased the total steam demand by 15%. Benali et. al. also performed assessments for water and energy demands. Their analysis demonstrates that while lignin recovery systems can improve pulp production, they disrupt the highly integrated kraft process. Demand for chemicals, water, steam, and energy change depending on a plant's capacity, lignin removal volume, and lignin end use, so each pulp plant that wants to add a lignin recovery process must conduct mass and energy balances to determine the resource demands and economic viability (Benali et al. 2014).

The cost of implementing a lignin recovery system in a pulp plant varies greatly depending on the price of chemicals and commodities, magnitude of pulp production, and value of lignin. Tomani estimated that as of 2008, the total investment cost for a LignoBoost plant was 106 million SEK ($9.8 million) and the operational costs were 230-580 SEK ($21-$53) per metric ton of lignin (Tomani 2010). LignoForce boasts lower acid requirements, so there are savings in the costs for $CO_2$ and H2SO4, but it also requires O2, which increases the overall cost of chemicals. Cost estimates for LignoForce are not available but can be calculated based on resource demands discussed in Kousini et. al. and current chemical and commodity prices (Kouisni et al. 2012). As a continuous process, SLRP's costs are lower than LignoBoost or LignoForce. Lake and Blackburn estimated that the capital costs of SLRP as of 2014 are about one half of LignoBoost's, while the operating costs are about 40% lower (Lake and Blackburn 2014).

Overall, studies show that lignin recovery processes are only profitable for kraft pulp plants if pulp production increases (Kienberger et al. 2021; Bertaud et al. 2023). Benali et. al. showed that 50 metric-tons/day of lignin recovery adds $12.5 million of revenue per year with a payback period of 2 years (Benali et al. 2014). In "Production of Biofuels and Chemicals from Lignin," Benali et. al. assess the costs of a LignoBoost and LignoForce plant and analyze the profitability of lignin recovery based on the lignin end use. They describe a feasible case for LignoBoost implementation with 100 metric-tons/day of lignin recovery, a 15% increase in pulp production, and a lignin market price of $500/metric-ton. In this case, the internal rate of return (IRR) is over 20%, making it a promising investment for a biorefinery. In a plant where an increase in pulp production is not possible, the lignin market price must be $780/metric-ton to achieve an IRR above 20%. Alternatively, government subsidies may cover a significant portion of the capital costs (43% in the case presented by Benali et. al.) and increase the IRR. As for the recovered lignin, Benali et. al. suggest that kraft plants develop a diverse portfolio of bioproducts, including biopolyols, lignin-based carbon fiber precursors, polyurethane, and lignin-based polyacrylonitrile carbon fiber (Benali et al. 2016).

### 2.1.4 Hydrogen Blend with Natural Gas

There is a long history of utility companies blending hydrogen into natural gas pipelines to reduce the carbon intensity of the fuel. This technology has been led by Hawaii Gas, who began blending up to 15% hydrogen, which was sourced as a byproduct from their synthetic natural gas plant, into their distribution network in 1974 (Hawai'i Gas n.d.). HyBlend is a Hydrogen Fuel Cell Technology Office (DOE-HFTO) initiative lead by the National Renewable Energy Laboratory to advance the technology to higher levels and more widespread use. The key challenge in many locations is the compatibility of high hydrogen content fuel gas with existing infrastructure in the broader and older mainland pipeline network (Topolski 2022). The current consensus among experts in the field is that most distribution networks and end users would be compatible with a blend of up to 30 vol% hydrogen in natural gas (a blend often marketed as hythane) without significant retrofitting costs (Chae et al. 2022; Mitsubishi Power 2023). Other industries, notably petroleum and petrochemical manufacturers, handle and combust fuel gases with even higher hydrogen content. Petroleum refineries get much of their energy by combusting refinery fuel gas, a mixture of light hydrocarbons similar to natural gas, but with hydrogen content up to 70% (Malek 2004). Methanol plants and other syn-gas-based chemical manufacturing processes commonly recirculate light ends containing similar mixtures of hydrogen, hydrocarbons, and carbon oxides to furnaces to drive reforming and synthesis reactions. Precedent is well established for specialized equipment to combust high hydrogen fuel gas blends at a manufacturing plant scale. New projects are targeting hydrogen content up to 100%, relying on specialized materials (Topolski 2022).

### 2.1.5 Carbon-Neutral and Clean Fuels

According to the 2015 “Best Available Techniques Reference Document for the Production of Pulp, Paper and Board,” 52.5% of heat and power generated in European pulp and paper plants is derived from biomass, 38.8% from gas, and the other 9.4% from fuel oil, coal, and other fossil fuels (Suhr 2015). Similarly, about 77% of the $CO_2$ emissions from U.S. pulp and paper mills are biogenic (Sagues et al. 2020). For example, WestRock, a U.S. paper packaging company, used renewable biomass to fulfill 61% of its own energy needs in 2023 (WestRock 2023). Billerud, a paper and packaging producer, has eliminated 98% of fossil fuels from production in their European plants, and 72% from their North American plants. Instead of fossil fuels they use a variety of biofuels, including forest biomass residues, raw methanol, tall oil, resin acid, biogas, rapeseed, and more (Billerud n.d.).

Within a pulp and paper plant, the major $CO_2$ emitters are the recovery boiler, multi-fuel boiler, and lime kiln (Sagues et al. 2020). The emissions from the recovery boiler are considered biogenic, as the black liquor burned in the BLRB is a biofuel derived from wood (Gardarsdóttir et al. 2018). The multi-fuel boiler can utilize waste biomass, fossil fuels, or other alternative fuels. The mixture of fuels depends on the volume of wood waste produced and the steam demand. Sagues et. al. presented a case in which only 47% of fuel was waste wood and the other 53% was fossil-based (Sagues et al. 2020), while Onarheim et. al. assumed a multi-fuel boiler that burned 95% bark waste and 5% bio-sludge from wastewater treatment (Onarheim et al. 2017).

The lime kiln is the only unit in a pulp plant that still uses fossil fuel for normal operation, but there are opportunities for fuel switching. Co-firing or complete fuel substitution in the lime kiln are technologically feasible with alternative fuels such as tall oil and tall oil pitch, producer gases, hydrogen, bark powder, lignin, and torrefied biomass (Kuparinen and Vakkilainen 2017). These alternative fuels have all been demonstrated at a lab or industrial scale. A 2005 survey of pulp mills revealed that at least six lime kilns operate by burning tall oil pitch (Francey, Tran, and Berglin 2011). Producer gas combustion has been utilized in multiple Scandinavian lime kilns (Kuparinen and Vakkilainen 2017). A hydrogen-fired lime kiln was demonstrated by the British Department for Business, Energy, and Industrial Strategy (British Lime Association 2022). Bark powder has been co-fired in lime kilns since the 1980s (Suhr 2015), but recently Scandinavian pulp mills proved the feasibility of 100% bark firing (Manning and Tran 2015). A 100% lignin-fired lime kiln was proven successful at the Sodra Monsteras mill (Suhr 2015), but lignin isolation from black liquor disrupts the heat and power integration of the pulp production process, so process economics must be considered (Kuparinen and Vakkilainen 2017). Torrefaction is a mild form of pyrolysis that reduces moisture content, increases energy density, and improves the grindability of biomass. Torrefied biomass is similar to coal, which is a common fuel for lime kilns (Kuparinen and Vakkilainen 2017). The combustion behavior of torrefied biomass has been studied (Sher et al. 2020), but the concept has not been proven with an industrial lime kiln. After analyzing the technological and economic feasibility of various fuel switching options, Kuparinen and Vakkilainen found that producer gas and torrefied biomass were the most profitable options (Kuparinen and Vakkilainen 2017).

### 2.1.6 Electric Lime Kilns

Within a pulp and paper plant, a rotary lime kiln serves to convert calcium carbonate into calcium oxide for further use ($CaCO_3 \rightarrow CaO + CO_2$). Unfortunately, this reaction produces $CO_2$ as a side product, creating unavoidable emissions. Additionally, conventional lime kilns are heated by fuel combustion or coal-firing within the kiln shell, creating $CO_2$ emissions that could be avoided through electrification.

One option for electrification is resistive electric heating. Rather than combusting fuel within the shell of the rotary kiln, the kiln would use electric heating elements arranged outside the perimeter of the shell. Powering the heating elements with renewable electricity rather than combustion can reduce the $CO_2$ emissions of the kiln by 35% (Tokheim 2019). Further, the electrified rotary lime kiln is an ideal candidate for pairing with CCUS. Without the contamination from combustion gases, the energy requirements for carbon capture with an electric kiln are lowered because of the virtually pure $CO_2$ emissions (Jacob and Tokheim 2023).

This technology has been demonstrated in literature through modeling and experimentation (Tokheim 2019; Katajisto 2020; Jacob and Tokheim 2023; Jacob, Pinheiro, and Tokheim 2023; Liu and Wang 2018; Parra and Romano 2023; Tokheim, Mathisen et al. 2019, Katajisto 2020; Liu, Jin et al. 2023; Quevedo Parra and Romano 2023). These papers mainly discuss the applications of the electrified kiln in the context of the concrete industry rather than the pulp and paper industry, but the same technology can be used. Major results show that the electrified rotary kiln paired with CCUS has the potential to avoid 72% of $CO_2$ emissions, with an associated cost of $72 per metric ton of $CO_2$ avoided (Tokheim 2019). The 72% emission reduction assumes electrical energy sourced from the grid with a $CO_2$ footprint of 47 g/kWh. Integrating nuclear energy would avoid the energy carbon footprint, leading to 100% $CO_2$ emission reduction.

The electric rotary kiln has now entered the market, and various versions are offered by kiln manufacturers (Agico Cement n.d.; IBU tec n.d.; FEECO n.d.; Kintek n.d.; Kurimoto n.d.; Noritake n.d.). One example is Agico Cement's electric heating rotary kiln, which uses 48 electrified silicon carbide rods arranged at the bottom of the rotary shell (Agico Cement n.d.). The process material is indirectly heated through the kiln shell. The other kilns use similar designs, with varied materials and arrangements of heating elements. These electric rotary kilns are advertised for use with concrete manufacturing, pulp and paper, glass, and more. In 2022, Japan's Ministry of Economy, Trade, and Industry released a "Technology Roadmap for 'Transition Finance' in Pulp and Paper Sector," which claimed that the electrification of lime kilns would be implemented in pulp manufacturing in the 2030s (Ministry of Economy Trade and Industry 2022),

Benefits of the electric lime kiln with resistive heating include direct and indirect $CO_2$ emission reduction, accurate heating control in multiple zones, and absence of lime contamination (Katajisto 2020; Jacob and Tokheim 2023). Still, the technology presents issues. First, the thermal energy requirements for the indirectly heated kiln are higher than that of the kiln directly heated with fuel combustion. Jacob and Tokheim showed that the electrified kiln requires 81% more effective thermal energy than a coal-fired scenario (Jacob and Tokheim 2023). This is due to multiple factors, including higher calcination temperature, heat losses through the shell material, and the heat to energy efficiency factor (Jacob and Tokheim 2023). The heat losses can be mitigated through further research of the heating elements and the kiln shell material. Further, the electrified kiln must use electricity that is non-carbon-emitting in order to take advantage of the carbon avoidance from electrification. Due to the increased energy demands, an electrified kiln using energy generated from natural gas would end up emitting more $CO_2$. Similarly, high costs of renewable energy may make the electric kiln economically infeasible. For these reasons, switching to an electric kiln is only recommended if the plant has reliable access to low-carbon energy, as in Pennsylvania where the steel industry utilizes electrified equipment (Pisciotta et al. 2022). Finally, electric rotary lime kilns have been shown to have decreased output. Specifically, FEECO and IBUtec report reduced throughput (Pisciotta et al. 2022). This is due to the heat transfer inefficiencies associated with indirect heating (Pisciotta et al. 2022). Therefore, further research of the heating elements and shell material can mitigate this issue.

One design that attempts to avoid the heat transfer inefficiencies is Jacob and Tokheim's novel internally heated electric rotary kiln (Jacob and Tokheim 2023).They explain that the indirectly heated electric rotary kilns on the market use expensive shell materials in order to improve heat transfer, making the equipment more expensive, so they tested a design using internal electric heating that can still utilize the cheaper refractory and steel materials utilized in conventional lime kilns (Jacob and Tokheim 2023). They built a computational model of the system, then validated the results experimentally. The design used three silicon carbide heating elements and two thermocouples. The internally heated electric kiln successfully ran for 4 days, which validated that the design is possible, but results showed 60% heat loss, showing that further research into heating elements and insulation is required (Jacob and Tokheim 2023).

Researchers are exploring more approaches to minimizing $CO_2$ emissions from lime kilns, including oxy-fuel combustion, plasma heating, electrochemical calcination, and more (Wilhelmsson 2018; Svensson, Wiertzema, and Harvey 2021; Pisciotta et al. 2022; Liu et al. 2023; Parra and Romano 2023).

# Carbon Capture

Carbon capture is likely the simplest solution to decarbonize existing industrial processes. $CO_2$ capture in flue gases is typically done in one of three ways: pre-combustion, post-combustion, or oxy-fuel combustion. Pre-combustion capture traps $CO_2$ before the fuel is burned by converting the fuel to syngas. Post-combustion capture separates the $CO_2$ from the flue gases as the final stage. Oxy-fuel combustion requires burning the fuel in an oxygen atmosphere instead of air, which results in flue gases that are mainly $CO_2$ and water vapor. This is considered a form of capture because the resulting $CO_2$ stream is nearly pure and requires minimal treatment. Because most of the $CO_2$ emissions come from black liquor, pre-combustion capture would require significant changes to the pulping process. Therefore, this study focuses on post-combustion capture and oxy-fuel combustion for the boilers at the mill. While there exist commercial post-combustion capture technologies that could be integrated immediately, oxy-fuel combustion would require more design considerations.

## 2.1.7 Post-Combustion Capture (Amine Scrubbing)

One of the most studied techniques for $CO_2$ capture is post-combustion capture. This approach directly removes $CO_2$ from a combustion flue gas, which is then compressed and transported at a higher concentration for further utilization or sequestration. For this purpose, several methods have been considered, including solid sorbents for physical absorption, and liquid solvents for chemical absorption. low-high temperature sorbents, membranes, ionic liquids, etc. Between the different alternatives found, the amine-based solvent scrubbing has been the most scalable technology and has been proven with high reliability. Amines such as monoethanolamine (MEA) have a strong affinity with $CO_2$ and provide a confident way to separate the carbon dioxide from a flue gas stream. The molecular formula of MEA is $C_2H_7NO$, and the equilibrium and kinetic reactions that represent the pathway of the $CO_2$ in contact with the MEA are represented in the Equations (1)–(5) (Madeddu, Errico, and Baratti 2019; Zhang et al. 2009):

$$2H_2O \leftrightarrow H_3O^+ + OH^- \quad (1)$$

$$MEA^+ + H_2O \leftrightarrow H_3O^+ + MEA \quad (2)$$

$$HCO_3^- + H_2O \leftrightarrow H_3O^+ + CO_3^{2-} \quad (3)$$

$$CO_2 + MEA + H_2O \leftrightarrow MEACOO^- + H_3O^+ \quad (4)$$

$$CO_2 + OH^- \leftrightarrow HCO_3^- \quad (5)$$

The fresh amine solvent is put in contact with the cooled flue gas (~40°C) containing $CO_2$ in a packing absorber column, where the size of the column and the packing prototype allow enough contact and residence time for the $CO_2$ to react and be trapped by the amine with the lowest pressure drop possible [Equations (1)–(5)]. Then, the amine-rich $CO_2$ is sent to a stripping column, where the solvent is heated up to ~120°C under low pressure (1-2 bar), releasing the $CO_2$. This step is very energy-intensive and demands a high amount of steam. Once the solvent is regenerated, it is sent back after cooling to the absorber to capture the $CO_2$ again. The concentrated $CO_2$ obtained from the top of the stripping column is further dehydrated and compressed to keep it liquefied for storing purposes.

Several technical evaluations and economic analyses of amine solvent carbon capture systems have been conducted at a commercial scale for power generation plants (Jones 2019; National Energy Technology Laboratory 2007) and different industrial sectors (Hughes 2022; Gardarsdóttir et al. 2018; Leeson et al. 2017), including pulp and paper manufacturing. In the case of the pulp and paper manufacturing sector, Onarheim et. al performed a comprehensive economic analysis of coupling a post-combustion $CO_2$ capture with a European integrated kraft pulp mill (Onarheim et al. 2017). In their work, they estimated the cost of capturing $CO_2$ from the different sources found in kraft processes, and combinations of them, in a range of \$70 to \$100 per metric ton of $CO_2$ captured. Nwaoha and Tontiwachwuthikul evaluated different amine blends and compared their performance against a conventional MEA system to capture $CO_2$ from a Canadian paper mill (Nwaoha and Tontiwachwuthikul 2019). They focused the analysis only for fossil $CO_2$ sources in the mill, estimating a cost of ~\$137 using MEA and a range of ~\$120-\$150 per metric ton of $CO_2$ captured for the different amine blend alternatives considered in the study. Finally, a concise study focused only on lime kiln flue gas emissions from the kraft mill process was conducted by Pakhi et. al. The estimated cost for $CO_2$ emissions from the lime kiln ranged between \$70 to \$82 per metric ton captured (Parkhi, Cremaschi, and Jiang 2022).

### 2.1.8 Oxy-Fuel Combustion

Oxy-fuel combustion can be implemented into the multi-fuel boilers, lime kiln, and BLRB, however, this will require a source of pure oxygen. This section describes how oxy-fuel combustion could be integrated into the lime kiln and BLRB and shows two methods for obtaining an oxygen-rich gas stream.

Oxy-fuel combustion is different than the gasification, although many of the reaction mechanisms are the same. In gasification, the fuel feedstock material is exposed to a controlled amount of oxygen, so only a portion of the fuel burns completely. The reaction products will be heat and syngas (a combination of H2, CO, and $CO_2$), which can be burned as fuel in a turbine or other application (National Energy Technology Laboratory n.d.-a).

In oxy-fuel combustion the purpose is to completely combust the fuel in an oxygen-rich atmosphere diluted with fuel or water. The primary reaction products are $CO_2$ and $H_2O$, and water can be removed from the stream by condensation. This results in a nearly pure $CO_2$ stream that can be separated and captured at a much lower energy requirement (National Energy Technology Laboratory n.d.-a).

Oxy-fuel combustion on its own is sometimes referred to as a $CO_2$ capture process. This is because the stream is not mixed with a large portion of nitrogen, and depending on the fuel used, could have contaminates such as sulfur-rich gas and NOx, which can be removed by conventional separation technologies.

Beyond the removal of controlled emissions, the level of additional separation or purification required depends on the final use of the $CO_2$. DOE/NETL completed a comparison study of air-fired combustion and capture technologies. Air-fired coal combustion with amine post-combustion capture generated a >99% pure stream of $CO_2$. Oxy-firing technologies produced an 84%-88% pure stream of $CO_2$ after controlled emissions were removed. Additional minor contaminants (nitrogen, oxygen, argon) were removed by a partial condensation purifier to increase the purity to 96% (Thimsen 2011).

#### *2.1.8.1 Lime Kiln*

The lime kiln is a high-value point source for $CO_2$ in a paper mill because the process of generating quicklime necessitates the release of $CO_2$. This is the most highly concentrated $CO_2$ source at the mill.

The endothermic reaction for calcite to form lime is

$$1g\ CaCO3\ (s) + 1.783\ kJ\ heat \longrightarrow 0.56g\ CaO(s) + 0.44g\ CO2\ (g) \quad (6)$$

This process is generally carried in a rotary kiln, where material flows through the kiln through different stages until it is calcined into calcium oxide. The limestone enters the kiln on the cooler side (800°C to 900°C) to be dried and heated by the flue gas flowing in the opposite direction. On the opposite end of the kiln is the burner, which releases $CO_2$ from the calcium carbonate at temperatures between 1000°C to 1200°C. As the lime exits the kiln, the product must be cooled quickly to minimize the uptake of $CO_2$ from the atmosphere. If too much $CO_2$ is absorbed, it will revert the CaO back to $CaCO_3$. In a traditional lime kiln, flue gases exiting the kiln are treated for pollutants and then released to the atmosphere. The flue gas consists of both residual $CO_2$ from the calcination process and combustion gases from fuel in the burner. Lime kilns are designed to fire a variety of fuels, depending on the availability: natural gas, coal, No. 6 fuel oil, incinerated non-condensable gases, and biomass residuals. Many modern plants use natural gas as the fossil fuels source. Across all the operating paper mills as of 2020, the average $CO_2$ concentration in the lime kiln flue gas stream is 21 mol% (Sagues et al. 2020).

There are many strategies to reducing combustion emissions from the lime kiln, such as increasing energy efficiency, using low-carbon fuels, and incorporating pre-combustion capture of carbon dioxide. However, because of the emissions of $CO_2$ from the calcination process itself, only two technologies can help achieve near-zero $CO_2$ emissions from the lime kiln: post-combustion capture of $CO_2$ and capture through oxy-fuel combustion (Eriksson, Hökfors, and Backman 2014).

In an oxy-fuel configuration, oxygen is substituted for air in the lime kiln, which concentrates the $CO_2$ stream even further by removing nitrogen from the combustion equation. Raising the oxygen levels also increases the flame temperature and heat load in the lime combustion area, therefore the temperature must be more carefully controlled. Flame temperature can be controlled by recirculating flue gas into the kiln, which raises the $CO_2$ concentration, increasing the calcination temperature of the raw material. From simulations by Eriksson et al., the $CO_2$ concentration in the flue gas using this method can reach 70-75%. This greatly reduces the energy required for carbon capture. Implementing oxy-fuel combustion also lowers the total $CO_2$ emitted from combustion and the calcination reaction. In a reference case using coal as the fuel, the ratio of $CO_2$ emitted per metric ton of product was 1.34. The lowest emitting oxy-fuel test case with acceptable product quality was a ratio of 1.23 (Eriksson, Hökfors, and Backman 2014). Although $CO_2$ capture can still be effective for flue gas from the lime kiln, oxy-fuel combustion adds the benefit of decreasing the energy required for the separation and capture of $CO_2$. Gerbelová et al. (2017), compared the energy requirements for MEA post-combustion capture and oxy-fuel combustion in a lime kiln for a cement plant. In the study, cryogenic air seperation was used to obtain the oxygen stream. The results, shown in Table 2, show that oxy-fuel combustion required less energy per metric ton $CO_2$ captured than MEA capture.

Table 2. Comparison of MEA post-combustion capture and oxy-fuel combustion energy requirements from (Gerbelová, van der Spek, and Schakel 2017).

| Parameter | Unit | MEA Post-Combustion Capture | Oxy-Fuel combustion $CO_2$ capture ($O_2$ from CAS) |
|---|---|---|---|
| $CO_2$ capture rate | % | 67.2 | 87.1 |
| $CO_2$ captured | Metric ton/hr | 161.9 | 161.9 |
| Additional Heat Requirement | MWhth/metric ton $CO_2$ | 1.17 | 0 |
| Electricity Consumption | MWhe/metric ton $CO_2$ | 0.06 | 0.19 |

It is unclear if oxy-fuel combustion has been demonstrated in lime kilns, although the technology has been commercialized. According to Maerz, a lime kiln vendor, "no technology has been developed to retrofit existing lime kilns with an oxy-fuel combustion system to reach a very high $CO_2$ concentration in the exhaust gas stream" (Pringer n.d.). The Maerz EcoKiln is a commercial lime kiln that can be used in either an air combustion or oxy-fuel combustion configuration but does not include a carbon capture system. In 2017, Gerbelová et al. published a feasibility assessment to retrofit an existing cement plant with post-combustion and oxy-fuel combustion $CO_2$ capture (Gerbelová, van der Spek, and Schakel 2017). In the modeling work, they made no changes to the preheater, calciner, or rotary kiln when considering retrofit needs or costs.

#### *2.1.8.2 Black Liquor Boiler*

The BLRB both supplies the most steam to a typical kraft mill and requires the some of that energy to be input through the evaporators. The recovery boiler is key to the kraft chemical recovery process. It contains several vital reactions. Figure 2 illustrates the components and operation of the BLRB.

Lignin solids, which precipitate from the digesting process, are the "fuel" powering the boiler. Black liquor contains about 35% water and 65% black liquor solids, which consist of about 60% organic matter (lignin) and 40% inorganic matter (pulping chemicals). As a fuel, black liquor has a high water content, meaning it has a low HHV compared to other fuels. Liquor is sprayed into the furnace to be combusted at temperatures over 1000 °C. The flue gases from combustion preheat water, which is sent to the generating section of the boiler, where the heat of combustion evaporates the liquid feedwater to steam. Cooled flue gas is typically routed to an electrostatic precipitator to remove particulate matter before being vented from the mill.

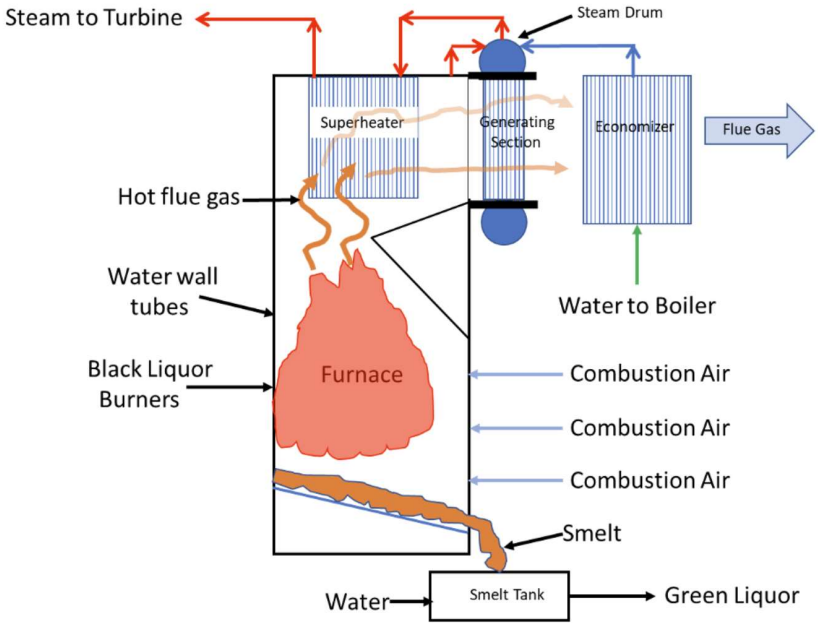


Figure 2. Schematic of a conventional BLRB. (Traubert 2022)

The other vital reaction is the reduction of sodium in the form of Na2SO4, which is recycled as Na2S to become a main component of white liquor. The combustion of organics in black liquor has the complementary effect of reducing sodium sulfate through carbothermal reduction. Carbon, when present in high temperatures, is one of the few oxidizing agents that can reduce or oxidize sodium sulfate. This reaction typically happens over a char bed, where un-reacted carbon from the black liquor solids collects. These reactions are as follows:

$$Organics(C,H) + O_2 = H_2O + CO_2 \quad (7)$$

$$Na_2SO_4 + 4C = Na_2S + 4CO \quad (8)$$

$$2NaOH + CO2 = Na2CO3 + H2O \quad (9)$$

The reduced sodium compounds, in the form of Na2CO3, and Na2S, are collected in the bottom of the furnace as smelt. This smelt is mixed with water and some white liquor to form "green liquor," which is sent to the causticizing plant, where the calcium coming from the lime kiln complements the chemical recovery cycle. The reactions form NaOH, the other main component of white liquor.

$$Na_2CO_3 + Ca(OH)_2 + Na_2S = CaCO_3 + 2NaOH + Na_2S \quad (10)$$

$$Na_2S + H_2O = NaOH + NaSH \quad (11)$$

In a perfect boiler system, all the sodium and sulfur would be recovered as $Na_2S$ and $Na_2CO_3$ in the smelt, however, some of the sulfur and sodium is evaporated in the flue gas, mainly in the form of Glauber salt dust ($Na_2SO_4$), and sulfur-containing gases ($SO_2$, $H_2S$, $CH_3SH$) (Hupa n.d.).

The careful balance of sulfur and sodium in a recovery boiler is relevant to this study because it complicates efforts to make the boiler process more economical or less polluting. At low operating temperatures, sulfur compounds (-$SO_2$ or -$SO_3$) in the smelt bed are less likely to be present in flue gases due to the reduced sulfur combustion conversion efficiency, at high boiler temperatures total sulfur content in the smelt bed is reduced, leading to an increase in sulfur content in the flue gas (Hupa n.d.). At higher operating temperatures, more salt dust is circulated. From Figure 3, the observed equilibrium temperature is between 1000°C and 1200°C.

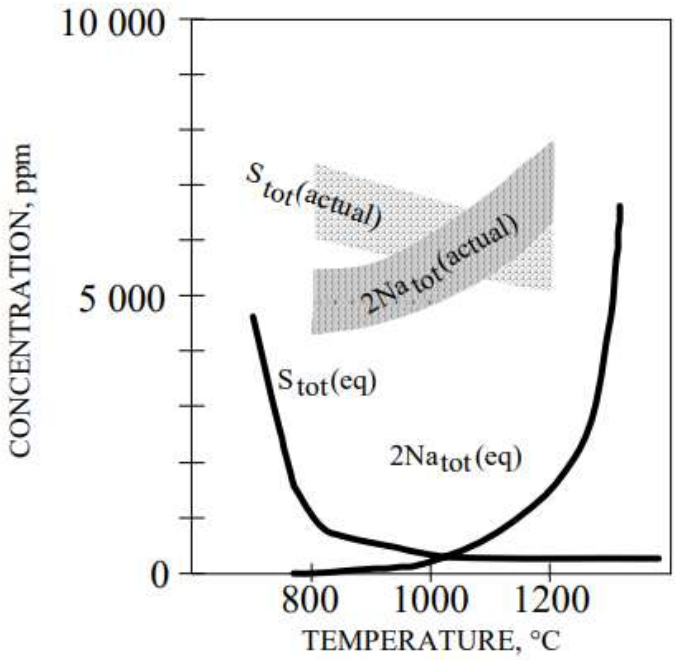


Figure 3. Resulting concentration of sulfur and sodium in the BLRB flue gases based on the boiler operating temperature. (Hupa n.d.)

There have been several demonstrations of oxy-fuel combustion in fossil fuel fired boilers, summarized in Figure 4. In 2012, the Fundación Ciudad de la Energia of Spain tested Foster Wheeler's 30 MW oxy-fuel combustion boiler using various fuel mixes (Lupion et al. 2013). The units ran for 920 hours under oxy-combustion conditions and 1300 hours overall. While the results from the test were promising, the design was never scaled up to the planned 320 MW boiler. In 2020, Research Institutes of Sweden (RISE) began a study of oxy-fuel combustion in black liquor boilers (RI.SE 2020). The goals of the project were to develop a model of the complex chemistry involved, experiment with the black liquor boiler under varied conditions, and estimate the costs associated with the technology and carbon savings. Although the study has ended, RISE has not yet published their results. Guo et al. summarized the known industrial oxy-fuel demonstration projects, including Shwaraze Pumpe, Lacq, CIUDEN, Callide, and Yingcheng (Guo et al. 2024). The oxy-fired black liquor boiler has not been implemented in the pulp and paper industry.

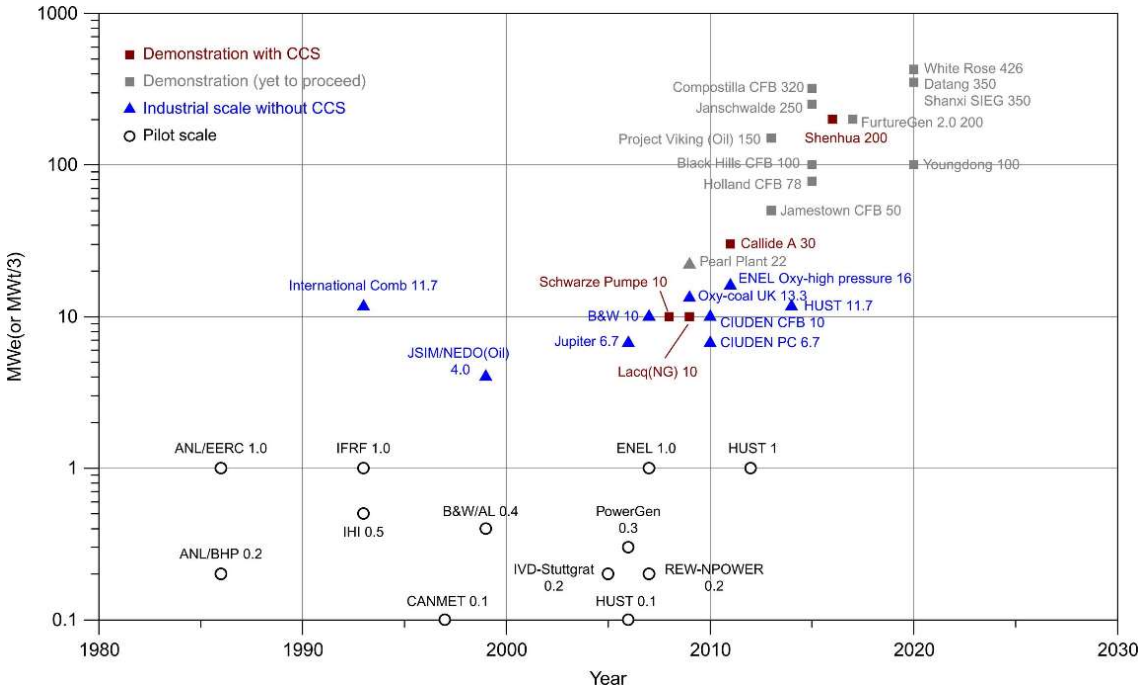


Figure 4. Progress and size of oxy-fuel combustion demonstration projects (Yadav 2022).

### *2.1.8.3 Oxygen Generation*

Oxy-fuel combustion of fossil fuels and biomass requires an air stream free of any inert gases. In conventional combustion, inert gases dilute the flue gas, requiring large and complicated systems if flue gas $CO_2$ capture is to be investigated. A typical flue gas is more than 70% nitrogen and less than 20% $CO_2$ on a dry molar basis. In contrast, a condensed flue gas from an oxy-fired natural gas burner may exceed 99% $CO_2$. Biomass such as the black liquor that is combusted at the reference pulp and paper mill will have a slightly dirtier flue gas due to the trace elements in the fuel matrix.

Various methods can be used to produce oxygen. The most common are cryogenic air separation units (ASU) and pressure swing adsorption (PSA). Cryogenic air separation separates the components of air based on their different boiling points. Air is liquefied, then distilled to separate pure oxygen and nitrogen. In PSA, air enters a pressurized tank filled with zeolites, which selectively adsorbs nitrogen molecules while allowing the remaining elements of air to flow through. When comparing ASU and PSA oxygen production, the required oxygen purity and flow rate help determine the best option. As shown in Figure 5, cryogenic separation provides oxygen at the lowest cost when the required flowrate is above 230,000 standard cubic feet per hour, or about 6,500 $m^3$/hr (Rao 2007).

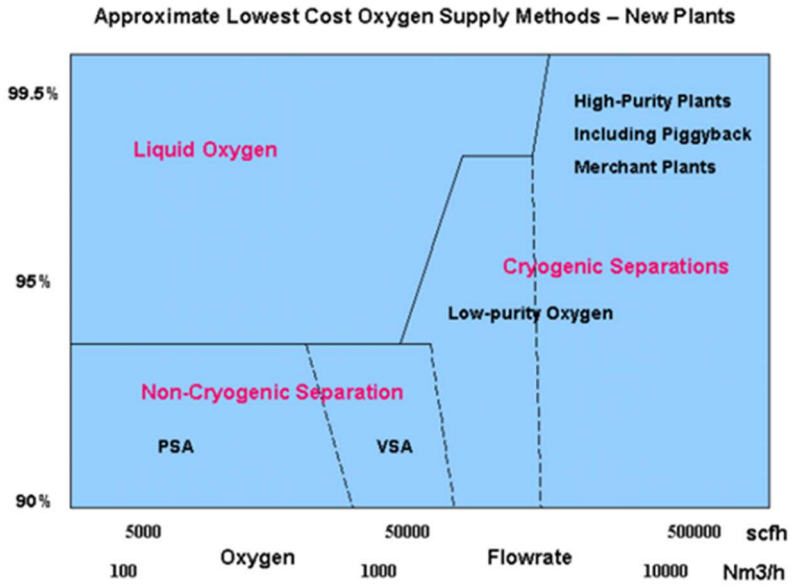


Figure 5. Lowest cost oxygen supply methods for new plants based on the required oxygen flowrate and purity (Rao 2007).

Oxy-fuel combustion furnaces do not simply run on pure oxygen, as this would cause the flame temperature to exceed metallurgical limits. Figure 6 depicts a generic oxy-fuel combustion schematic, where oxygen purified by cryogenic air separation is mixed with recycled flue gas to produce an "air" feed composed primarily of oxygen, carbon dioxide, and water vapor. The unrecycled flue gas, which is highly enriched in $CO_2$, is then sent to the $CO_2$ capture block, where the combustion water is condensed, and other impurities are removed. Cryogenic air separation uses compression and is an electricity-intensive process that could benefit from nuclear power. A literature source found that 99 mol% oxygen requires around 0.3 kWh/kg of $O_2$ (Hu, Li, and Yan 2010), with higher purity increasing the specific energy consumption exponentially.

Cryogenic air separation has been in use since 1895 (Rao 2007). Cryogenic air separation is most efficient when oxygen is required in high volumes and high purity, so it is mainly used in large-scale industrial processes like steel and petroleum manufacturing. Air Products sells ASUs with production capacities up to 3800 metric tons per day to serve customers with industrial-scale oxygen needs. For example, Shandong Qingdao Iron & Steel Gases Co., Ltd steel plant requires 2812 metric-tons/day of oxygen, and a Saudi Aramco refining plant requires 18,600 metric-tons/day of oxygen (Air Products n.d.).

Cryogenic air separation is currently thought to be the most technologically feasible oxygen generation method for oxy-fuel combustion because of the high volumes of oxygen required (Yadav 2022). For example, a 500 $MW_e$ oxy-coal power plant would require 10,000 metric tons per day of oxygen (Higginbotham et al. 2011). Pilot and industrial-scale oxy-combustion demonstration plants, including Vattenfall's Schwarze Pumpe plant and Air Liquide's Lacq pilot plant, utilized cryogenic air separation. The 30 $MW_{th}$ Schwarze Pumpe plant sourced 99.5% pure oxygen from a GOX 6000 ASU on site (Strömberg et al. 2009). Figure 6 shows how oxy-fuel combustion capture would work with cryogenic air separation as the oxygen source.

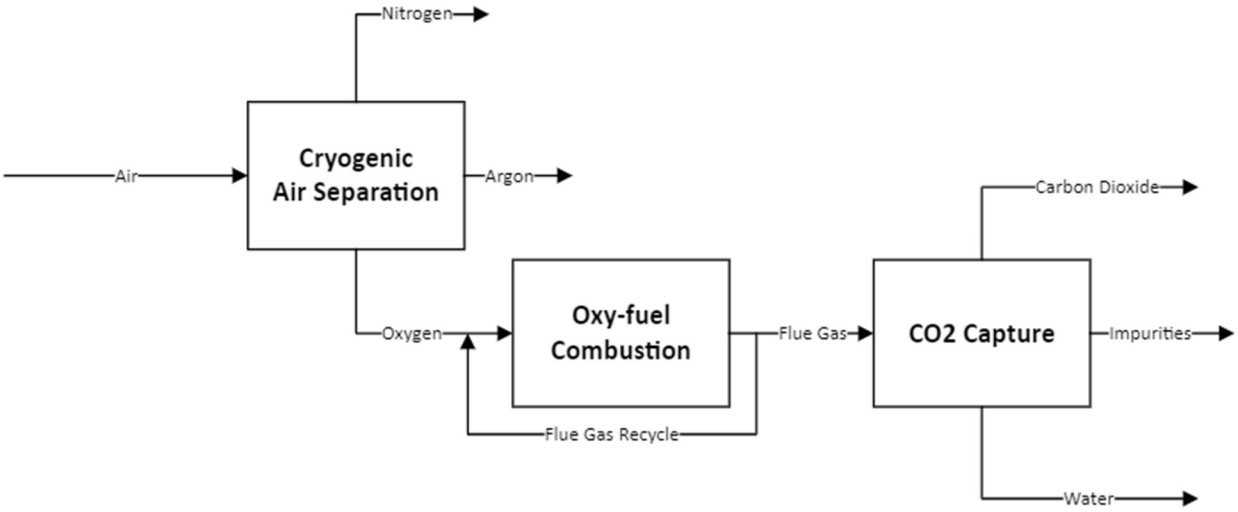


Figure 6. Oxy-fuel combustion schematic with cryogenic air separation sourced $O_2$.

The nitrogen byproduct of such a configuration is of relatively low value. Due to the high cooling requirements in ASUs, cryogenic air separation is an extremely energy-intensive process. Additionally, if there is no immediate use for the nitrogen produced, it is vented to the atmosphere. Rather than producing nitrogen to be wasted, electrolysis can produce the required oxygen and valuable hydrogen.

Because of this, we investigate a second oxygen source: high temperature steam electrolysis (HTSE). HTSE uses DC power to split the water molecule. In most applications, the oxygen is expected to be simply exhausted as an enriched air, as the oxygen market is relatively small compared to the hydrogen market. However, $CO_2$ can be used as the oxygen sweep instead of air to result in a "carboxy air" of 40 mol% $O_2$ and 60 mol% $CO_2$. Figure 7 depicts such a system, where a portion of the captured $CO_2$ is returned to sweep the $O_2$ gas away from the anode of the electrolysis stack. This $CO_2$ sweep prevents high temperature pure oxygen from reacting with system piping. The $CO_2$ portion of the carboxy air is inert in the oxy-fuel furnace, but because $CO_2$ is also the key product, it does not dilute the flue gas. Figure 7 shows how oxy-fuel combustion capture would work with cryogenic air separation as the oxygen source.

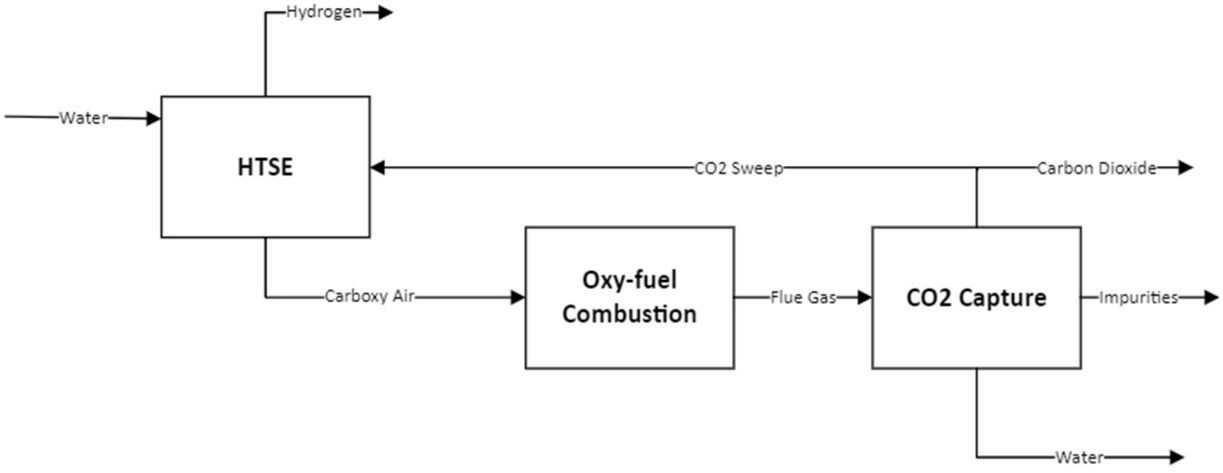

Figure 7. Oxy-fuel combustion schematic with HTSE sourced $O_2$.

HTSE is an emerging technology, with one demonstration project underway at the Prairie Island NPP in the U.S. (Office of Nuclear Energy 2022). However, the impacts of scaling this technology beyond a few MW is unclear. HTSE is used in this study to make oxygen because of the high value of hydrogen as a byproduct compared to nitrogen, the value of tax credits available for clean hydrogen production, and the future possibility of using hydrogen to convert biomaterial at the pulp mill into biofuels.

# 3. NUCLEAR INTEGRATION CASE STUDIES

The pulp and paper industry is a significant source of both biogenic and non-biogenic $CO_2$ emissions (U.S. Environmental Protection Agency 2022) and therefore is a sector that could benefit from decarbonization. The potential for nuclear integration is based on the mill size and configuration. Figure 8 shows the location and emissions of pulp and paper facilities in the U.S.

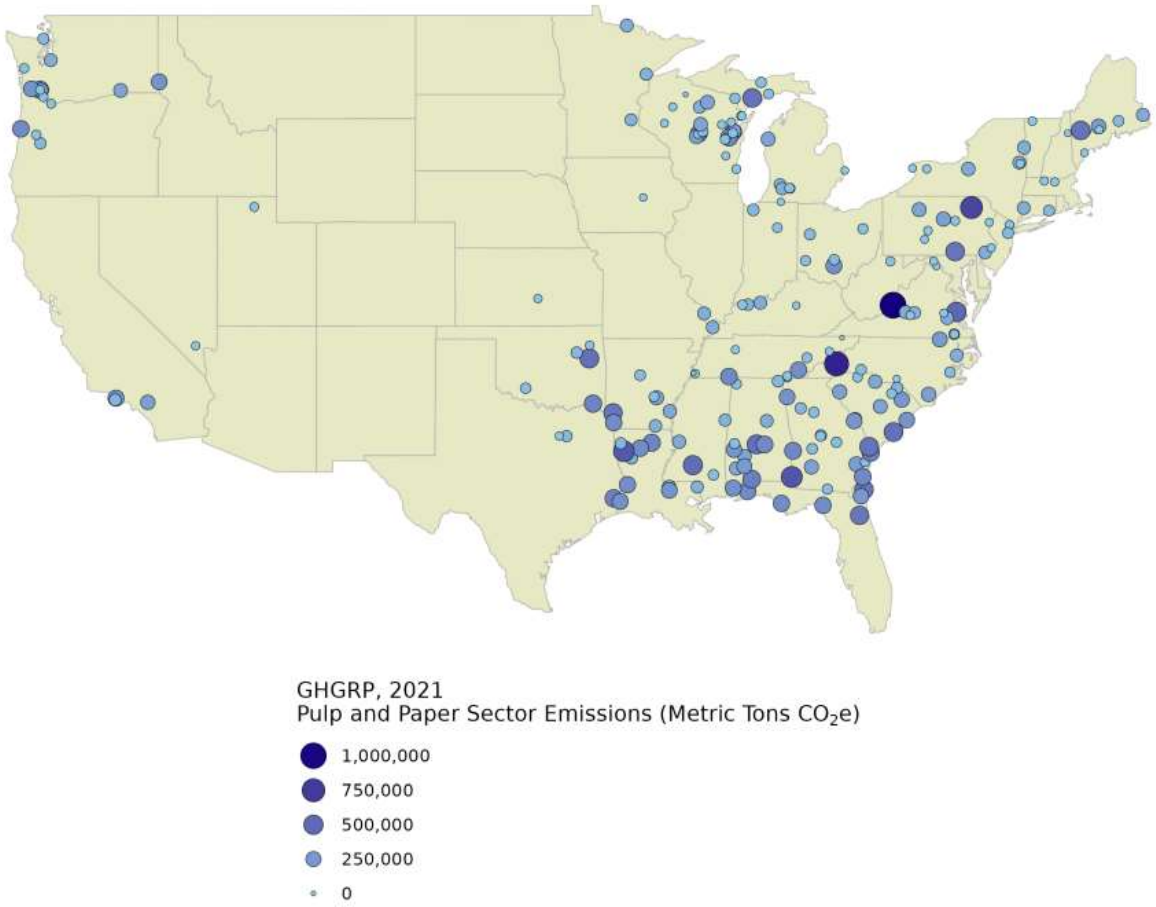


Figure 8. 2021 Greenhouse Gas Reporting Program Sector Profile: Pulp and Paper (U.S. Environmental Protection Agency 2022).

We evaluated six scenarios for the decarbonization of the reference unbleached softwood kraft mill. The net present value of the total profits from the reactor coupling and tax credits are estimated for each. The cases are separated into three decarbonization phases to reflect the technical readiness of each scenario. Phase 1 consists of conventional carbon capture at the plant using MEA and nuclear steam as a drop-in fuel. Phase 2 includes oxy-fuel combustion of the boilers. Phase 3 is not quantified here but would consist of converting the biomass burned in the BLRB and multi-fuel boilers to liquid fuels, chemicals, or bioproducts. A description of the five cases across three decarbonization phases is presented in Table 3.

Table 3. Scenarios for nuclear integration case studies and technoeconomic analysis.

| | | Description |
|---|---|---|
| Phase 0: Business as Usual Scenario | Case 1 | Baseline |
| Phase 1: Conventional Carbon Capture Scenarios | Case 2 | Carbon Capture with MEA technology, powered by an auxiliary NG boiler |
| | Case 3a | Carbon capture with MEA technology, powered by nuclear steam and electricity. Nuclear steam integrated to replace multi-fuel boilers |

| | | |
|---|---|---|
| | Case 3b | Alternative configuration for nuclear integration with carbon capture |
| Phase 2: Oxy-fuel combustion Carbon Capture Scenario | Case 4 | Oxy-Fuel combustion of all boilers and lime kiln with carbon capture. Oxygen steam from nuclear-powered HTSE unit. |
| | Case 5 | Case 4 with nuclear steam integration to eliminate multi-fuel boilers. |
| Phase 3: Biomass Conversion | Future Work | Waste biomass and lignin are extracted and converted to bioproducts or biofuels. |

In all cases, no distinction was made between the biogenic and non-biogenic $CO_2$. For the purposes of the carbon capture credit, section 45Q, $CO_2$ from all sources is eligible to receive the credits for capture. From a cost perspective, it would be disadvantageous for the pulp mill to capture only the non-biogenic $CO_2$, as evidenced by the results in Sagues et al. (2020). Case 2 is included to compare the results of a non-nuclear decarbonization case to the nuclear decarbonization case.

The analysis also assumed that all captured carbon was diverted to sequestration. This is because the credit for sequestration is higher than the credit for utilization, and it is unlikely that the mill operators would want to invest in building and operating the utilization equipment alongside the mill itself. In future work, the $CO_2$ utilization will be considered and compared to the sequestration cases. An analysis of the location of the mill and the feasibility of sequestration using pipelines is not in the scope of this study.

## Nuclear Integration with a Kraft Pulp Mill

The reference pulp mill produces 400,000 ADt unbleached southern softwood pulp annually. The assumed final pulping yield was 46 wt.%, which falls within the range of industrial operation yields (40%–55%). For the purposes of this study, the reference mill produces pulp only, so no paper making line is included. The reference plant has a robust CHP system that generates electricity while producing the various levels of steam required for the different unit operations. The reference mill was created as a steady-state model from on a variety of sources, and detailed information can be found in (Novotny et al. 2024). Only the black liquor boiler and lime kiln were modeled in Aspen Plus, and the results are included in Appendix A, BLRB and Lime Kiln Oxy-Fuel Combustion- Aspen Plus Process Model Simulation, Heat and Mass Balances and Modeling Validation.

The delignification that occurs in the BLRB is necessary for the operation of the plant. Chemical processes that do not convert lignin to $CO_2$ are also discussed in this report, but for this case it is assumed that the recovery boiler must remain. Therefore, nuclear cogeneration aims to decarbonize the reference mill by removing the natural gas auxiliary boiler and the hog boiler. The bark and fines that would otherwise be burned in the hog boiler would need to be disposed of in some other way.

This analysis is focused on HTGR type SMNRs. A generic HTGR was modeled in Aspen HYSYS using the conditions listed in Table 4. Although high-temperature gas-gas heat exchangers are being developed, it is assumed that the steam generator may not be bypassed. In other words, the highest quality heat accessible from the generic HTGR is the main steam, which has a saturation temperature of approximately 350°C and is superheated to 565°C. The generic HTGR is assumed to be available in increments of 200 MWth. Attached to a typical Rankine cycle with a thermal efficiency of about 40%, electrical production may be 80 MW. Co-generation, particularly the generation of main CHP steam, will lower the electricity production of the power cycle according to the total amount and grade of heat extracted.

The kraft mill's CHP system attenuates the main steam to the specified HP, MP, and LP conditions required at the plant, cogenerating electricity in the process. The existing CHP system will be leveraged in the case studies—wherever possible, the equipment is to be operated on-design. In some cases, the decarbonization systems will require additional energy, which will be supplied by increasing the main steam flow rate, operating the CHP off-design. In each case study, decarbonization opportunities will be analyzed ensuring that the production capacity of the key product (pulp) of the mill is unaffected.

Table 4. Summary of generic HTGR stream conditions used for this report.

| Coolant | | Temperature (°C) | Pressure (bar) | Phase | Flow Rate (kg/s) |
|---|---|---|---|---|---|
| Primary Helium | Core Inlet | 260 | 60 | Supercritical | 80.4 |
| | Core Outlet | 750 | 58.8 | | |
| Secondary Steam | Steam Gen. Inlet | 220 | 168.4 | Sub-cooled liquid | 81.1 |

In each case, the nuclear integration design followed the following assumptions and limitations.

1. Nuclear steam was implemented in the least invasive design, meaning that the HTGR steam was injected at the same quality as the boilers it was replacing (500˚C). This was to avoid a full thermodynamic analysis of the plant steam systems, given that changes in the injected steam quality could affect heat outputs to other areas of the plant. This type of analysis was performed in (Worsham and Terry 2022). However, this required taking main steam off the HTGR, and this is not necessarily the most thermally efficient configuration. A comparison of different integration techniques for this reference plant can also be found in (Novotny et al. 2024). More configurations will be explored in future work.
2. Steam delivered from the SMNR is injected into the plant's existing CHP system. The CHP system can use this steam to generate more electricity, and this strategy ensures that steam delivery to the plant's processes is unaffected.
3. When nuclear steam was integrated with the mill, the multi-fuel boilers were eliminated, including the hog boiler. This assumed that in future work (Phase 3), the waste biomass would be more valuable once converted to products or liquid fuels. The downside to this assumption is that (1) there is no current incentive for paper mills to send this material off-site, (2) less tax credits are harvested for carbon capture, and (3) in some cases, the elimination of the hog boiler increased the required size of the SMR.
4. Any additional SMR capacity that was not used to fulfill plant heat and electricity demands was used to generate electricity sold to the grid.

Other types of advanced SMNRs could be suitable for integration with the reference mill. Notable varieties include liquid metal, molten salt, and light-water cooled reactors. Each type has its own advantages. Light-water reactors operate at lower temperatures than the other reactor types; lower-temperature steam would have to be injected into the reference mill's CHP cycle at a header with steam at lower pressure and temperature.

An Aspen HYSYS model was developed to replace the 90 bar superheated steam lost when decommissioning the hog boiler and natural gas auxiliary boiler. The main 165 bar/565°C steam from the HTGR is required to generate CHP steam at the required conditions. By producing the same mass flow rate of steam at the same conditions, the existing CHP equipment can be operated in an identical manner to the BAU case (see Figure 9). This model, which demonstrates that the required 63 MWth of steam can be produced while cogenerating 51.2 MWe, is detailed in Appendix G.

## Phase 0: Business as Usual Scenario

Shown in this phase is the BAU scenario for the kraft mill. A typical mill does not include any carbon capture or mitigation equipment, and only manages emissions based on the Environmental Protection Agency's NESHAP and NSES guidelines. The plant is connected to a natural gas pipeline to fuel the auxiliary boiler and lime kiln.

### 3.1.1 Case 1: Baseline

Figure 9 depicts the utility requirements for the reference kraft pulp mill. Under normal operation, a natural gas auxiliary boiler is required to supplement the main steam produced by the BLRB and hog boiler.

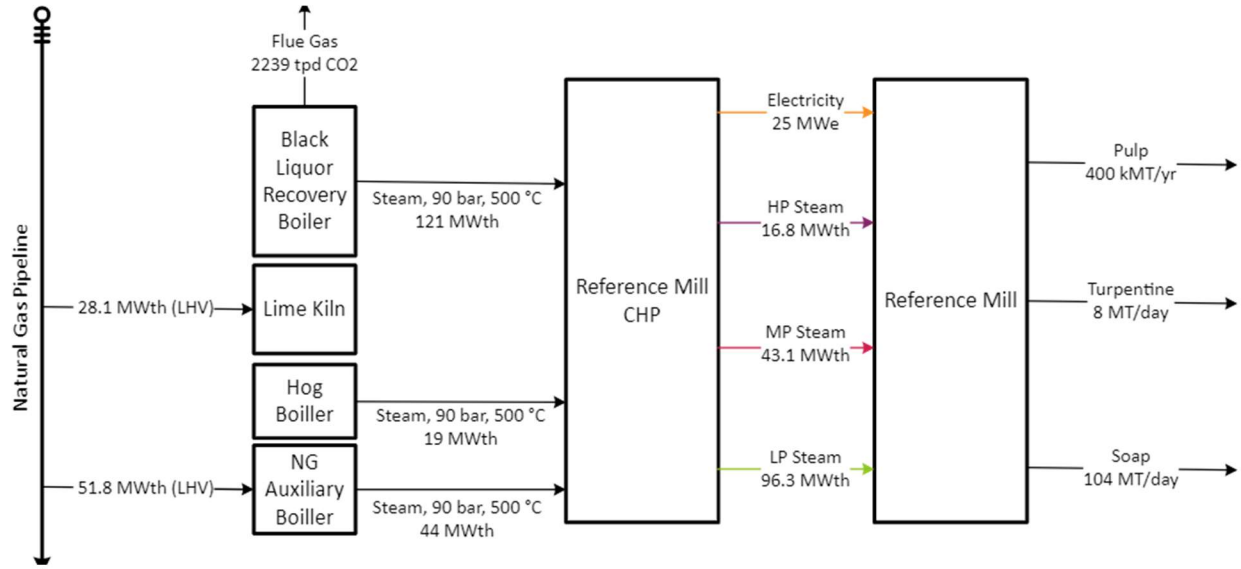


Figure 9. Utility system and unit operation BFD for BAU reference kraft pulp mill. LHV designates the fuel's lower heating value.

Table 5 shows the material and energy balance for the BAU case. Note that the reference mill only consumes 25 MW of electricity, which is supplied from the plant CHP system. Because of this, no cases were explored to integrate the plant with nuclear electricity only. The reference mill consumes 129.8 metric-tons/day natural gas from the pipeline to supply both the lime kiln and natural gas auxiliary boiler and emits 2256 metric-tons/day $CO_2$.

Table 5. Material and energy balance for Case 1.

| Inputs | Value |
|---|---|
| Natural Gas | 79.9 MWth (129.8 metric-tons/day) |
| Hog Fuel | 19 MWth |
| Energy Consumed | — |
| Steam | 156.2 MWth |
| Electricity | 25 MWe |
| Outputs | — |
| $CO_2$ (emitted) | 2239 metric-tons/day |

# Phase 1: Conventional Carbon Capture

This phase focuses on high technology readiness level (TRL) technologies that are drop-in ready to a pulp and paper mill for decarbonization. A large proportion of the $CO_2$ emissions from the reference kraft pulp mill come from the BLRB, but as discussed in Section 2, demonstrated BLRB decarbonization technologies would require an overhaul of the pulping system or major equipment investments. Theoretically, the plant could reduce its carbon footprint by switching to 100% renewable fuels, but this option would not have much effect on the actual carbon emissions of the plant and would not harvest any credits from the Inflation Reduction Act (IRA). Rather, the least capital-intensive option with an immediate return on investment is adding a carbon capture system to sequester emissions.

MEA carbon capture is a commercially available option to capture carbon emitted from a point source. This is likely the most attractive near-term option for decarbonization in the pulp and paper industry because a capture system can be powered by any fuel source, and mills could take advantage of tax credit 45Q for carbon sequestration. Case 2 shows the system changes and resulting revenues using the natural gas auxiliary boiler to power the MEA capture and compression unit. Case 3 is the same configuration, with an NPP providing steam and electricity to the unit through the plant's CHP system.

### 3.1.2 Case 2: MEA-Based $CO_2$ Capture

Figure 10 depicts the addition of MEA-based $CO_2$ capture to the reference mill. The MEA capture system has a 90% $CO_2$ recovery and requires 2.9 GJ/metric-ton-$CO_2$ captured in low-pressure steam, based on the analysis in Appendix D, MEA Carbon Capture Cost Estimation. The captured $CO_2$ is compressed and liquefied to be transported to long-term storage, requiring 77.8 kWh-e/metric-ton-$CO_2$. The added requirements in this case must be supplied by increasing the duty of the natural gas auxiliary boiler, which slightly increases the total $CO_2$ that goes to the MEA capture system.

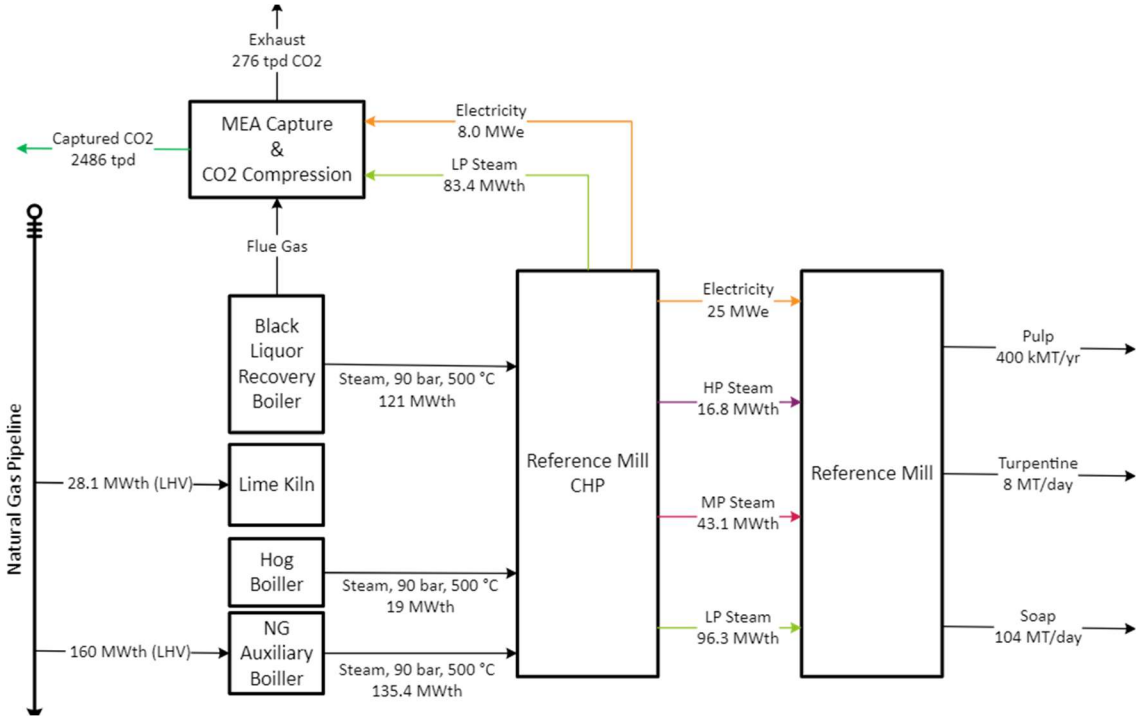


Figure 10. Utility system BFD for Case 2 - MEA-based CO2 capture.

The energy and material balance for the carbon capture case using a natural gas auxiliary boiler is presented in Table 6. This case uses more than double the natural gas required for the BAU case and generates more $CO_2$. However, the implementation of the carbon capture system decreases the $CO_2$ emitted by 88%.

Table 6. Energy and material balance for Case 2.

| Inputs | Value | Difference from BAU |
|---|---|---|
| Natural Gas | 188.1 MWth (317.9 metric-tons/day) | +108 MWth |
| Hog Fuel | 19 MWth | — |
| Energy Consumed | — | — |
| Steam | 239.6 MWth | +83.4 MWth |
| Electricity | 33.1 MWe | +8 MWe |
| Outputs | — | — |
| $CO_2$ (captured) | 2,486 metric-tons/day | — |
| $CO_2$ (emitted) | 276 metric-tons/day | -1,963 metric-tons/day (-88%) |

### 3.1.3 Case 3: MEA-Based $CO_2$ Capture + Nuclear Steam Integration

This case contains two subcases that compare the results of the same system with two HTGR sizes (200 MWth and 400 MWth). Originally, the case only used the 400 MWth design. Based on the TEA results of Case 3a, the authors wanted to explore the results with a smaller HTGR, so the thermal integration was modified. Both the 200 MWth and 400 MWth cases are shown here to describe how SMNR size impacts the TEA results.

### 3.1.3.1 Case 3a: 400 MWth HTGR

Figure 11 demonstrates that a 400 MWth HTGR can be used to replace the hog boiler and natural gas auxiliary boiler, reducing the natural gas usage and the $CO_2$ emissions that need to be captured. The 90 bar, 500°C steam that the reference mill CHP requires must be generated by the main 165 bar, 565°C steam from the HTGR. Although the main steam extraction for this case is only 128 MWth, a 200 MWth unit was not used in this integration configuration because the mixture of the main condensate and the turbine cycle condensate would be too hot to cool the primary HTGR coolant unless heat is wasted, as in Case 3b. An alternative integration strategy that allows a 200 MWth reactor to be used is shown in Case 3b. The integration of nuclear steam reduces the natural gas usage to only that required by the lime kiln, reducing $CO_2$ emissions and $CO_2$ captured.

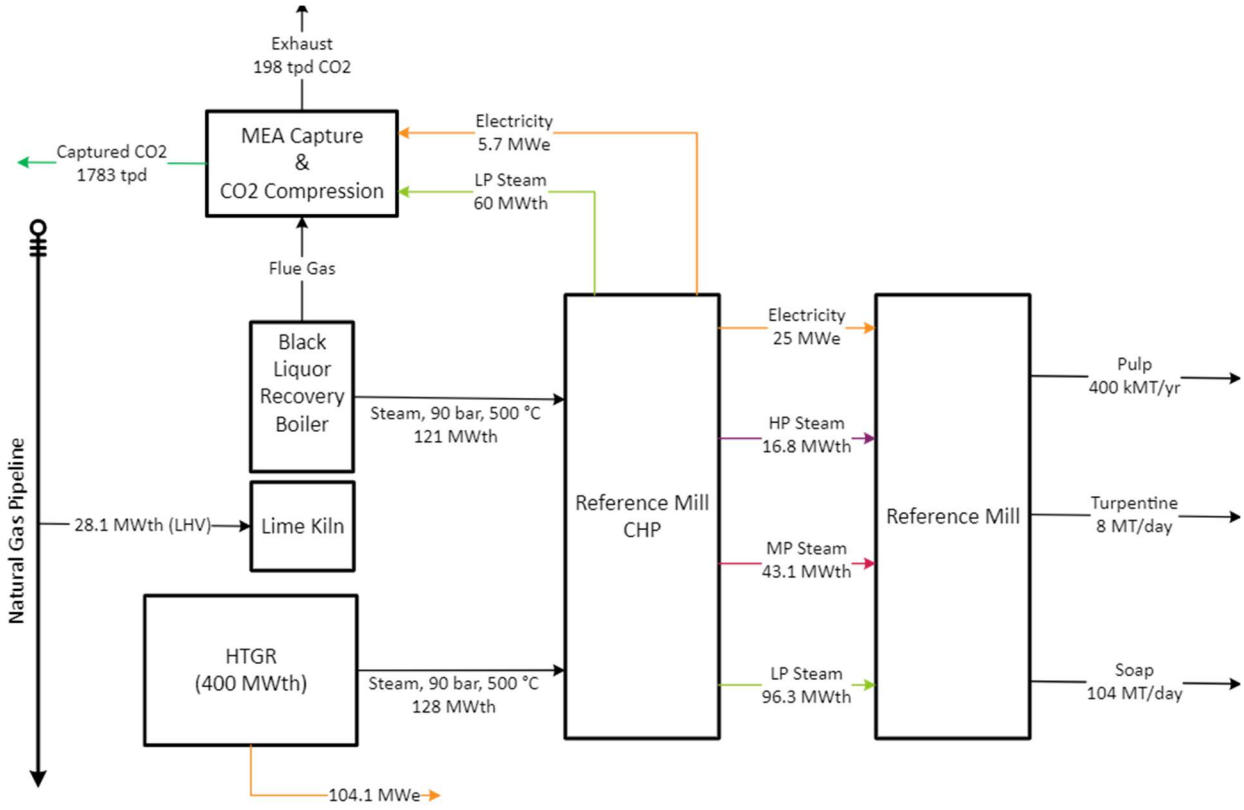


Figure 11: Utility system BFD for Case 3a - MEA-based $CO_2$ capture + nuclear steam integration.

Table 7 gives the energy and material balance for this case. The natural gas usage is reduced from the baseline because the multi-fuel boilers are eliminated. This case reduces the overall $CO_2$ produced by the mill and decreases the total $CO_2$ emitted by 91%. Note that this is a slightly higher reduction than in Case 2 because the same percentage of $CO_2$ is captured by the MEA system, but the total $CO_2$ produced is slightly less because the energy for capture is coming from a non-carbon-emitting fuel.

Table 7. Material and energy balance for Case 3a.

| Inputs | Value | Difference from BAU |
|---|---|---|
| SMNR Capacity | 400 MWth | — |
| Natural Gas | 28.1 MWth (39.8 metric-tons/day) | -51.8 MWth |
| Hog Fuel | 0 MWth | -19 MWth |
| Energy Consumed | — | — |
| Steam | 216.2 MWth | +60 MWth |
| Electricity | 30.7 MWe | +5.7 MWe |
| Outputs | — | — |
| Electricity (to grid) | 104.1 MWe | — |
| $CO_2$ (captured) | 1783 metric-tons/day | — |
| $CO_2$ (emitted) | 198 metric-tons/day | -2041 metric-tons/day (-91%) |

#### *3.1.3.2 Case 3b: 200 MWth HTGR*

Figure 12 demonstrates that a 200 MWth HTGR can be used to replace the hog boiler and natural gas auxiliary boiler, reducing the natural gas usage and the $CO_2$ emissions that need to be captured. The 90 bar, 500°C steam that the reference mill CHP requires must be generated by the main 165 bar, 565°C steam from the HTGR. With such a large percentage of the main steam being extracted for thermal use, the condensate from this process steam generator needs to be cooled to 268.5°C before mixing with the turbine condensate. This is done by using the condensate to reheat the turbine interstage and wasting 10 MWth. The integration of nuclear steam reduces the natural gas usage to only that required by the lime kiln, reducing $CO_2$ emissions and $CO_2$ captured.

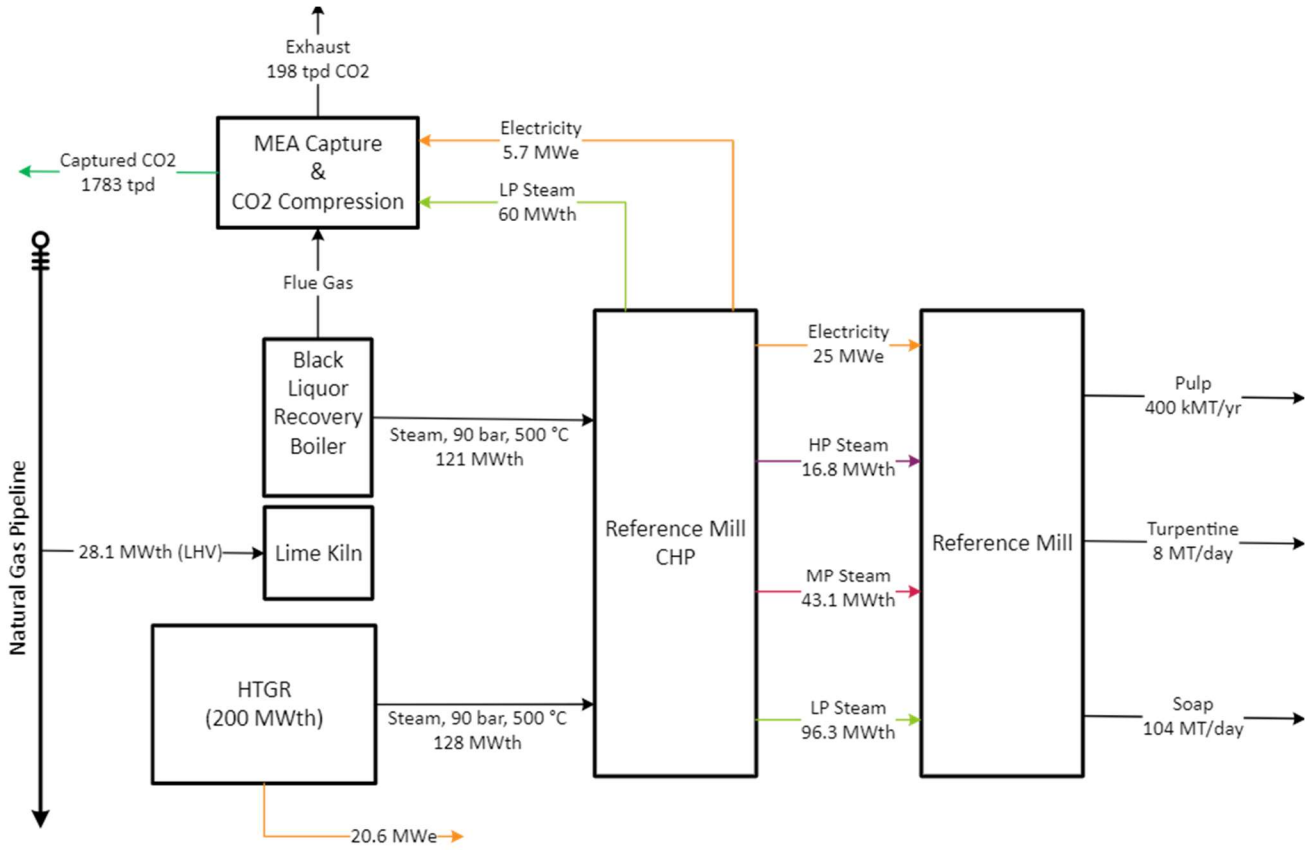


Figure 12: Utility system BFD for Case 3b - MEA-based $CO_2$ capture + nuclear steam integration.

Table 8 gives the energy and material balance for this case. The natural gas usage is reduced from the baseline because the multi-fuel boilers are eliminated. This case reduces the overall $CO_2$ produced by the mill, and reduces the total $CO_2$ emitted by 91%. Note that this is a slightly higher reduction than in Case 1 because the same percentage of $CO_2$ is captured by the MEA system, but the total $CO_2$ produced is slightly less because the energy for capture is coming from a non-carbon-emitting fuel.

Table 8. Material and energy balance for Case 3b.

| Inputs | Value | Difference from BAU |
|---|---|---|
| SMNR Capacity | 200 MWth | — |
| Natural Gas | 28.1 MWth (39.8 metric-tons/day) | -51.8 MWth |
| Hog Fuel | 0 MWth | -19 MWth |
| Energy Consumed | — | — |
| Steam | 216.2 MWth | +60 MWth |
| Electricity | 30.7 MWe | +5.7 MWe |
| Outputs | — | — |
| Electricity (to grid) | 20.6 MWe | — |
| $CO_2$ (captured) | 1783 metric-tons/day | — |
| $CO_2$ (emitted) | 198 metric-tons/day | -2041 metric-tons/day (-91%) |

# Phase 2: Oxy-Fuel Combustion

As an alternative for the MEA-based $CO_2$ capture, oxy-fired combustion has been studied. Oxy-fuel combustion, unlike air-firing, produces a flue gas with a very high $CO_2$ content which has lower associated sequestration costs. For the purposes of this study, the oxygen is supplied by HTSE, where the oxygen electrode is swept by a recycled portion of the $CO_2$ product to produce an air analogue that is 40 mol% oxygen and 60 mol% $CO_2$. A model was developed in Aspen HYSYS to couple such an HTSE stack to an HTGR type SMNR, where nuclear heat and electricity are used to split water into oxygen and a hydrogen byproduct.

### 3.1.4 Case 4: Oxy-Fuel Combustion-Based $CO_2$ Capture

Figure 13 depicts the nuclear integration schematic for oxy-fuel combustion in the BLRB, lime kiln, hog boiler, and natural gas auxiliary boiler. The only difference between this case and BAU operation (Case 1) is that the combustion equipment is fired by a blend of $CO_2$ and $O_2$ rather than normal air, yielding a flue gas devoid of nitrogen gas. The flue gas can be cleaned up simply using existing emission controls at the mill (venturi scrubber, electrostatic precipitator). A portion of the $CO_2$ is recirculated to the oxygen electrode of the HTSE stack, while the surplus is compressed and liquefied. Because the electricity for compression is supplied by the HTGR, the reference mill CHP can be operated on-design.

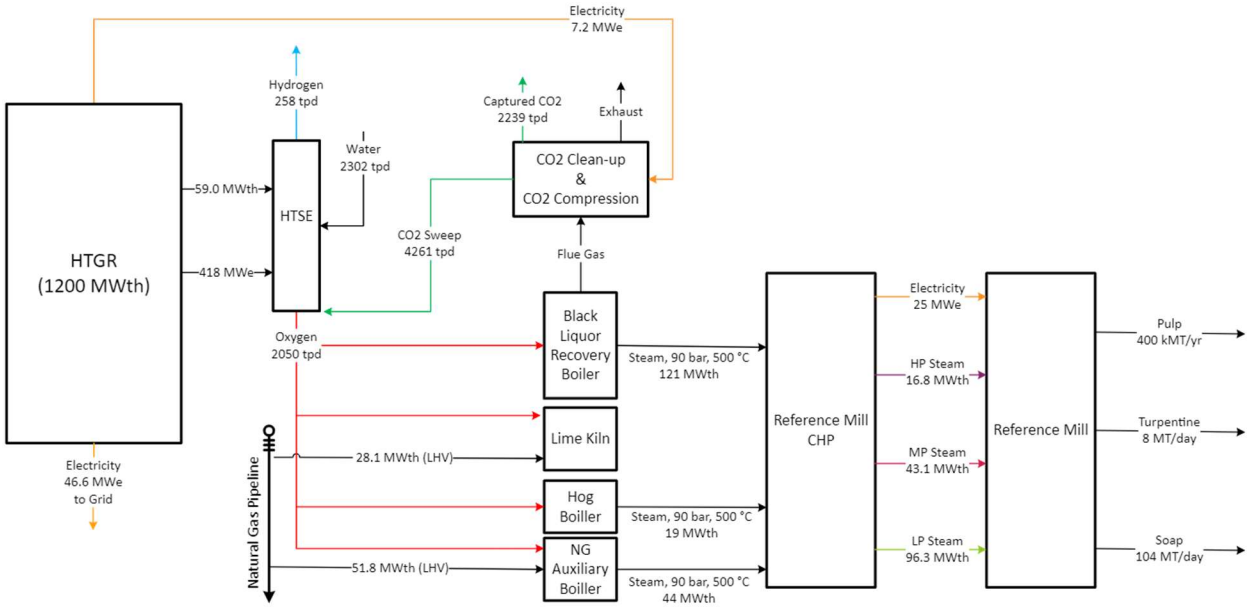


Figure 13. Utility system BFD for Case 4 - oxy-fuel combustion-based $CO_2$ capture.

Table 9 summarizes the material and energy balances for Case 4. In this case, 258 metric-tons/day of hydrogen is produced as a byproduct, and very little of it can be used on-site. This hydrogen must be transported to another location, or, ideally, used nearby in an energy park application. A potential synergistic approach would be to send both the hydrogen byproduct and the captured $CO_2$ to a nearby synfuel plant. This decarbonization pathway also reduces the $CO_2$ emissions of the kraft mill to virtually zero.

Table 9. Material and energy balance for Case 4.

| Inputs | Value | Difference from BAU |
|---|---|---|
| SMNR Capacity | 1200 MWth | — |

| | | |
|---|---|---|
| Natural Gas | 79.9 MWth (129.8 metric-tons/day) | 0 MWth |
| Hog Fuel | 0 MWth | -19 MWth |
| Oxygen | 2050 metric-tons/day | — |
| Energy Consumed | — | — |
| Steam | 215.2 MWth | +59 MWth |
| Electricity | 450.2 MWe | +425.2 MWe |
| Outputs | — | — |
| Hydrogen | 258 metric-tons/day | +258 metric-tons/day |
| Electricity (to grid) | 46.6 MWe | — |
| $CO_2$ (captured) | 2239 metric-tons/day | — |
| $CO_2$ (emitted) | 0 metric-tons/day | -2239 metric-tons/day (-100%) |

### 3.1.5 Case 5: Oxy-Fuel Combustion-Based $CO_2$ Capture with Nuclear Steam Integration

Figure 14 depicts a similar schematic as Figure 13, except the HTGR supplies steam to the CHP system. The hog boiler and natural gas auxiliary boiler are removed, reducing the oxygen demand and allowing a 1000 MWth HTGR (as opposed to 1200 MWth in Case 4) to be used, reducing the total investment. 203 metric-tons/day of hydrogen is produced as a byproduct, and very little of it can be used on-site. This hydrogen must be transported to another location, or, ideally, used nearby in an energy park application. A potential synergistic approach would be to send both the hydrogen byproduct and the captured $CO_2$ to a nearby synfuel plant.

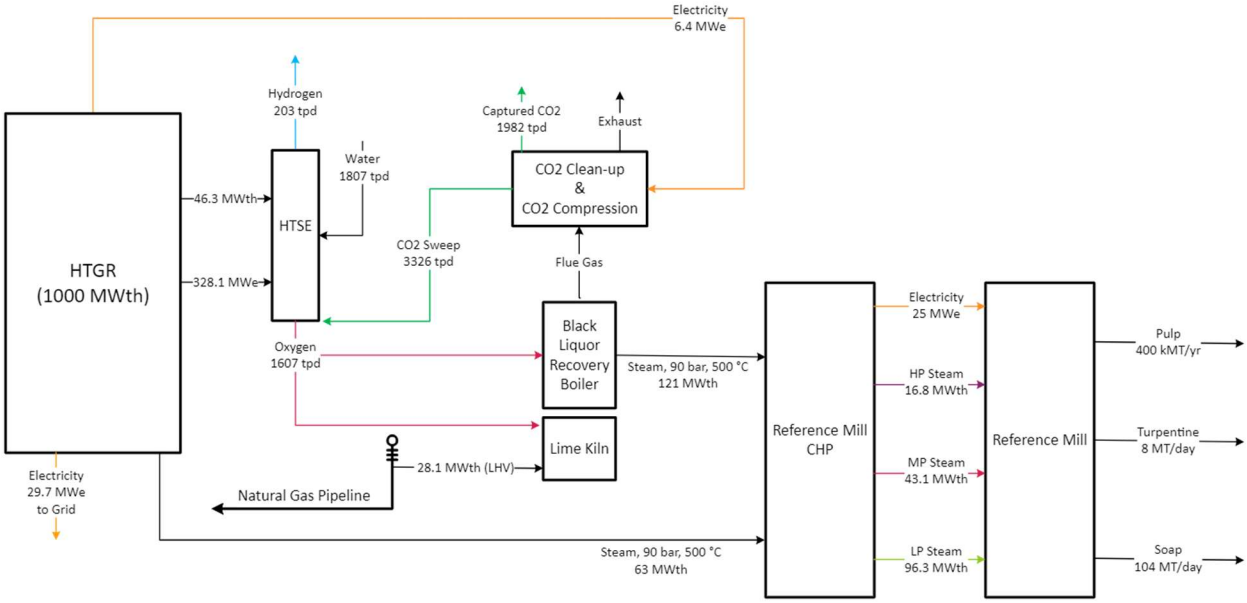


Figure 14. Utility system BFD for Case 5 - oxy-fuel combustion-based $CO_2$ capture + nuclear steam integration.

Table 10 summarizes the material and energy balances for Case 5. As in Case 4, Case 5 eliminates virtually all $CO_2$ emissions from the mill. Also, because the HTGR is supplying steam rather than generating oxygen for the multi-fuel boilers, the energy requirements of the system are reduced.

Table 10. Material and energy balance for Case 5.

| Inputs | Value | Difference from BAU |
|---|---|---|
| SMNR Capacity | 1000 MWth | — |
| Natural Gas | 28.1 MWth (39.8 metric-tons/day) | -51.8 MWth |
| Hog Fuel | 0 MWth | -19 MWth |
| Oxygen | 1607 metric-tons/day | — |
| Energy Consumed | — | — |
| Steam | 202.5 MWth | +46.3 MWth |
| Electricity | 359.5 MWe | +334.5 MWe |
| Outputs | — | — |
| Hydrogen | 203 metric-tons/day | — |
| Electricity (to grid) | 29.7 MWe | — |
| $CO_2$ (captured) | 1982 metric-tons/day | — |
| $CO_2$ (emitted) | 0 metric-tons/day | -2239 metric-tons/day (-100%) |

## Phase 3: Carbon Utilization and Biomass Conversion

In the cases considered above, the biomass typically burned in the hog boiler was replaced with nuclear steam wherever possible. From a business and lifecycle perspective, it makes sense for the mill to utilize its waste material as a carbon-neutral fuel to provide steam from the plant. However, when nuclear steam is available, replacing the biomass with a non-carbon-emitting fuel provides deeper decarbonization. Consequentially, the biomass can be converted to valuable fuels or products that can help to decarbonize other sectors, such as transportation. In theory, the hydrogen produced in Cases 4 and 5 would be used to upgrade the wood waste to liquid fuels. In addition to providing decarbonization, it is possible that upgraded biomass and extracted lignin from black liquor would be more monetarily valuable to the mill as other products when nuclear steam is available to replace them. Another valuable product in phase 3 is the captured $CO_2$ from each integration scenario. Although the tax credit for $CO_2$ utilization is less than that for sequestration, there is additional value to be gained from creating and selling additional products. These future pathways are described further in Section 6.

# 4. Economic Modeling Methods

Two tools that were created in-house at INL were used to complete the TEA: The Standardized Economic Tool (SET) and Nuclear Integrated Hydrogen Production Analysis (NIHPA). SET was developed as a versatile TEA tool capable of performing discounted cash flow analysis to estimate levelized costs for a specific product, net present value (NPV) of an investment, and internal rate of return (IRR) for an investment. It requires inputs such as financial parameters and cost contributors, including revenue streams, capital expenditures (CAPEX), annual variable operation and maintenance (O&M), annual fixed O&M, and annual received tax credits.

NIHPA has built-in formulas to estimate annual revenue streams, CAPEX, annual variable O&M, annual fixed O&M, and annual received tax credits for nuclear-integrated H2 production. In this study, the NIHPA tool's features are expanded to integrate SMNR and HTSE with the mill by adding the feedstock and product unit costs of the entire facility, including the SMNR, HTSE, and mill. The outputs of the NIHPA tool are then used by SET to perform cash flow analysis. Detailed descriptions of the calculations developed in each tool are provided in this chapter.

The following financial assumptions were used for all cases:

- Cost of equity: A 10% cost of equity is assumed for all the scenarios.
- Depreciation: This includes all depreciable capital costs, both direct (DCCs) and indirect (ICCs), for the nuclear reactors, carbon capture equipment, and HTSE. These costs are considered over a depreciation period of 15 years using the modified accelerated cost recovery system.
- Project timeline: The project is assumed to start on January 1, 2030, with a construction period of 1 year for the carbon capture equipment, HTSE, and SMNR, implying overnight construction. The project lifetime is set at 40 years, based on the SMNR license, with a debt term of 30 years beginning January 1, 2031.
- Plant type design: The nth-of-a-kind plant type design is assumed for the three systems, SMNR, carbon capture, and HTSE. The resulting values represent a commercial build between the second and fourth units deployed, assuming demonstrations by 2030, termed between-of-a-kind (BOAK).
- Inflation: No inflation rate is considered in this TEA for verification purposes.
- Tax credits: The IRA 45V tax credit is applied for clean H2 production for the HTSE, the 45Q Carbon Capture Credit is applied for the carbon capture equipment, and the IRA 48E tax credit is applied for the SMNR investment tax credits. A detailed description of the IRA tax credits can be found in Appendix B, Tax Credit Information.

## SET Tool

The SET tool discounts future cash flows to the same dollar year to calculate the NPV. Using a discounted cash flow method allows for consistent comparison between project investments and revenues. This is necessary because the value of money today differs from its value in the future due to its potential to earn interest. For example, $100 invested today at a hypothetical risk-free rate of 10% would be worth $110 next year. Conversely, $100 received a year from now is worth about $90 today when considering the time value of money. The discount factor, DF, for year "t" depends on the discount rate "r" and t. As t increases, future cash flows are worth less in present terms due to greater discounting, as shown by Equation (12).

$$DF_t = \frac{1}{(1+r)^t} \tag{12}$$

The previous equation (12) is applied to a series of cash flows to calculate their present value, determining profitability through NPV. Mathematically, this is expressed as:

$$NPV = \sum_{t=1}^{T} \frac{CF_t}{(1+r)^t} \quad (13)$$

*where*

NPV = net present value

$t$ = specific year

$T$ = project's total length (80 years is the maximum amount of time available)

$CF_t$ = cash flow in year $t$ (positive for returns, negative for investments or losses)

$r$ = project's discount rate, equal to the cost of equity.

Note that the discount factor is the cost of equity, as the cash flow in SET includes debt principal payments (see Table 11). Therefore, it is appropriate to discount the resulting cash flow using the cost of equity rate rather than the weighted average cost of capital (WACC).

Another key metric is the IRR, which is calculated similarly to NPV but with NPV set to zero to solve for r. The IRR represents the discount rate at which the project breaks even. If the IRR exceeds the cost of equity, the project is considered profitable and meets the required returns for equity.

Cash flows for each year are calculated based on revenues, costs, and taxes. In this model, a simplified version of the calculation shows direct additions and subtractions from revenue to cash flow, though the comprehensive method is detailed in Table 11.

Table 11. Simplified model calculation methodology.

| |
|---|
| + Revenue |
| - Variable Operation and maintenance (O&M) |
| - Fixed O&M |
| = Earnings before interest taxes depreciation, and amortization (EBITDA) |
| - Tax Depreciation |
| - Interest Expense |
| = Earnings before taxes (EBT) |
| - Taxes |
| + Tax Credits |
| = Net Income |
| + Tax Depreciation |
| - Debt Principal Payment |
| = cashflow |

Once the cashflow has been calculated. It is possible to utilize the cost structure in it to calculate the Levelized Cost of Energy (LCOE). The LCOE formula provides a high-level approach to calculating at what price should the electricity generated be sold to recover the total cost of the investment to produce that electricity. In other words, the cost level of producing one unit of electricity for a specific renewable energy technology. The total cost includes capital costs, operation and maintenance (O&M) costs, performance, and fuel expenses. However, the basic version of this formula does not account for factors like financing, discount rates, future replacements, or degradation costs. The simplest formula for the LCOE is:

$$LCOE_{\square} = \sum_{t}^{T} \frac{\left(\frac{1}{(1+r)^t}\right) * TotalCosts_t}{\left(\frac{1}{(1+r)^t}\right) * Productio_t} \quad (14)$$

*where*

$TotalCosts_t$ = overnight capital costs, variable O&M, fixed O&M, tax payment, loan interest expense, and loan principal payments.

In summary, LCOE measures the total lifetime costs of a technology divided by its energy output. Note that this study includes financial costs such as interest during construction, principal loan repayment, debt costs (interests of loan repayment), cost of equity, and taxes. In this sense, it treats debt principal payments as an additional cost that must be subtracted from the revenue generated by the IES investment project. Consequently, the total profits from the IES are lower compared to a scenario where principal payments are not considered an extra cost.

## NIHPA Tool

Although NIHPA was initially developed for nuclear-integrated H2 production via HTSE, its existing formulas for estimating CAPEX, annual variable O&M, and annual fixed O&M have been generalized for use with SMNR, HTSE, and pulp and paper plants. The formulas for SMNR CAPEX, annual variable O&M, and annual fixed O&M are presented in Equations (15), (16), and (17), respectively.

$$CAPEX_{SMNR} = C_{OC} * 1000 * Cap_{th} * E_{th} \quad (15)$$

*where*

$CAPEX_{SMNR}$ = is the CAPEX for SMNR in the unit of U.S. dollars

$C_{OC}$ = is the overnight capital costs (OCC) in the units of $/kWe

$Cap_{th}$ = is the thermal capacity for a SMNR in the unit of MWth

$E_{th}$ = is the thermal efficiency for a SMNR converting thermal energy to electricity in the unit of %.

$$AnnVarO\&M_{SMNR} = \left(O\&M_{nonfuel} + O\&M_{fuel}\right) * Cap_{th} * E_{th} * F_{cp} * 8760 \quad (16)$$

*where*

$AnnVarO\&M_{SMNR}$ = annual variable O&M costs for SMNR in the unit of U.S. dollars

$O\&M_{nonfuel}$ = non-fuel O&M costs in the unit of $/MWh

$O\&M_{fuel}$ = nuclear fuel O&M costs in the unit of $/MWh

$F_{cp}$ = capacity factor of an NPP in the unit of %.

$$AnnFixedO\&M_{SMNR} = O\&M_{fixed} * Cap_{th} * E_{th} * F_{cp} * 8760 \quad (17)$$

*where*

$AnnFixedO\&M_{SMNR}$ = annual fixed O&M costs for SMNR in the unit of U.S. dollars

$O\&M_{fixed}$ = fixed O&M costs in the unit of $/MWh.

The formula for HTSE CAPEX, annual variable O&M, and annual fixed O&M are shown in Equations (18), (19), and (20), respectively.

$$CAPEX_{HTSE} = (C_{dir} + C_{indir}) * E_{HTSE} * 1000 + C_{land} \quad (18)$$

*where*

$CAPEX_{HTSE}$ = CAPEX for HTSE in the unit of U.S. dollars

$C_{dir}$ = DCCs including the installed stack manufacturing costs and the balance of plant costs in the units of $/kW-dc

$C_{indir}$ = ICCs including site preparation, engineering and design, process and project contingency, and upfront permitting costs in the units of $/kW-dc

$E_{HTSE}$ = electricity required for HTSE operation in the units of MW-dc

$C_{land}$ = land costs that are not depreciable in the unit of U.S. dollars.

$$AnnVarO\&M_{HTSE} = \left(C_{cw} * U_{cw} + C_{pw} * U_{pw}\right) * F_{cp} * 365 * F_p \quad (19)$$

*where*

$AnnVarO\&M_{HTSE}$ = annual variable O&M costs for HTSE in the unit of U.S. dollars

$C_{cw}$ = cooling water cost in the unit of $/gallon

$C_{pw}$ = process water cost in the unit of $/gallon

$U_{cw}$ = cooling water usage in the unit of gallon/day

$U_{pw}$ = process water usage in the unit of gallon/day

$F_p$ = performance factor of the HTSE plant considering the degradation factors.

$$AnnFixedO\&M_{HTSE} = C_{labor} + C_{GA} + C_{ins} + C_{main} + (C_{dec} - C_{sal}) * H(T - t) \quad (20)$$

*where*

$AnnFixedO\&M_{HTSE}$ = annual fixed O&M costs for HTSE in the unit of U.S. dollars

$C_{labor}$ = annual labor costs in the unit of U.S. dollars

$C_{GA}$ = annual general and administrative costs in the unit of U.S. dollars

$C_{ins}$ = annual property tax and insurance costs in the unit of U.S. dollars

$C_{main}$ = annual maintenance and repair costs in the unit of U.S. dollars

$C_{dec}$ = decomposing costs in the unit of U.S. dollars that would appear at the end of the project

$C_{sal}$ = salvage value in the unit of U.S. dollars that would appear at the end of the project

$H(T - t)$ = Heaviside step function where $H(T - t)$ is one only when $T \geq t$; otherwise, $H(T - t)$ is zero.

The formulas for the annual variable O&M and annual fixed O&M for the mill are shown in Equations (21) and (22), respectively.

$$AnnVarO\&M_{MILL} = (C_{NG} * U_{NG} * F_{cv}) * 365 \quad (21)$$

*where*

$C_{NG}$ = NG price in the unit of $/Million British Thermal Unit (MMBtu)

$U_{NG}$ = NG usage in the unit of metric-tons/day

$F_{cv}$ = conversion factor from MMBtu to equivalent metric tons.

$$AnnFixedO\&M_{MILL} = C_{labor} + C_{GA} \quad (22)$$

## Discounted Cash Flow Model

A discounted cash flow model is employed to estimate the revenue generated from the mill under different scenarios. Variable and fixed O&M costs are subtracted from total revenue to obtain earnings before interest, taxes, depreciation, and amortization (EBITDA). Depreciation and interest expenses are then deducted from EBITDA to determine earnings before taxes (EBT). After accounting for taxes and applying any available tax credits, net income is calculated. Depreciation, a non-cash expense, is added back to the net income to adjust for its impact on actual cash levels. Payments toward debt principal are subtracted to arrive at the final cash flow. To estimate the NPV of these cash flows, the annual cash flows are discounted back to their present value using an appropriate discount rate. Finally, the discounted cash flows are summed to determine the total NPV.

## Avoided Cost of Carbon

Integrating clean energy systems into an existing industrial facility reduces emissions but incurs additional costs. These extra costs for building cleaner integrated energy systems can be considered the cost of avoiding carbon emissions. This concept is mathematically described in Equation (23).

$$acc_{ref} = \frac{C_{add}}{CO_{2,avoid}} \quad (23)$$

*where*

$acc_{ref}$ = mill onsite $CO_2$ avoided costs in the units of U.S. dollars per metric ton of $CO_2$ production

$C_{add}$ = mill additional cost, which is calculated as the difference between the total cost (CAPEX + O&M costs) in scenario "i" and the total cost in the BAU Case in the units of U.S. dollars per day

$CO_{2,avoid}$ = avoided $CO_2$ that is the difference between the total $CO_2$ emissions from the mill in scenario "i" and the total $CO_2$ emissions from the mill in scenario BAU in the units of metric ton $CO_2$ production per day.

Additionally, the avoided net cost of carbon is estimated according to Equation (24).

$$acc_{ref,net} = \frac{C_{add} - [PTC + ITC]}{CO_{2,avoid}} \quad (24)$$

*where*

$acc_{ref,net}$ = mill onsite $CO_2$ net avoided costs in the units of U.S. dollars per metric ton of $CO_2$ production

PTC = amount of dollars per day received from the tax credit 45V and 45Q during the total period the credit is available

ITC = amount of dollars per day received as a percentage of the CAPEX according to the tax credit 48E.

## Cost Analysis for Individual Components

The cost contributors of each case include the CAPEX, variable O&M, and fixed O&M for SMNR, carbon capture equipment, and HTSE and the variable O&M for the pulp and paper mill. A detailed breakdown for the cost estimates of each component is described herein.

### 4.1.1 Nuclear Power Plant

This study leverages data estimated by INL's Gateway for Accelerated Innovation in Nuclear (GAIN) (Abou-Jaoude et al. 2024), which identified reference overnight capital costs (OCC) and O&M costs, as well as trends for large and small advanced nuclear reactors, focusing on cost projections for 2030–2050. GAIN developed a methodology to estimate these costs using a comprehensive and publicly available set of detailed cost estimates from the literature. These estimates were meticulously mapped, escalated, and processed to provide a robust data foundation.

To ensure a statistically neutral determination of cost ranges and reduce the impact of outliers, the data were normalized to a common baseline. Cost ranges were derived by analyzing quartiles within data groupings, resulting in a spectrum of cost estimates from different estimators rather than selecting single data points. The analysis includes both first-of-a-kind (FOAK) and nth-of-a-kind (NOAK) costs, with the resulting quartile values termed between-of-a-kind (BOAK), which refers to the next commercial offering, typically between the second and fourth unit deployed of a given type. This assumes demonstrations would occur by 2030 through DOE's Advanced Reactor Demonstration Program (ARDP) or other commercial efforts.

The TEA was conducted under three scenarios consistent with GAIN (2024): advanced, moderate, and conservative, following the National Renewable Energy Laboratory annual technology baseline National Renewable Energy Laboratory 2024 definitions. The advanced scenario represents data points with minimal cost overruns, suggesting a well-executed project with thorough application of lessons learned or substantial government investment to de-risk the technology. The moderate scenario, considered the baseline, includes data points in the middle range of estimates and anticipates some cost overruns and inefficiencies. The conservative scenario accounts for substantial cost overruns, reflecting limited learning between the initial demonstration and the BOAK estimate, with unresolved challenges from the FOAK project. The O&M costs were divided into fixed and variable categories, with variable costs influencing the bid price for market clearance, including front-end expenses like natural uranium, enrichment, and fabrication. The overall overnight capital costs, variable O&M, and fixed O&M estimates were sourced from GAIN (Abou-Jaoude et al. 2024), as detailed in Table 12. The thermal capacity of the SMNR in each case was used to estimate the total CAPEX, annual variable O&M, and annual fixed O&M. The nominal thermal efficiency of the SMNR used for all cases was 40%, and the SMNR was assumed to have a 93% capacity factor.

Table 12. SMNR cost structure. Adapted from GAIN (Abou-Jaoude et al. 2024).

| Cost contributors for SMNR | Advanced | Moderate | Conservative |
|---|---|---|---|
| BOAK OCC ($/KWe) | 3,000 | 5,500 | 8,000 |
| Non-fuel costs for variable O&M ($/MWh) | 2.2 | 2.6 | 2.8 |
| Fuel costs for variable O&M ($/MWh) | 10.0 | 11.0 | 12.1 |
| Fixed O&M costs ($/MWh) @93% capacity factor | 14.5 | 16.6 | 26.5 |
| Construction periods (months) | 60 | 82 | 125 |

### 4.1.2 Reference Mill Operations

It is assumed that the mill has been fully depreciated, and that no additional CAPEX are required to integrate the mill with HTSE and SMNR. Integration costs are excluded from the scope of the TEA because their magnitude is significantly smaller than the CAPEX of the SMNR. The cost structure of the reference mill plant is detailed in Table 13.

The reference mill plant produces 400,000 ADt pulp-based products to meet yearly demand. The revenue generated from selling these products constitutes the primary source of income for the TEA. Table 14 details the prices for each mill product used in this analysis.

Table 13. Cost structure of reference mill plant.

| Costs Contributors for mill Plant | Unit Cost | Reference |
|---|---|---|
| Waste wood Purchase | $11.04/metric-ton-of-final product | (Fishersolve International 2024) |
| Chemicals | $15.15/metric-ton-of-final product | (Fishersolve International 2024) |
| Wood Logs Softwood | $75 per 1000 board-foot | (Fishersolve International 2024) |
| Natural Gas price | $6.4/MMBtu | (U.S. Energy Information Administration 2024) |
| Annual labor costs (for 100 staff-members) | $116/FST | (Fishersolve International 2024) |
| Annual general and administrative costs ($) | 1% of Labor costs | (Wendt and Knighton 2022) |

Table 14. Sale price of finished products in 2022 dollars.

| | | | |
|---|---|---|---|
| Unbleached Pulp price | $/metric-ton | $1,487 | (Fastmarkets 2024) |
| Turpentine price | $/metric-ton | $3,380 | (Indexbox 2023) |
| Soaps (Tall Oil Fatty Acids) price | $/metric-ton | $1,650 | (Chemanalyst n.d.) |
| Electricity | $/MWh | $74.6 | (U.S. EIA n.d.) |

### 4.1.3 High-Temperature Steam Electrolysis

The CAPEX for HTSE includes DCC, ICC, depreciation, and replacement costs. The DCC for building HTSE facilities encompass the installed stacks and the balance of plant costs, both of which are dependent on the HTSE capacity. A linear regression analysis was conducted to fit the DCC data, which ranges from 10 MW-dc to 1600 MW-dc, as illustrated in Figure 15. This study assumes an NOAK design for HTSE.

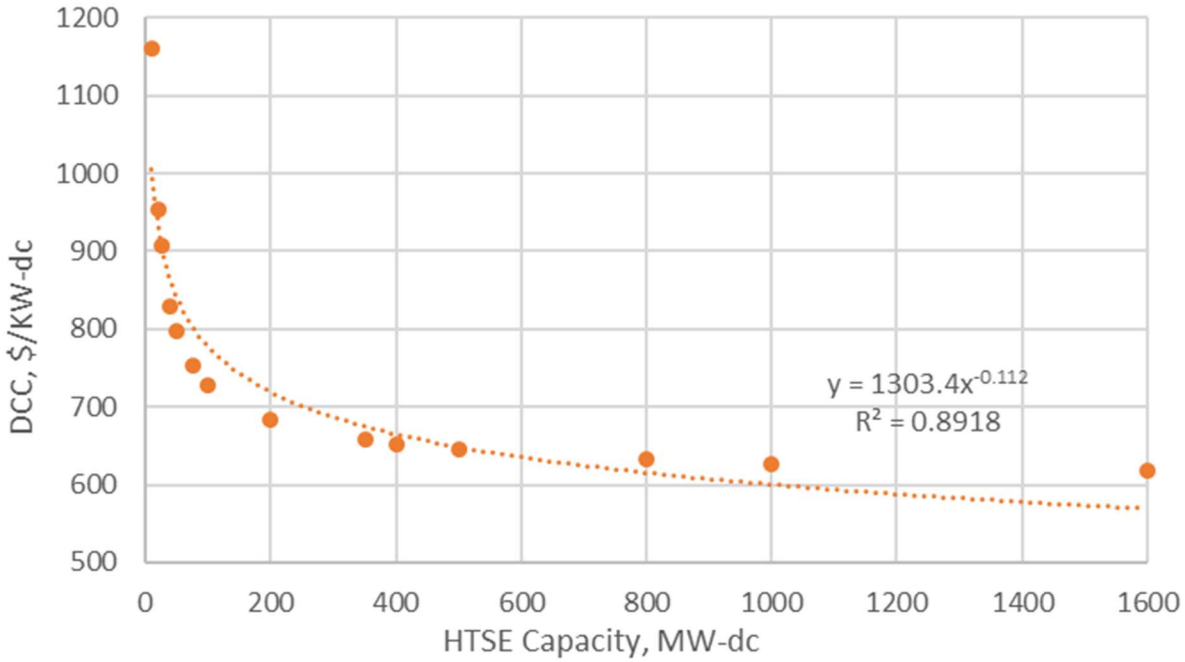


Figure 15. DCCs for an HTSE facility as a function of NOAK HTSE capacity.

In this study, the $H_2$ production capacity is defined for Scenarios 4 and 5, while no HTSE is necessary for Cases 1, 2, and 3. The HTSE costs structure is reported in Table 15, including the performance factors due to fuel cell replacements.

Table 15. HTSE cost structure. Adapted from (Wendt and Knighton 2022).

| | Case 4 | Case 5 |
|---|---|---|
| DCCs ($/kW-dc) | 264 | 214 |
| ICCs ($/kW-dc) | 665.6 | 683.8 |
| Land costs ($) | 75 million | 60 million |
| Cooling water costs ($/Gallon) | 2.79e-3 | |
| Process water costs ($/Gallon | 2.79e-5 | |
| Cooling Water Usage (gallon/day) | 31 million | 25 million |
| Process water usage (gallon/day) | 0.7 million | 0.55 million |
| Performance factor at the 1st, 6th, 11th, 16th, 21st, 26th 31st, and 36th year (%) | 100% | |
| Performance factor at the 2nd, 7th, 12th, 17th, 22nd, 27th 32nd, and 37th year (%) | 98% | |
| Performance factor at the 3rd, 8th, 13th, 18th, 23rd, 28th 33rd, and 38th year (%) | 96% | |
| Performance factor at the 4th, 9th, 14th, 19th, 24th, 29th 34th, and 39th year (%) | 94% | |
| Performance factor at the 5th, 10th, 15th, 20th, 25th, 30th 35th, and 40th year (%) | 92% | |
| Annual labor costs ($ for 10 staff-members) | $1,504,759 | $1,417,216 |
| Annual general and administrative costs ($) | $15,048 | $14,172 |

| | Case 4 | Case 5 |
|---|---|---|
| Annual property tax and insurance costs ($) | $8,963,197 | $7,244,918 |
| Annual maintenance and repair costs ($) | $7,926,522 | $6,406,978 |
| Decomposing costs ($) | $37 million | $30 million |
| Salvage value ($) | $45 million | $36 million |

### 4.1.4 Carbon Capture Systems

This analysis included two types of carbon capture systems: MEA and the Linde-Hampson process for $CO_2$ liquefaction.

The cost for MEA capture was based on an amine solvent-based $CO_2$ capture system modeled in Aspen Plus. The model was adapted to handle the different total flow amount, and the inherent $CO_2$ concentration found in the sources of the kraft process: recovery boiler, biomass boiler, natural gas boiler, and lime kiln (Sagues et al. 2020). The mass and energy balance results from the amine system modeling were integrated with a TEA to estimate the cost per metric ton of $CO_2$ captured. The cost is given as a function of the total flue gas rate (metric-tons/h) and $CO_2$ concentration (%mol). The results are presented in Appendix D. Table 38 in Appendix D summarizes the amine carbon capture costs reported in literature, which were used to validate the results of Equation 25. The economic metrics for the TEA considered a 96% plant utilization, and an internal rate of return of 10%. The cost of the equipment was estimated using the Aspen Process Economic Analyzer (APEA) and escalated using a scaling factor equation:

$$\frac{Equipment\ A}{Baseline\ cost} = \left(\frac{Equipment\ A\ capacity}{Baseline\ capacity}\right)^{n} \quad (25)$$

Where equipment A and its capacity corresponds to the value to be estimated, baseline cost and capacity are the known costs to be used for scaling the size of the equipment, and n is the capacity factor equal to 0.6 (Humbird et al. 2011). For the combined flue gases in Case 2 (total flue gas flowrate 553.2 metric-tons/h, and 14.2% $CO_2$ concentration) using the MEA carbon capture system, the cost per metric ton of $CO_2$ captured is $76.49.

In the technical work, the $CO_2$ compression system was based on the Linde-Hampson process to liquefy the $CO_2$ in a four-stage compression system. The cost of the capture system was estimated using several data sources and the APEA output from the compression model. The capital cost estimation includes capital costs for compression, duct work and piping, balance of plant, and a cooling water system. The high purity $CO_2$ capture costs presented in Table 16 are in accordance with the $CO_2$ compression system costs assessed. The estimate does not include financial assumptions such as interest on debt, as that will be applied within in the modeling tools used for the TEA. Detailed information on these financial assumptions can be found in Appendix E, CO2 Compression Cost Estimation. The resulting OCC was used in NIHPA and SET as the cost of compression.

The OCC, Fixed, O&M, and variable O&M costs used for each case are listed in Table 16. The O&M costs were assumed to be a conservative value for all cases. These are more conservative than the compression O&M costs listed in Appendix E.

Table 16. Cost of carbon capture used for each case study.

| Case | Capture type | OCC ($/metric-ton-$CO_2$ captured annually) | Fixed O&M ($/metric-ton-$CO_2$ captured annually) | Variable O&M ($/metric-ton-$CO_2$) |
|---|---|---|---|---|
| 1 | None | 0 | 0 | 0 |
| 2 | MEA | $76.49 | 2.5 | 5.5 |
| 3a | MEA | $72.43 | 2.5 | 5.5 |
| 3b | MEA | $72.43 | 2.5 | 5.5 |
| 4 | Oxy-fuel + Compression | $25 | 2.5 | 5.5 |
| 5 | Oxy-fuel + Compression | $25 | 2.5 | 5.5 |

# 5. TECHNOECONOMIC ANALYSIS RESULTS

Compared to the BAU case, the five cost and revenue drivers for the integrated mill are the size of the NPP (Tax Credit section 48E), the $CO_2$ captured (Tax Credit section 45Q), hydrogen produced (Tax Credit section 45V), natural gas purchased, and excess electricity from the SMNR capacity that can be sold to the grid. The product-related feedstock expenses and product outputs are assumed to be the same for all cases. For reference, a summary of these drivers for the five TEA cases are listed in Table 17.

Table 17. Summary of results from the nuclear integration case studies.

| Case | Description | NPP Size (MWth) | Natural Gas usage | Carbon Captured | Hydrogen Produced | Electricity Sold |
|---|---|---|---|---|---|---|
| 1 | BAU | 0 | 139 metric-tons/day | 0 | 0 | 0 |
| 2 | MEA Capture (NG) | 0 | 279 metric-tons/day | 0.91 MMT/yr | 0 | 0 |
| 3a | MEA Capture (Nuclear) | 400 | 49 metric-tons/day | 0.65 MMT/yr | 0 | 104.1 MWe |
| 3b | MEA Capture (Nuclear) | 200 | 49 metric-tons/day | 0.65 MMT/yr | 0 | 20.6 MWe |
| 4 | Oxy-Fired boilers | 1200 | 139 metric-tons/day | 0.82 MMT/yr | 0.09 MMT/yr | 46.6 MWe |
| 5 | Oxy-fired boilers and steam integration | 1000 | 49 metric-tons/day | 0.72 MMT/yr | 0.7 MMT/yr | 29.7 MWe |

These results are summarized in Table 18, Table 19, and

Table 20, respectively. The results are further discussed in the following sections. More scenarios reach an NPV higher than the BAU case when the capital costs of nuclear reactors go down. For instance, when capital costs are around $8,000/kWe, Scenario 2 is more profitable than the BAU case. When capital costs are around $5,500/kWe, Scenarios 2, 3a, and 3b are more profitable than the BAU. Finally, when the capital costs fall to $3,000/kWe, all scenarios are more profitable than the BAU case.

These results are only relevant for this specific mill and the specific assumptions in the TEA. These results should not be applied generally to pulp and paper mills in the U.S. However, these results help us to understand the economic drivers behind the decarbonization pathways that utilize nuclear integration.

Table 18. Summary of key data outputs for high CAPEX ($8,000/kWe).

| 40 years Project Lifetime | | | | | | | |
|---|---|---|---|---|---|---|---|
| CAPEX HTGR = $8,000/kWe | | Case 1 | Case 2 | Case 3a | Case 3b | Case 4 | Case 5 |
| IRA Benefits | Tax Credits | — | TC 45Q | ITC 48E + TC 45Q | ITC 48E + TC 45Q | ITC 48E + PTC 45V + TC 45Q | ITC 48E + PTC 45V + TC 45Q |
| Finance | NPV Cash Flow | $2763M | $2991M | $2603M | $2709M | $776M | $1340M |
| | Delta NPV of Total Costs (Relative to BAU) | — | $229M | -$159M | -$54M | -$1987M | -$1422M |
| | Avoided Cost of Carbon ($/metric-ton-CO2) | — | $9.3 | $30.6 | $15.6 | $111.7 | $90.5 |
| | Avoided Net Cost of Carbon ($/metric-ton-CO2) w/ tax credits | — | -$7.2 | $7.5 | -$2.9 | $21.6 | $13.3 |
| | IRR | — | 962.0% | 73.0% | 123.0% | 22.0% | 30.0% |

Table 19. Summary of key data outputs for medium CAPEX ($5,500/kWe).

| 40 years Project Lifetime | | | | | | | |
|---|---|---|---|---|---|---|---|
| CAPEX HTGR = $5,500/kWe | | Case 1 | Case 2 | Case 3a | Case 3b | Case 4 | Case 5 |
| IRA Benefits | Tax Credits | — | TC 45Q | ITC 48E + TC 45Q | ITC 48E + TC 45Q | ITC 48E + PTC 45V + TC 45Q | ITC 48E + PTC 45V + TC 45Q |
| Finance | NPV Cash Flow | $2763M | $2991M | $2900M | $2859M | $2309M | $2371M |
| | Delta NPV of Total Costs (Relative to BAU) | — | $229M | $138M | $97M | -$454M | -$392M |
| | Avoided Cost of Carbon ($/metric-ton-CO2) | — | $9.3 | $21.8 | $11.2 | $87.6 | $70.4 |
| | Avoided Net Cost of Carbon ($/metric-ton-CO2) w/ tax credits | — | -$7.2 | $2.4 | -$5.5 | $7.6 | $1.6 |
| | IRR | — | 962.0% | 103.0% | 168.0% | 43.0% | 49.0% |

Table 20. Summary of key data outputs for low CAPEX ($3,000/kWe).

| 40 years Project Lifetime | | | | | | | |
|---|---|---|---|---|---|---|---|
| CAPEX HTGR = $3,000/kWe | | Case 1 | Case 2 | Case 3a | Case 3b | Case 4 | Case 5 |
| IRA Benefits | Tax Credits | — | TC 45Q | ITC 48E + TC 45Q | ITC 48E + TC 45Q | ITC 48E + PTC 45V + TC 45Q | ITC 48E + PTC 45V + TC 45Q |
| Finance | NPV Cash Flow | $2763M | $2991M | $3141M | $3006M | $2911M | $2927M |
| | Delta NPV of Total Costs (Relative to BAU) | — | $229M | $378M | $243M | $149M | $164M |
| | Avoided Cost of Carbon ($/metric-ton-CO2) | — | $9.3 | $13.5 | $6.3 | $64.8 | $51.9 |
| | Avoided Net Cost of Carbon ($/metric-ton-CO2) w/ credits | — | -$7.2 | -$2.3 | -$8.6 | -$5.2 | -$8.7 |
| | IRR | — | 960.0% | 170.0% | 326.0% | 68.0% | 76.0% |

## NPV Comparison

Using NIHPA and SET tools, the five previously described scenarios are modeled to obtain the present value of cash flows for the five potential mill decarbonization pathways. Cash flow growth is calculated using Equation (26).

$$Cash\ Flow\ Growth = \frac{NPV_{case_i} - NPV_{BAU}}{NP_{BAU}} \quad (26)$$

The results for each scenario, considering three different CAPEX levels with and without tax credits, are summarized in Figure 16. The findings indicate that CAPEX is the primary cost driver affecting the difference in the net present value of profits between scenarios. The selected tax credits (ITC-48E, PTC-45V, and PTC-45Q) serve as the main revenue driver in each scenario.

With tax credits, Case 2 always has a higher NPV of cashflows than Case 1. This confirms the important assumption of this study that biogenic and non-biogenic $CO_2$ emissions be treated and captured equally. This result suggests that even without nuclear integration, implementing carbon capture at existing kraft pulp mills by 2030 may be a profitable business decision. These results should be confirmed on an individual basis for each mill.

The highest NPV of cashflows scenario evaluated was Case 3a, with tax credits ITC-48E and PTC-45Q and low capital costs. Case 3a, which has the same carbon capture system as Case 2 but is powered by nuclear instead of natural gas, has a higher NPV of cashflows than Case 1 and 2 with tax credits and a low capital cost. However, as capital costs rise, the NPV of cashflows for the capture system powered by nuclear in Case 3a is lower than that for natural gas (Case 2). This suggests that a carbon capture system powered by natural gas may be equally cost-effective or more cost-effective than one powered by nuclear. However, these results would have to be confirmed by comparing Case 2 with several other integration scenarios.

Importantly, the tax credits reduce the net investment costs and make all the nuclear integration scenarios (Cases 3, 4, and 5) more cost-competitive than the BAU when the capital costs are low ($3,000 per kilowatt electrical [KWe]). With high capital costs and without tax credits, there are no scenarios that have a higher NPV than the BAU.

Cases 3a and 3b investigate some of the drivers behind this competitiveness. In Case 3a a 400 MWth reactor is used, and in Case 3b a 200 MWth reactor is used. The tradeoff is that the 200 MWth has less excess electricity available to sell to the grid (about 80% less than Case 3a). When captial costs are only $3,000 per KWe, the 400 MWth scenario has a higher NPV of cashflows. As capital costs rise, the 200 MWth scenario has a higher NPV. The only difference between these two cases is the reactor capital cost as the revenue from exported electricity. This suggests that in addition to the capital cost, the electricity revenue is also a major cost driver. In the low capital cost scenario, the 400 MWth case has a higher NPV of cashflows with and without tax credits, meaning that the additional electricity sold is making up for the additional investment. In the high capital cost scenario, the 200 MWth case is more competitive because it requires less initial capital investment. This result, however, is specific to the high electricity prices in the region, and may change in a different location. This result is important because (1) it suggests that investing in more capacity spread across several markets and commodities can help recoup initial investments, and (2) it strengthens the argument for utilities to own and operate reactors for the grid and contract a portion of their capacity to industrial customers.

Between the two oxy-fuel combustion configurations, Case 5 always has a higher NPV than Case 4. Case 5 is likely more profitable because similar tax credits can be harvested with a smaller capital investment in the SMNR (1000 MW for Case 5, compared to 1200 MW for Case 4). Case 4, however, has a larger demand for oxygen and therefore produces more hydrogen as a byprodut. This indicates that for this configuration, the capital cost of the reactor is driving the NPV more than the hydrogen production credit. However, Case 5 is extremely sensitive to the capital cost of the SMNR and the availability of tax credits. In all scenarios except for the low capital costs with tax credits, Cases 4 and 5 have the lowest NPV of all cases, and in the highest capital cost scenario generate a negative NPV of cashflows, meaning that the total costs of the project were greater than the revenues.

With tax credits, Case 2 always has a higher NPV of cashflows than Case 1. This confirms the important assumption of this study that biogenic and non-biogenic $CO_2$ emissions be treated and captured equally. This result suggests that even without nuclear integration, implementing carbon capture at existing kraft pulp mills by 2030 may be a profitable business decision. These results should be confirmed on an individual basis for each mill.

As described in Section 0, the integration method chosen is not the most thermally efficient, and different integration scenarios could change the competitiveness between nuclear-powered carbon capture and natural gas-powered carbon capture. Additionally, if the multi-fuel boilers were re-included into the thermal systems, more total $CO_2$ would be captured, increasing the share of positive NPV of cashflows from harvested tax credit 45Q. In future work, these cases will be explored thoroughly.

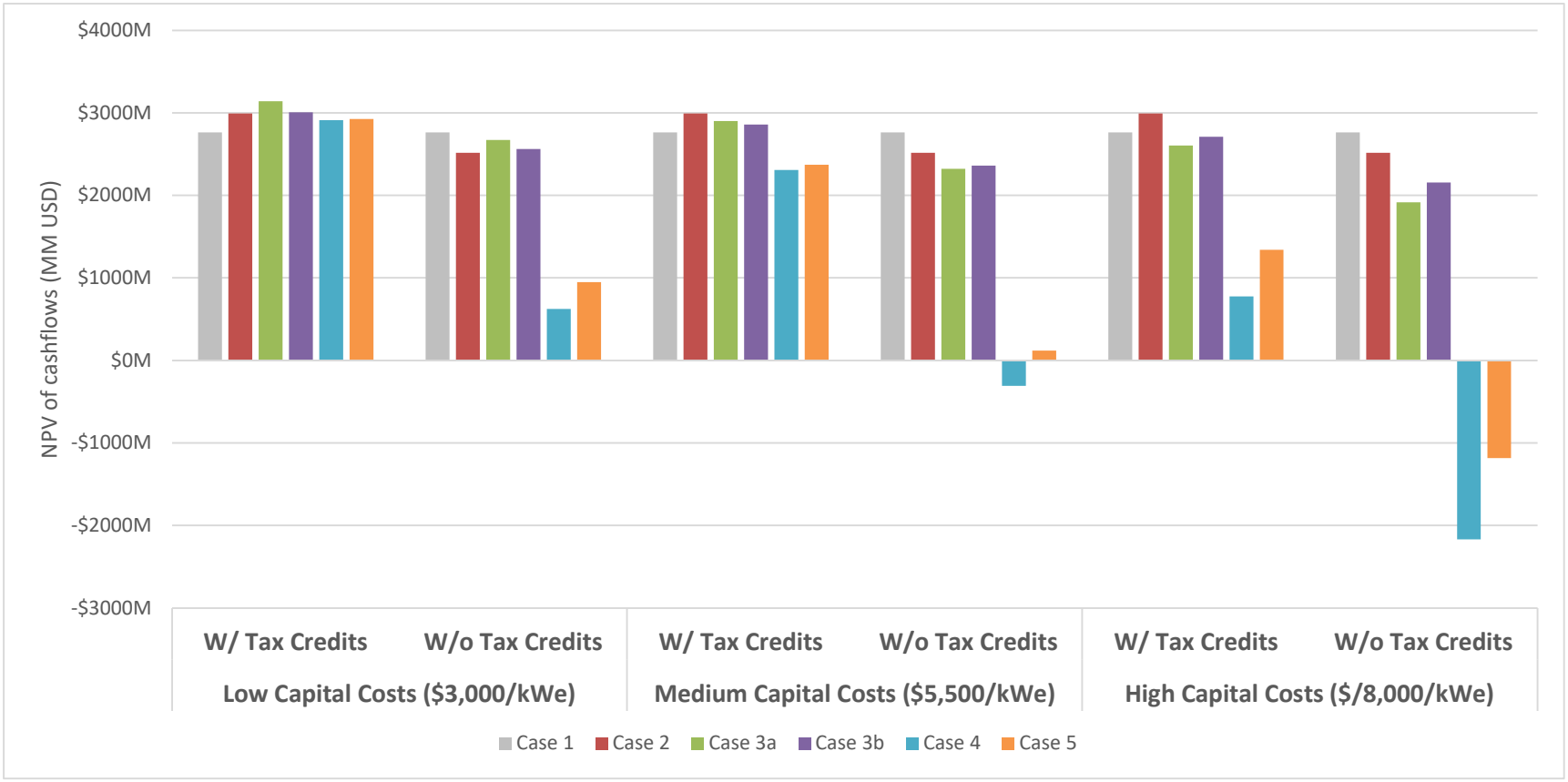


Figure 16. NPV cumulative cash flow for all TEA scenarios (2022 USD).

## Avoided Cost of Carbon

The calculations are based on $CO_2$ emissions reductions at various scopes, along with the cost of power, heat, and hydrogen for each scenario. Scope 1 emissions are estimated annually throughout all ACC calculations, assuming a 40-year project life. A sensitivity analysis for the cost of natural gas was also performed for a 40-year project life, as shown in Appendix F, Sensitivity Analysis. Using Equations (27) and Equation (28), the ACC and ANCC for cases without tax credits and with tax credits are presented in Figure 17 and Figure 18, respectively.

ACC and ANCC illustrate the annual $CO_2$ avoidance cost as a function of the total onsite $CO_2$ avoidance for each scenario, both excluding and including the IRA Investment Tax Credits (ITCs) and Production Tax Credits (PTCs). The ACC was analyzed for three SMNR costs: \$8,000/kWe, \$5,500/kWe, and \$3,000/kWe. The total onsite $CO_2$ avoidance is expressed in MMT of $CO_2$ per year, based on the 1.59 MMT/year of $CO_2$ emissions associated with the referenced 400,000 metric-ton/year mill.

Figure 17 and Figure 18 also show the decarbonization cost as a function of the amount of $CO_2$ emissions avoided, for scenarios excluding and including the IRA ITCs and PTCs. In these figures, the ACC is presented on a normalized basis in terms of \$/metric-ton-$CO_2$. This normalization allows for comparison of each case's ACC while maintaining perspective on which scenarios provide the highest level of mill decarbonization.

Figure 17 is a measure ratio of the total capital investment to the $CO_2$ avoided.

$$acc_{ref} = \frac{C_{add}}{CO_{2,avoid}} \tag{27}$$

Figure 18 is the net cost when tax incentives are included. This does not include any additional revenue streams, such as electricity sold.

$$acc_{ref,net} = \frac{C_{add} - [PTC + ITC]}{CO_{2,avoid}} \tag{28}$$

When the IRA ITCs and PTCs are excluded, Figure 17 demonstrates that higher levels of decarbonization generally correlate with higher annual costs. The total carbon avoided increases along the X-axis of the chart, but the ACC increases as well. Reducing the reactor costs also reduces the ACC., but no scenario has a negative ACC when no tax credits are applied.

Figure 18 shows the ANCC for each case with tax credits included. Cases 4 and 5 have the most impact, with 100% reduction in $CO_2$ emissions. However, the ANCC for Case 4 is the highest compared to other cases when the reactor costs are \$8,000/kWe. At \$5,500/kWe, Case 4 has the highest ANCC, but only slightly less than the ANCC of Case 3a. At the lowest reactor costs, both case 4 and 5 have a negative ANCC, meaning that the tax credits have covered the entire cost of decarbonization and provided a revenue stream. At \$3,000/kWe, Case 5 provides greater decarbonization (100%) compared to Case 3b (90%) for a similar, negative ANCC. Case 3a and 3b have the same decarbonization potential at different costs.

Despite Case 3a having a higher NPV than 3b, 3a has a higher ANCC. In other words, the cost of abating one unit of CO2 is higher for Case 3a, although value of total cash flows in 3a are greater. This is because the ANCC does not include the revenue of electricity that benefit Case 3a. Case 3b always has a negative ACC regardless of reactor costs, but Case 2, using natural gas, has a more negative ACC than Case 3b at a reactor cost of \$5,500/kWe and above. This result shows that the value of carbon capture credits is greater than the cost of carbon capture using MEA, with or without nuclear integration, and can provide an additional revenue stream to the mills.

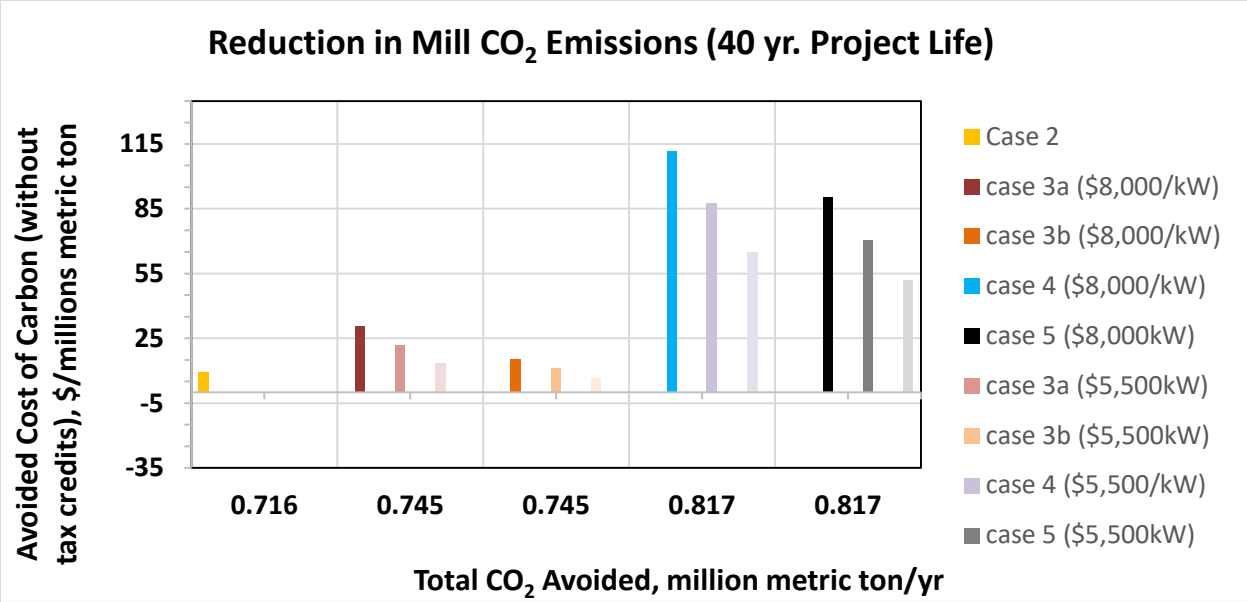


Figure 17. **ACC** results for each case. HTGR-type SMNR pulp and paper mill plant decarbonization total onsite CO2 avoidance and annual cost by case without IRA ITCs and PTCs.

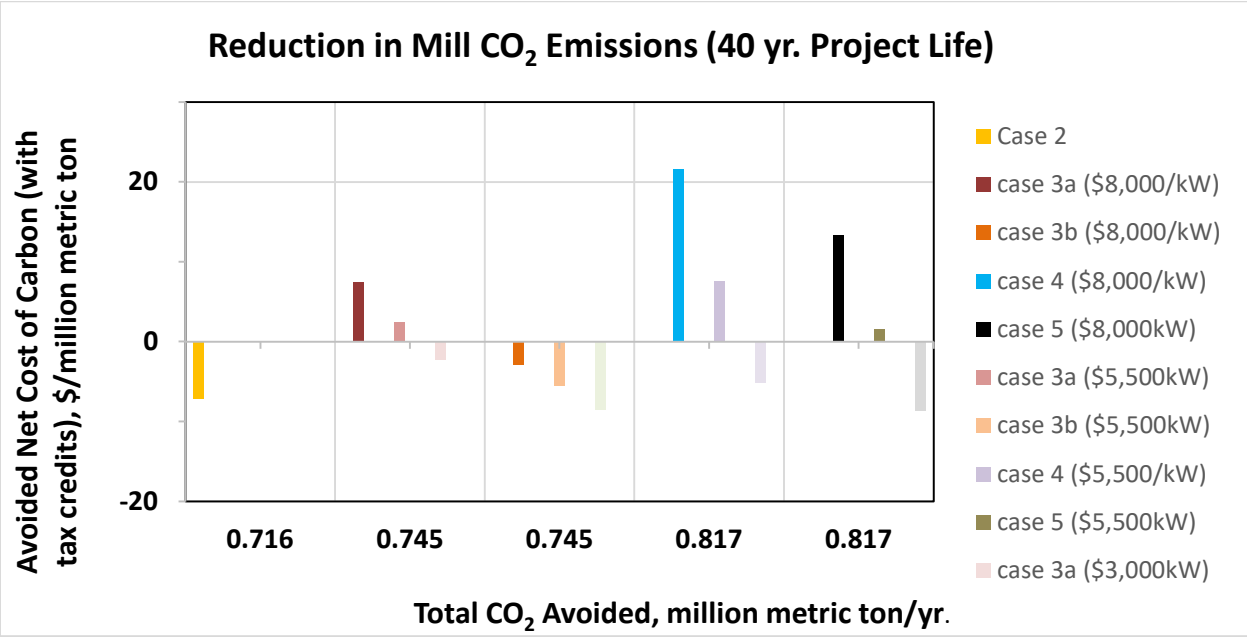


Figure 18. **ANCC** results for each case. HTGR-type SMNR pulp and paper mill plant decarbonization total onsite CO2 avoidance and annual cost by case with IRA ITCs and PTCs.

# 6. FUTURE DECARBONIZATION PATHWAYS

### 6.1.1 Decarbonization Through $CO_2$ Utilization

The IRA 45Q tax credit provides up to $85 per metric ton of $CO_2$ sequestered, compared to $60 for each metric ton of $CO_2$ diverted to a qualified use. Naturally, this incentivizes industrial point sources to sequester their $CO_2$. Also, pulp mills are uninterested in owning and operating tertiary processes. This conclusion is based on feedback from pulp and paper industry leaders at "The Use of Nuclear Energy in the Pulp and Paper Industry" workshop hosted by the Electric Power Research Institute (EPRI), Massachusetts Institute of Technology (MIT), and North Carolina State University in 2023 (Forsberg 2023). However, the availability of geological stores for $CO_2$ is limited by both location and space. Transportation costs for $CO_2$ may be prohibitive, if available at all. Therefore, it is important to assess the life cycle value of $CO_2$ utilization versus storage in each location, rather than relying on the tax credit value.

One possible $CO_2$ product that could be collocated with pulp and paper mills is methanol synthesis. Methanol is both a fuel and a potential building block for other fuels and chemical products. Methanol capacity in the U.S. has increased in the last decade and is "among the most natural gas-intensive industrial end users," requiring natural gas both as a feedstock and for process heat (U.S. Energy Information Administration 2019). Now, demand for green methanol is increasing primarily as renewable marine transportation fuel (S&P Global 2023). In 2023, OCI Global announced increasing their capacity of green methanol to approximately 400,000 metric tons per year, and has projected an "incremental demand of more than 6 million metric tons by 2028, due to the adoption of green methanol as a shipping fuel, based on the 225 dual-fueled methanol vessels now on order" (OCI Global 2023) Green methanol can be used to decarbonize a variety of sectors, whether it is used as a fuel or as a chemical feedstock to processes.

$CO_2$ can be converted to methanol through two mid-TRL technologies: co-electrolysis and the reverse water gas shift (RWGS) reaction. A suggested coupling between a pulp mill, NPP, and methanol synthesis using co-electrolysis is shown in Figure 19. In co-electrolysis, water and $CO_2$ are electrolyzed together to produce two product streams: (1) a syngas stream containing hydrogen and carbon monoxide and (2) a mixture of O2 and $CO_2$. The oxygen and $CO_2$ stream could be sent back to the mill for oxy-fuel combustion, while the syngas can be converted to methanol through the standard synthesis process. The DOE has recently awarded funding for a 50 kW demonstration plant for co-electrolysis coupled with an NPP (United States Department of Energy 2023).

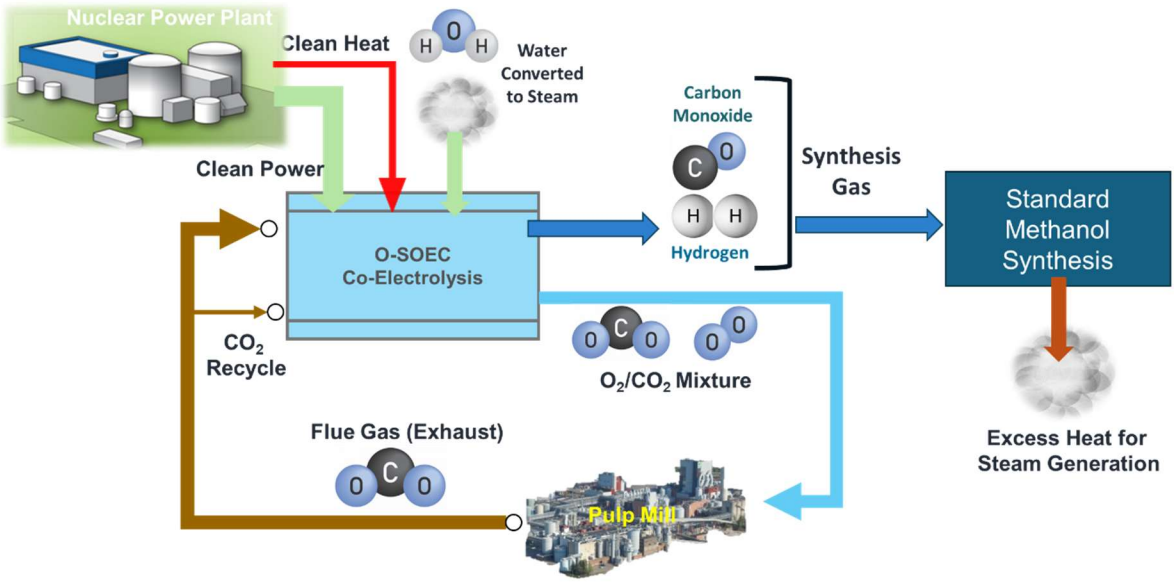


Figure 19. Pathway for decarbonizing a pulp mill through co-electrolysis and conventional methanol synhesis (Boardman 2023).

A second pathway for methanol is through the RWGS reaction, as shown in Figure 20. In this case, co-electrolysis or electrolysis would provide a hydrogen stream to a methanol synthesis reactor. The captured $CO_2$ flue gas from the oxy-fired process would be combined with hydrogen in the RWGS reactor to be selectively converted to CO and water. The resulting syngas mixture is then synthesized to methanol. In both pathways, the standard methanol synthesis process is highly exothermal, and could be used to generate additional steam for the mill.

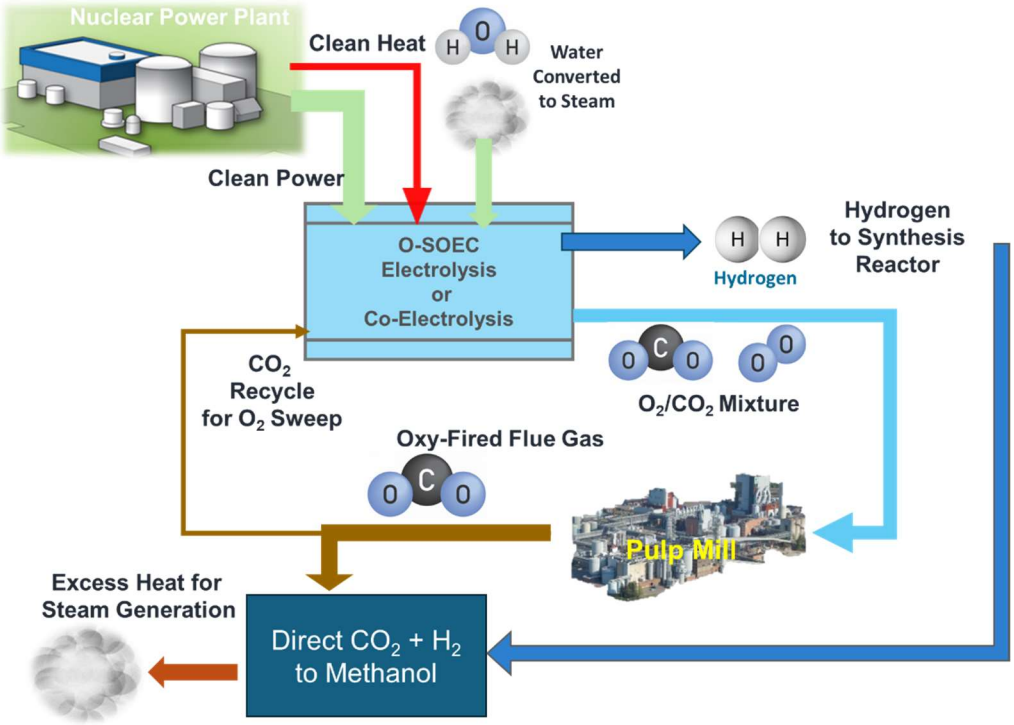


Figure 20. Pathway for decarbonizing a pulp mill through co-electrolysis and a direct methanol synthesis process (Boardman 2023).

### 6.1.2 Decarbonization Through Biomass Upgrading

With nuclear power providing clean steam to the pulp mill, its conventional biomass fuels could be upgraded to liquid fuels, which could replace combustion heat needs in the lime kiln or displace fossil fuel use in other sectors. Biomass can be upgraded to fuels through several pathways, including:

- Pyrolysis: Carbonaceous materials are heated and broken down without oxygen. The results are solids (char), tar, oil, and gases. This is the step prior to gasification, and on its own typically produces a higher percentage of solid and liquid products.
- Gasification: Proceeding after pyrolysis, gasification heats the char, tar, and oil products to high temperatures. This is a partial oxidation process resulting in methane, carbon dioxide, carbon monoxide, and hydrogen gases. This syngas product can be used as a fuel on its own or converted to liquid fuels with further treatment.
- Hydrotreating: Hydrotreating is used to upgrade oil products by removing oxygen and increasing the hydrogen content of the fuel. This step is usually done after treating the biomass with gasification or pyrolysis.

Other researchers have already investigated the possible fuel pathways for kraft pulp mills, but converting the biomass to usable fuel products requires energy for treatment. Mäki et al. (2021) studied the retrofit opportunities to produce fuel products at pulp mills and identified the TRL of each fuel pathway. The results are shown in Table 21. The demonstration projects cited reported $CO_2$ emissions savings due to replacing oil and natural gas consumption with the renewable fuels. As of 2021, these pathways have a high TRL—most potential retrofit pathways had a TRL of 8 or 9.

Table 21. Retrofit opportunities for biofuels production in pulp and paper mills. (adapted from Mäki et al. 2021).

| Retrofit technology | TRL |
|---|---|
| Kraft Mills | |
| Raw methanol purification | 8 |
| Black liquor gasification to DME/biomethanol/FT | 7 |
| Kraft lignin extraction from black liquor | 9 |
| Renewable diesel production from tall oil | 9 |
| Hydrothermal Liquefaction (HTL) of black liquor and lignin | 6/7 |
| All Pulp Mills | |
| Bark Gasification | 9 |
| All Pulp and Paper Mills | |
| Hydrothermal carbonization (HTC) of sludge | 7 |
| Anaerobic fermentation of sludge | 8/9 |

Jafri et al. (2020) studied the energy consumption, greenhouse gas (GHG) footprint, and cost of two pathways for biofuels production at three different mills. In the first pathway, lignin was separated from black liquor and sent to a refinery to be upgraded to diesel through hydrocracking. The hydrogen came from either steam methane reforming or polymer electrolyte membrane (PEM) electrolysis. Lignin separation from black liquor occurs through pH changes, where $CO_2$ can be utilized for this purpose. In the second pathway, black liquor was gasified and sent to a refinery to be converted using the methanol to gasoline pathway. In case 2b, the water gas shift reactor was eliminated and instead, hydrogen from PEM electrolysis of water was added to the gases. In Case 2c, the black liquor was mixed with pyrolysis oil before gasification.

The results showed that while biofuels production increased energy demand at the mill, energy efficiency of the mill systems increased when the value of the refined products was considered. Jafri notes the reason for this is that "relatively inefficient electricity generation from BL is substituted with more efficient biofuels production." In terms of GHG footprint, a significant reduction was estimated, especially when hydrogen is obtained through electrolysis rather than methane reforming. In this context, hydrogen produced via electrolysis powered by nuclear energy serves as a promising alternative for reducing the carbon footprint. This result reinforces the need for decarbonization efforts in the pulp and paper industry by moving towards more efficient fuels.

### 6.1.3 Decarbonization Through Lignin Extraction

The economic significance of lignin lies in its role in papermaking, where it is removed from lignocellulose during processes such as the kraft or sulfite process at pulp mills. According to the FAO Pulp and Paperboard Capacity Survey, the U.S. had a capacity of 48,661 million metric tons in 2023 (Food and Agricultural Organization of the United Nations 2023). Also, the survey shows that 87% of lignin is produced by chemical pulping, which involves thermal chemical digestion of woody feedstock. In this context, it is important to mention that the lignin is mainly burned on-site to recover the process chemicals and obtain energy (Cline and Smith 2017). Each metric ton of pulp manufactured through the kraft pulping method yields approximately 10 metric tons of weak black liquor or around 1.36 metric tons (1.5 short tons) of black liquor dry solids, necessitating processing via the chemical recovery procedure. Each year, 181 million metric tons (200 million short tons) of black liquor dry solids are burned to produce high-pressure steam (Larson, Consonni, and Katofsky 2003). Given this, black liquor could be considered the fifth most important fuel in the world, next to coal, oil, natural gas, and gasoline. However, because the availability of the liquor depends on technical factors of the production process, it's not possible for a mill to achieve a perfect balance between the supply of black liquor and its demand of fuel requirements (Tran and Vakkilainnen 2012).

Despite the large quantities of technical lignin available from the dominant kraft process and the recent research into lignin material use that could significantly impact the whole decarbonization of the pulp and paper industry and their supply chain (Tardy et al. 2023; Wenger and Stern 2019), lignin has not been established and expanded as much as the lignosulphonates. Lignin is still in the developmental stage, with few commercial production facilities and limited larger-scale applications currently available (Dessbesell et al. 2020). For instance, available evidence suggests that there is enough biomass to serve as a viable alternative to fossil fuels for transportation and chemical feedstocks if substantial external inputs of hydrogen and heat, particularly in large-scale refineries, are included (Forsberg et al. 2021, Joelsson and Gustavsson 2012, Larson et al. 2007).

Potential product applications and development have gained traction in recent years, despite variations in the lignin refining complex structure and extraction methods employed. The complicated lignin structure results in diverse, but inefficient, utilization methods. The achievable utilization methods are low value. For example, lignin could be utilized as a fertilizer modifier, a pesticide release agent, a feed binding agent, a liquid film, or a soil ameliorant, as well as for applications in high polymer materials, lignin-based polymer blends, carbon materials, and carbon fiber. (Chen 2015) A summary of potential market applications for kraft lignin is shown in Table 22.

Table 22. Potential applications for kraft lignin.

| Marketed Commodity | Potential kraft lignin applications |
|---|---|
| Input as fuel | The precipitated lignin is mostly used as a solid fuel, for example, in the lime kiln of the pulp mill, where it can replace fossil fuels. |
| Material Applications | 1. Thermoplastics<br>2. Thermosets<br>3. Fillers<br>4. Composites<br>5. Blends |
| Material integration potential | Replacing fossil-based chemicals<br>6. Polymers<br>7. Derivatives |
| Biomedical uses | 1. Cosmetic and topical formulations<br>2. Hydrogels<br>3. 3D printed<br>4. Excipient to improve the bioavailability<br>5. Films for biomedical applications |

Hermansson, Janssen, and Svanström (2020), highlighting the importance of understanding market dynamics, analyzes the potential environmental benefits of utilizing lignin as a renewable substitute in various industrial processes, such as carbon fiber production, tert-butyl catechol's (TBC) production, and medium density fiberboards (MDF boards) manufacturing. The study estimates the climate impact of lignin in these substitution scenarios, considering different allocation methods and potential $CO_2$ emissions savings. The study's results show that the choice of allocation method significantly influences the climate impact of lignin. A summary of the results is provided below. Table 23 shows the $CO_2$ emissions reductions, the product substitute, and the product replaced.

Table 23. Alternative uses for products from pulp and paper mills. Adapted from (Hermansson, Janssen, and Svanström 2020).

| | Replaced product | Avoided impacts per kg of replaced product (kg $CO_2$/kg or per MWh replaced product) | Reference |
|---|---|---|---|
| Pulp (kg): Alternative 1 | Cotton | 2.9 | Ecoinvent 3.3 (Wernet et al. 2016) |
| Pulp (kg): Alternative 2 | Reading a magazine on a tablet | 0.35 | (Ahmadi Achachlouei, Moberg, and Hochschorner 2015; Achachlouei and Moberg 2015) |
| Lignin (kg): Used as a material product | Polyacrylonitrile (PAN) | 0.56 | (ELCD 2018) |
| Lignin (kg): Used as a fuel precursor | Crude petroleum | 0.24 | Ecoinvent 3.3 (Wernet et al. 2016) |
| Soap leaving the kraft pulp mill (kg) | Crude petroleum | 0.24 | Ecoinvent 3.3 (Wernet et al. 2016) |
| Heat output of the mill (MWh) | District heating | 58 | (Werner 2017) |

Moretti et al. (2020) analyze the environmental impact of utilizing lignin from local biorefineries as a sustainable alternative in asphalt production in the Netherlands. The results show that:

- Top-layer asphalt, when using biorefinery lignin, showed a climate change impact reduction of 35%-70% compared to conventional asphalt.
- Base-layer asphalts: for base-layer asphalts, a climate change impact reduction of 25%-50% was calculated when compared to conventional asphalts.
- Lignin-based polypropylene demonstrated climate change benefits like other lignin-based products, indicating a substantial reduction in environmental impact.
- Lignin-based adipic acid also showed significant climate change mitigation potential, aligning with the positive environmental performance of lignin-based products.
- Lignin-based transportation fuels exhibited climate change benefits, contributing to the overall reduction of greenhouse gas emissions.
- Lignin-based phenol showcased climate change mitigation potential, emphasizing the environmental advantages of utilizing lignin in place of conventional materials.
- These percentages reflect the positive impact of incorporating lignin-based alternatives in various products, highlighting the potential for significant reductions in climate change impacts compared to their conventional counterparts.

Recent research on the economic aspects of lignin examines its potential applications and economic implications. Studies have explored various application areas, including lignin-derived materials, energy storage, and renewable chemicals, with life cycle assessments suggesting environmental benefits. TEAs have highlighted the sensitivity of lignin feedstock costs and achievable product prices. An overview of some recent papers is presented in Table 24.

Table 24. Literature review of TEAs for lignin feedstock conversion. Adapted from Wenger et al. (2020)

| Raw material/input | Product | Applications | Substituted product | Country | Reference |
|---|---|---|---|---|---|
| Kraft lignin, lignosulfonate | Lignin microparticles and nanoparticles (LMNPs) | Several; e.g., emulsion stabilizers, UV protection | Particles (synthetic or mineral) | U.S. | (Abbati de Assis et al. 2018) |
| LignoBoost Lignin | Colloidal lignin particles (CLP dry powder) | Several; e.g., phenol--formaldehyde (PF) resins, foams | PE, PP, PET, phenol | (probably Finland) | (Bangalore Ashok et al. 2018) |
| Wood chips | Organosolv-like lignin | (Not indicated) | (Not indicated) | (probably U.S.) | (Chrisandina et al. 2019) |
| Softwood kraft lignin + LignoForce | DKL (powder) and Oxy-DKL (viscous liquid) | Polyurethane foams and phenolic resins | Phenols and polyols | Canada | (Dessbesell et al. 2017) |
| Kraft lignin | Depolymerized kraft lignin | PF resins in engineered wood products (e.g., plywood) | Phenols and polyols | Canada | (Dessbesell et al. 2018) |
| Softwood kraft lignin + LignoForce | Pyrolysis dry oil | (Phenolic) chemicals, e.g., for resins | Petro-chemical phenolics | Canada | (Farag and Chaouki 2015) |
| Indulin AT kraft lignin, Protobind 1000 soda lignin | Mixed oxygenated aromatic monomers (MOAMON), light organics, heavy organics, char | Bio-based chemicals | Petro-chemical aromatics | Netherlands | (Vural Gursel et al. 2019) |
| Olive tree pruning | Catechol | (Not indicated) | (Not indicated) | Spain | (Mabrouk et al. 2018) |
| Oil palm empty fruit bunches (OPEFB) | Ethanol, xylitol and lignin | (Not indicated) | (Not indicated) | Brazil | (Coral Medina et al. 2018) |
| Beech wood | Polymer-grade ethylene (main product), Organosolv lignin, methane, hydrolysis lignin | Chemicals (polymer-grade ethylene, Organosolv lignin), fuels (methane, hydrolysis lignin) | Petro-chemicals | Germany | (Nitzsche, Budzinski, and Grongroft 2016) |

While technical perspectives dominate the literature, there is a smaller body of economic statements focusing on lignin underutilization, market limitations, resource abundance, and utilization barriers (Hall et al. 2018. However, there is a need for greater consideration of external factors beyond production processes to fully understand lignin's economic dynamics (Wenger, Haas, and Stern 2020).

# 7. CONCLUSION

The technoeconomic assessment and gap analysis for advanced nuclear reactor integration into a 400,000 ADt/yr reference kraft pulp mill considered in this report reveals some potential for profitably decarbonizing production by leveraging energy-efficient processes such as HTSE and CHP. When capital costs are low ($3,000/KWe) and IRA tax credits are in place, coupling an NPP for decarbonization can slightly increase the NPV of the baseline refinery while eliminating up to 100% of the $CO_2$ emissions from the mill. In some scenarios, the ACC is pushed negative, meaning that decarbonization is creating an additional revenue stream for the mill. These results, however, are specific to this reference mill configuration and market location. Of the two decarbonization pathways investigated—MEA carbon capture and oxy-fuel combustion—MEA carbon capture was the most promising, although the oxy-fuel combustion scenarios can eliminate virtually 100% of carbon emissions and harvest the ITC hydrogen production tax credit.

The inclusion of tax credits is vital to making carbon capture and nuclear integration profitable for the pulp mill. Without tax credits, no scenario studied had a higher NPV than the baseline scenario. The ACC describes how the tax credits can cover the cost of decarbonization entirely and become a revenue stream for the mill. When the nuclear capital cost was $3,000/kWe, all scenarios have a negative ACC, meaning that the value of the tax credits was greater than the decarbonization cost. In case 3b, the ACC was negative at any reactor capital cost up to $8,000 kWe.

Case 2 and 3 compared the baseline scenario to MEA carbon capture fueled by natural gas (case 2) or nuclear (case 3). The Case 2 NPV was always above the baseline with tax credits included and was the highest NPV case when the nuclear capital cost was $5,500/KWe or higher. Additionally, the ACC for Case 2 was negative. Carbon capture through conventional methods, powered by natural gas, is likely going to be a cost-effective solution for pulp mills for as long as the tax credits are in place. Because the PTC does not distinguish between the source of the $CO_2$, capturing biogenic $CO_2$ can provide a new revenue stream for pulp mills and potentially drive their life cycle carbon accounting into the net-negative. When nuclear capital costs are sufficiently low, the NPV of Case 3a is the highest of all cases. Using nuclear to power the carbon caputre system provides additional tax credits, and may be more advantageous depending on the price of nuclear power and natural gas.

Case 3a and 3b compared the effect of reactor size on the overall NPV. In Case 3b, only a 200 MWth reactor module was used and there was some excess electricity to sell. In Case 3b, a 400 MWth reactor was used for the same thermal demands, and three times the electricity was available to sell. Case 3a has a higher ACC than Case 3a, but a higher NPV. This is due to the revenue of electricity sales in Case 3a. Depending on the cost of electricity in a region, it may be advantageous to oversize the reactor in order to sell excess electricity generation. Pulp and paper mills, in general, will likely only require a small portion of a reactor to meet their low-pressure steam demand needs. This result is important because (1) it suggests that investing in more capacity spread across several markets and commodities can help recoup initial investments and (2) it strengthens the argument for utilities to own and operate reactors for the grid and contract a portion of their capacity to industrial customers.

In the two oxy-fuel combustion cases, Case 4 and Case 5, oxygen was generated through HTSE to produce a $CO_2$ rich stream from the boilers. These cases were able to capture the hydrogen credit as well as the carbon capture credit. In the scenario studied, the hydrogen tax credit was not a better revenue driver than the investment costs of the reactor. In case 5, generating less hydrogen and using a smaller reactor was more cost-effective than case 4, in which a larger reactor was used and more hydrogen generation. Oxy-fuel combustion, in general, was not a cost-effective solution compared to MEA. More decarbonization pathways should be explored to confirm if this is the case. Also, using the hydrogen generated from HTSE in these cases to upgrade biomass to new products could increase the NPV of both Case 4 and Case 5 significantly.

Overall, the results of this study were too specific to a single case to make any overall claims about the prospects of nuclear to be cost-effective for the pulp and paper industry, however, these findings illuminate the cost and revenue drivers for decarbonization and nuclear integration. These findings lead us to believe that if pulp mills are decarbonized using nuclear power, it is advantageous for them to share the capacity of an NPP with other users. Regardless, pulp mill operators should consider investing in carbon capture equipment to harvest the tax credits, with or without integrating nuclear. Future work will assess the results for a variety of mill configurations and include deeper decarbonization pathways.

# 8. REFERENCES


Abbati de Assis, C., L. G. Greca, M. Ago, M. Y. Balakshin, H. Jameel, R. Gonzalez, and O. J. Rojas. 2018. "Techno-Economic Assessment, Scalability, and Applications of Aerosol Lignin Micro- and Nanoparticles." *ACS Sustainable Chemistry & Engineering* 6, no. 9: 11853–11868. https://doi.org/10.1021/acssuschemeng.8b02151.

Abou-Jaoude, A., L. M. Larsen, N. Guaita, I. Trivedi, F. S. Joseck, C. S. Lohse, E. Hoffman, N. Stauff, K. Shirvan, and A. Stein. 2024. *Meta-Analysis of Advanced Nuclear Reactor Cost Estimations*. NL/RPT-24-77048 Rev. 1. Idaho National Laboratory. https://inldigitallibrary.inl.gov/sites/sti/sti/Sort_107010.pdf.

Achachlouei, Mohammad Ahmadi, and Åsa Moberg. 2015. "Life Cycle Assessment of a Magazine, Part II: A Comparison of Print and Tablet Editions." *Journal of Industrial Ecology* 19, no. 4: 590–606. https://doi.org/10.1111/jiec.12229.

Agico Cement. n.d. "Electric Heating Rotary Kiln." Accessed September 5, 2024. https://www.rotarykilnfactory.com/electric-heating-rotary-kiln/.

Ahmadi Achachlouei, Mohammad, Åsa Moberg, and Elisabeth Hochschorner. 2015. "Life Cycle Assessment of a Magazine, Part I: Tablet Edition in Emerging and Mature States." *Journal of Industrial Ecology* 19, no. 4: 575–589. https://doi.org/10.1111/jiec.12227.

Air Products. n.d. "Cryogenic Air Separation Plant." Accessed September 5, 2024. https://www.airproducts.com/supply-modes/cryogenic-air-separation-plant.

Alpiq Group. 2010. "Alpiq Makes It Possible: Nuclear Power Plant Fires Up Cartaseta." Accessed September 5, 2024. https://www.alpiq.com/en/media-relations/news-stories/news-stories-detail/alpiq-makes-it-possible-nuclear-power-plant-fires-up-cartaseta/.

Alpiq Group. n.d. "Model AG Paper Mill." Accessed September 5, 2024. https://www.alpiq.com/en/view/steam-supply-for-the-cardboard-factory/.

Andritz. 2024. "ANDRITZ to Supply World's Largest Lignin Production System to Södra Pulp Mill in Sweden." Accessed September 5, 2024. https://www.andritz.com/newsroom-en/pulp-paper/2024-07-03-soedra-lignin-group.

Bangalore Ashok, Rahul Prasad, Pekka Oinas, Kalle Lintinen, Golam Sarwar, Mauri A. Kostiainen, and Monika Österberg. 2018. "Techno-Economic Assessment for the Large-Scale Production of Colloidal Lignin Particles." *Green Chemistry* 20, no. 21: 4911–4919. https://doi.org/10.1039/c8gc02805b.

Benali, M., Z. Périn-Levasseur, L. Savulescu, L. Kouisni, N. Jemaa, T. Kudra, and M. Paleologou. 2014. "Implementation of Lignin-Based Biorefinery into a Canadian Softwood Kraft Pulp Mill: Optimal Resources Integration and Economic Viability, Assessment." *Biomass & Bioenergy* 67: 473–482. https://doi.org/10.1016/j.biombioe.2013.08.022.

Benali, Marzouk, Olumoye Ajao, Jawad Jeaidi, Banafsheh Gilani, and Behrang Mansoornejad. 2016. "Integrated Lignin-Kraft Pulp Biorefinery for the Production of Lignin and Its Derivatives: Economic Assessment and LCA-Based Environmental Footprint." In *Production of Biofuels and Chemicals from Lignin*, edited by A. A. del Río and R. G. da Silva, 379–418. Springer. https://link.springer.com/chapter/10.1007/978-981-10-1965-4_13.

Bertaud, F., P. Ottenio, A. Aubigny, and A. Dufour. 2023. "Recovering Lignin in a Real-Case Industrial Kraft Pulp Mill: Pilot-Scale Experiment and Impact on the Mill Commodities." *ACS Sustainable*

*Chemistry & Engineering* 11, no. 16: 6311–6318. https://doi.org/10.1021/acssuschemeng.2c07678.

Billerud. n.d. "Resource Efficient Production." Accessed September 5, 2024. https://www.billerud.com/sustainability/sustainability-foundation/resource-efficient-production.

Blum, William. 1982. "Plans for Nuclear District Heating in Switzerland." *Nuclear Engineering International*. Accessed September 5, 2024. https://inis.iaea.org/search/searchsinglerecord.aspx?recordsFor=SingleRecord&RN=14717781.

Boardman, R. 2023. "One Path to Convert Black Liquor into a More Valuable Product." EPRI Workshop to Explore the Use of Nuclear Energy in the Pulp & Paper Industry, Charlotte, NC.

British Lime Association. 2022. *Alternatives to Natural Gas for High Calcium Lime Manufacturing: Hydrogen*. Accessed September 5, 2024. https://assets.publishing.service.gov.uk/media/637e4d28e90e072346aae0cb/phase_3_alternatives_to_natural_gas_for_high_calcium_lime_manufacturing_hydrogen.pdf.

Chae, M. J., J. H. Kim, B. Moon, S. Park, and Y. S. Lee. 2022. "The Present Condition and Outlook for Hydrogen-Natural Gas Blending Technology." *Korean Journal of Chemical Engineering* 39, no. 2: 251–262. https://doi.org/10.1007/s11814-021-0960-8.

ChemAnalyst. n.d. "Tall Oil Price Trend and Forecast." Accessed September 5, 2024. https://www.chemanalyst.com/Pricing-data/tall-oil-1328#:~:text=Towards%20the%20end%20of%20Q4,Houston%20USA%20in%20December%202022.&text=In%20the%20Asia%20Pacific%20region,the%20fourth%20quarter%20of%202022.

Chemical Engineering. n.d. "The Chemical Engineering Plant Cost Index ®." Accessed September 7, 2024. https://www.chemengonline.com/pci-home.

Chen, Hongzhang. 2015. "Lignocellulose Biorefinery Feedstock Engineering." In *Lignocellulose Biorefinery Engineering*, edited by Hongzhang Chen, 37–86. Woodhead Publishing.

Cheremisinoff, Nicholas P., Paul Rosenfeld, and Anton R. Davletshin. 2008. "The Wood Preserving Industry." In *Responsible Care*, 317–82.

Chrisandina, Natasha J., Thomas T. Kwok, Andreas S. Bommarius, and Matthew J. Realff. 2019. "Techno-Economic Analysis of Water Precipitation for Lignin Value Prior to Pulping." *Chemical Engineering Research and Design* 143: 4–10. https://doi.org/10.1016/j.cherd.2018.10.042.

Clean Air Task Force. 2017. "The Role of 45Q Carbon Capture Incentives in Reducing Carbon Dioxide Emissions." Accessed September 27, 2024. https://www.catf.us/resource/45q-carbon-capture-incentives/.

Cline, Stephen P., and Paul M. Smith. 2017. "Opportunities for Lignin Valorization: An Exploratory Process." *Energy, Sustainability and Society* 7, no. 1. https://doi.org/10.1186/s13705-017-0129-9.

Congressional Research Service. 2023. *The Section 45Q Tax Credit for Carbon Sequestration*. https://crsreports.congress.gov/product/pdf/IF/IF11455/4.

Coral Medina, Jesus David, Adenise Lorenci Woiciechowski, Arion Zandona Filho, Satinder Kaur Brar, Antonio Irineudo Magalhães Júnior, and Carlos Ricardo Soccol. 2018. "Energetic and Economic Analysis of Ethanol, Xylitol and Lignin Production Using Oil Palm Empty Fruit Bunches from a

Brazilian Factory." *Journal of Cleaner Production* 195: 44–55. https://doi.org/10.1016/j.jclepro.2018.05.189.

Damasceno, A., L. Carneiro, N. Andrade, S. Vasconcelos, R. Brito, and K. Brito. 2020. "Simultaneous Prediction of Steam Production and Reduction Efficiency in Recovery Boilers of Pulping Process." *Journal of Cleaner Production* 275: 124103. https://doi.org/10.1016/j.jclepro.2020.124103.

Davis, R., L. Tao, C. Scarlata, E.C.D. Tan, J. Ross, J. Lukas, and D. Sexton. 2015. *Process Design and Economics for the Conversion of Lignocellulosic Biomass to Hydrocarbons: Dilute-Acid and Enzymatic Deconstruction of Biomass to Sugars and Catalytic Conversion of Sugars to Hydrocarbons*. NREL/TP-5100-62498. National Renewable Energy Laboratory, Harris Group Inc. https://www.nrel.gov/docs/fy15osti/62498.pdf.

Dessbesell, Luana, Michael Paleologou, Mathew Leitch, Reino Pulkki, and Chunbao Xu. 2020. "Global Lignin Supply Overview and Kraft Lignin Potential as an Alternative for Petroleum-Based Polymers." *Renewable and Sustainable Energy Reviews* 123. https://doi.org/10.1016/j.rser.2020.109768.

Dessbesell, Luana, Zhongshun Yuan, Shawn Hamilton, Mathew Leitch, Reino Pulkki, and Chunbao Xu. 2017. "Bio-Based Polymers Production in a Kraft Lignin Biorefinery: Techno-Economic Assessment." *Biofuels, Bioproducts and Biorefining* 12, no. 2: 239–250. https://doi.org/10.1002/bbb.1834.

Dessbesell, Luana, Zhongshun Yuan, Mathew Leitch, Michael Paleologou, Reino Pulkki, and Chunbao Charles Xu. 2018. "Capacity Design of a Kraft Lignin Biorefinery for Production of Biophenol via a Proprietary Low-Temperature/Low-Pressure Lignin Depolymerization Process." *ACS Sustainable Chemistry & Engineering* 6, no. 7: 9293–9303. https://doi.org/10.1021/acssuschemeng.8b01582.

European Commission. 2018. *European Platform on Life Cycle Assessment (ELCD)*. Accessed September 5, 2024. https://eplca.jrc.ec.europa.eu/ELCD3/index.xhtml.

Eriksson, M., B. Hökfors, and R. Backman. 2014. "Oxyfuel Combustion in Rotary Kiln Lime Production." *Energy Science & Engineering* 2, no. 4: 204–215. https://doi.org/10.1002/ese3.40.

Farag, S., and J. Chaouki. 2015. "Economic Evaluation for On-Site Pyrolysis of Kraft Lignin to Value-Added Chemicals." *Bioresource Technology* 175: 254–261. https://doi.org/10.1016/j.biortech.2014.10.096.

Fastmarkets. 2024. "RISI." Accessed September 27, 2024. https://www.fastmarkets.com/forest-products/risi-is-part-of-fastmarkets/.

FEECO. n.d. "Rotary Kilns." Accessed September 5, 2024. https://feeco.com/rotary-kilns/.

Fishersolve International. 2024. "Fishersolve Database." https://www.fisheri.com/products-services/fishersolve/.

Food and Agricultural Organization of the United Nations. 2023. *Pulp and Paper Capacities*. Accessed September 5, 2024. https://www.fao.org/3/cc7461t/cc7461t.pdf.

Forsberg, Charles. 2023. "Nuclear Energy in the Pulp and Paper Industry." *Paper 360* 18, no. 5: 21-23.

Forsberg, C. W., B. E. Dale, D. S. Jones, T. Hossain, A. R. C. Morais, and L. M. Wendt. 2021. "Replacing Liquid Fossil Fuels and Hydrocarbon Chemical Feedstocks with Liquid Biofuels from Large-Scale Nuclear Biorefineries." *Applied Energy* 298. https://doi.org/10.1016/j.apenergy.2021.117225.

FPInnovations. n.d. "The LignoForce System™: A Process for the Production of High-Quality Lignin from Black Liquor." Accessed September 5, 2024. https://web.fpinnovations.ca/lignin-from-black-liquor/.

Francey, S., H. Tran, and N. Berglin. 2011. "Global Survey on Lime Kiln Operation, Energy Consumption, and Alternative Fuel Usage." *Tappi Journal* 10, no. 8: 19–26. https://doi.org/10.32964/Tj10.8.19.

Gardarsdóttir, S. O., F. Normann, R. Skagestad, and F. Johnsson. 2018. "Investment Costs and $CO_2$ Reduction Potential of Carbon Capture from Industrial Plants - A Swedish Case Study." *International Journal of Greenhouse Gas Control* 76: 111–124. https://doi.org/10.1016/j.ijggc.2018.06.022.

Gerbelová, H., M. van der Spek, and W. Schakel. 2017. "Feasibility Assessment of $CO_2$ Capture Retrofitted to an Existing Cement Plant: Post-Combustion vs. Oxy-Fuel Combustion Technology." *Energy Procedia* 114: 6141–6149. https://doi.org/10.1016/j.egypro.2017.03.1751.

Guaita, Nahuel, and Jason K. Hansen. 2024. *Analyzing the Inflation Reduction Act and the Bipartisan Infrastructure Law for Their Effects on Nuclear Cost Data*. INL/RPT-23-72925: Idaho National Laboratory. https://doi.org/10.2172/2335485.

Guo, J. J., J. Z. Liu, T. Zhang, F. Hu, P. F. Li, Z. H. Liu, and C. G. Zheng. 2024. "Review on Research and Development of Oxy-Coal Burner for Carbon Capture." *Science China-Technological Sciences* 67, no. 3: 647–672. https://doi.org/10.1007/s11431-023-2536-9.

Hall, Jeremy, Stelvia Matos, Stefan Gold, and Liv S. Severino. 2018. "The Paradox of Sustainable Innovation: The 'Eroom' Effect (Moore's Law Backwards)." *Journal of Cleaner Production* 172: 3487–3497. https://doi.org/10.1016/j.jclepro.2017.07.162.

Hawai'i Gas. n.d. "Hydrogen." Accessed September 5, 2024. https://www.hawaiigas.com/sustainability/hydrogen#:~:text=Hawai%CA%BBi%20Gas%20blends%20the%20SNG,highly%20versatile%20energy%20sources%20available.

Hermansson, Frida, Matty Janssen, and Magdalena Svanström. 2020. "Allocation in Life Cycle Assessment of Lignin." *The International Journal of Life Cycle Assessment* 25, no. 8: 1620–1632. https://doi.org/10.1007/s11367-020-01770-4.

Higginbotham, P., V. White, K. Fogash, and G. Guvelioglu. 2011. "Oxygen Supply for Oxyfuel $CO_2$ Capture." *International Journal of Greenhouse Gas Control* 5: S194–S203. https://doi.org/10.1016/j.ijggc.2011.03.007.

Hruška, Michal, Miroslav Variny, Juma Haydary, and Ján Janošovský. 2020. "Sulfur Recovery from Syngas in Pulp Mills with Integrated Black Liquor Gasification." *Forests* 11, no. 11: 1173. https://doi.org/10.3390/f11111173.

Hu, Y., H. Li, and J. Yan. 2010. "Integration of Evaporative Gas Turbine with Oxy-Fuel Combustion for Carbon Dioxide Capture." *International Journal of Green Energy* 7, no. 6: 615–631. https://doi.org/10.1080/15435075.2010.529405.

Hughes, Sydney, and Alexander Zoelle. 2022. *Cost of Capturing $CO_2$ from Industrial Sources*. National Energy Technology Laboratory. Accessed September 5, 2024. https://netl.doe.gov/projects/files/CostofCapturingCO2fromIndustrialSources_071522.pdf.

Humbird, D., R. Davis, L. Tao, C. Kinchin, D. Hsu, A. Aden, P. Schoen, J. Lukas, B. Olthof, M. Worley, D. Sexton, and D. Dudgeon. 2011. *Process Design and Economics for Biochemical Conversion of Lignocellulosic Biomass to Ethanol*. NREL/TP-5100-47764. National Renewable Energy Laboratory and Harris Group Inc. Accessed September 5, 2024. https://www.nrel.gov/docs/fy11osti/47764.pdf.

Hupa, M. n.d. "Combustion of Black Liquor Droplets." Edited by Åbo Akademi University: TAPPI. Accessed September 5, 2024. https://www.tappi.org/content/events/08kros/handouts/4-2.pdf.

IBU-tec. n.d. "Rotary Kilns." Accessed September 5, 2024. https://www.ibu-tec.com/facilities/rotary-kilns/.

IEAGHG. 2011. *Effects of Impurities on Geological Storage of CO2*. International Energy Agency. https://ieaghg.org/docs/General_Docs/Reports/2011-04.pdf.

IndexBox. 2023. *U.S. - Methanol (Methyl Alcohol) - Market Analysis, Forecast, Size, Trends and Insights*. Accessed September 5, 2024. https://www.indexbox.io/store/u-s-methanol-methyl-alcohol-market-analysis-forecast-size-trends-and-insights/.

Institutt for Energiteknikk - Halden Reactor Project. 2008. *50 Years of Safety-Related Research*. Accessed September 5, 2024. https://www.oecd-nea.org/jointproj/docs/halden/the-halden-project-1958-2008.pdf.

Intergovernmental Panel on Climate Change. 2023. *Climate Change 2022 - Mitigation of Climate Change*. Cambridge: Cambridge University Press.

Internal Revenue Service. "Section 45V Credit for Production of Clean Hydrogen; Section 48(a)(15) Election to Treat Clean Hydrogen Production Facilities as Energy Property." *Federal Register* 88, no. 246 (December 26, 2023). https://www.federalregister.gov/documents/2023/12/26/2023-28359/section-45v-credit-for-production-of-clean-hydrogen-section-48a15-election-to-treat-clean-hydrogen.

International Atomic Energy Agency. 2007. *Advanced Applications of Water Cooled Nuclear Power Plants*. IAEA-TECDOC-1584. Austria. Accessed September 5, 2024. https://www-pub.iaea.org/MTCD/Publications/PDF/te_1584_web.pdf.

International Atomic Energy Agency. 2019. *Guidance on Nuclear Energy Cogeneration*. IAEA Nuclear Energy Series. Accessed September 5, 2024. https://www-pub.iaea.org/MTCD/Publications/PDF/P1862_web.pdf.

Jacob, R. M., J. P. Pinheiro, and L. A. Tokheim. 2023. "Electrified Externally Heated Rotary Calciner for Calcination of Cement Raw Meal." *Heliyon* 9, no. 11 (November): e22023. https://doi.org/10.1016/j.heliyon.2023.e22023.

Jacob, R. M., and L. A. Tokheim. 2023. "Electrified Calciner Concept for $CO_2$ Capture in Pyro-Processing of a Dry Process Cement Plant." *Energy* 268 (October): 126673. https://doi.org/10.1016/j.energy.2023.126673.

Jafri, Yawer, Elisabeth Wetterlund, Sennai Mesfun, Henrik Rådberg, Johanna Mossberg, Christian Hulteberg, and Erik Furusjö. 2020. "Combining Expansion in Pulp Capacity with Production of Sustainable Biofuels – Techno-Economic and Greenhouse Gas Emissions Assessment of Drop-In

Fuels from Black Liquor Part-Streams." *Applied Energy* 279 (November): 115879. https://doi.org/10.1016/j.apenergy.2020.115879.

Joelsson, J. M., and L. Gustavsson. 2012. "Reductions in Greenhouse Gas Emissions and Oil Use by DME (Di-Methyl Ether) and FT (Fischer-Tropsch) Diesel Production in Chemical Pulp Mills." *Energy* 39, no. 1 (January): 363-374. https://doi.org/10.1016/j.energy.2012.01.001.

Jones, Dale A. 2019. *Technoeconomic Evaluation of MEA versus Mixed Amines and a Catalyst System for $CO_2$ Removal at Near-Commercial Scale at Duke Energy Gibson 3 Pulverized Coal Plant and Duke Energy Buck Natural Gas Combined Cycle (NGCC) Plant*. https://www.osti.gov/biblio/1499969/.

Katajisto, Oona. 2020. "Calcination of Calcium Carbonate Based Materials in Electric Heated Rotary Kiln." Master's thesis, Engineering and Natural Sciences, Tampere University. https://trepo.tuni.fi/bitstream/handle/10024/123811/KatajistoOona.pdf?sequence=2&isAllowed=y .

Kienberger, M., S. Maitz, T. Pichler, and P. Demmelmayer. 2021. "Systematic Review on Isolation Processes for Technical Lignin." *Processes* 9, no. 5 (May): 804. https://doi.org/10.3390/pr9050804.

Kintek. n.d. *Electric Rotary Kiln Pyrolysis Furnace Plant Pyrolysis Machine Electric Rotary Calciner*. Accessed September 5, 2024. https://feeco.com/rotary-kilns/.

Kouisni, L., P. Holt-Hindle, K. Maki, and M. Paleologou. 2012. "The Lignoforce System™: A New Process for the Production of High-Quality Lignin from Black Liquor." *Journal of Science & Technology for Forest Products and Processes* 2, no. 4 (October): 6-10.

Kuparinen, Katja, and Esa Vakkilainen. 2017. "Green Pulp Mill: Renewable Alternatives to Fossil Fuels in Lime Kiln Operations." *BioResources* 12, no. 2 (April): 4031-4048. https://doi.org/10.15376/biores.12.2.4031-4048.

Kurimoto. n.d. *Continuous, External Heating Type Rotary Kiln*. Accessed September 5, 2024. https://www.global-kurimoto.com/id/id/product/item/07pw/380.php.

Lake, M. A., and J. C. Blackburn. 2014. "SLRP™ - An Innovative Lignin-Recovery Technology." *Cellulose Chemistry and Technology* 48, no. 9-10 (September-October): 799-804.

Larson, Eric D., Stefano Consonni, and Ryan E. Katofsky. 2003. *A Cost-Benefit Assessment of Biomass Gasification Power Generation in the Pulp and Paper Industry*. Princeton University, USA. https://acee.princeton.edu/wp-content/uploads/2016/10/BLGCC_FINAL_REPORT_8_OCT_2003.pdf.

Larson, Eric D., Stefano Consonni, Ryan E. Katofsky, Iisa Kristiina, and James W. Jr. Frederick. 2007. "Gasification-Based Biorefining at Kraft Pulp and Paper Mills in the United States." Paper presented at the International Chemical Recovery Conference, Quebec City, Canada. https://acee.princeton.edu/wp-content/uploads/2016/10/Larson-etal-ICRC07-FINAL-19-Mar-2007-WITH-CITATION.pdf.

Leeson, D., N. Mac Dowell, N. Shah, C. Petit, and P. S. Fennell. 2017. "A Techno-Economic Analysis and Systematic Review of Carbon Capture and Storage (CCS) Applied to the Iron and Steel, Cement, Oil Refining, and Pulp and Paper Industries, as Well as Other High Purity Sources." *International Journal of Greenhouse Gas Control* 61 (July): 71-84. https://doi.org/10.1016/j.ijggc.2017.03.020.

Liu, C. L., and W. J. Wang. 2018. "Chemical Looping Gasification of Pyrolyzed Biomass and Coal Char with Copper Ferrite as an Oxygen Carrier." *Journal of Renewable and Sustainable Energy* 10, no. 6 (November): 063101. https://doi.org/10.1063/1.5040379.

Liu, X. K., K. Y. Jin, X. B. Li, and R. G. Yang. 2023. "Low-Carbon Cement Manufacturing Enabled by Electrified Calcium Looping and Thermal Energy Storage." *International Journal of Greenhouse Gas Control* 129 (August): 103986. https://doi.org/10.1016/j.ijggc.2023.103986.

Lupion, M., I. Alvarez, P. Otero, R. Kuivalainen, J. Lantto, A. Hotta, and H. Hack. 2013. "30 MWth CIUDEN Oxy-CFB Boiler - First Experiences." *Energy Procedia* 37: 6179-6188. https://doi.org/10.1016/j.egypro.2013.06.547.

Mabrouk, Aicha, Xabier Erdocia, Maria González Alriols, and Jalel Labidi. 2018. "Economic Analysis of a Biorefinery Process for Catechol Production from Lignin." *Journal of Cleaner Production* 198 (July): 133-142. https://doi.org/10.1016/j.jclepro.2018.06.294.

Madeddu, Claudio, Massimiliano Errico, and Roberto Baratti. 2019. *$CO_2$ Capture by Reactive Absorption-Stripping*. Springer. https://link.springer.com/book/10.1007/978-3-030-04579-1.

Mäki, Elina, Heidi Saastamoinen, Kristian Melin, Doris Matschegg, and Hanna Pihkola. 2021. "Drivers and Barriers in Retrofitting Pulp and Paper Industry with Bioenergy for More Efficient Production of Liquid, Solid and Gaseous Biofuels: A Review." *Biomass and Bioenergy* 148 (November): 106036. https://doi.org/10.1016/j.biombioe.2021.106036.

Malek, Aicha, and Shaukat Farooq. 2004. "Hydrogen Purification from Refinery Fuel Gas by Pressure Swing Adsorption." *AIChE Journal* 44, no. 9 (September): 1826-1837. https://doi.org/10.1002/aic.690440906.

Manning, R., and H. Tran. 2015. "Impact of Cofiring Biofuels and Fossil Fuels on Lime Kiln Operation." *Tappi Journal* 14, no. 7 (July): 474-480. https://doi.org/10.32964/Tj14.7.474.

Massood, Ramezan, Timothy Skone, Nsakala Nsakala, and Gregory N. Lilijedhal. 2007. *Carbon Dioxide Capture from Existing Coal-Fired Power Plants*. DOE/NETL-401/110907. National Energy Technology Laboratory, Alston Power Inc. http://large.stanford.edu/courses/2012/ph240/maas1/docs/NETL-401-110907.pdf.

Ministry of Economy Trade and Industry. 2022. *Technology Roadmap for "Transition Finance" in Pulp and Paper Sector*. https://www.meti.go.jp/policy/energy_environment/global_warming/transition/transition_finance_technology_roadmap_paper_eng.pdf.

Mitsubishi Power. 2023. "Mitsubishi Power Successfully Operates an Advanced Class Gas Turbine with 30% Hydrogen Fuel Co-Firing at Grid-Connected T-Point 2." Accessed September 5, 2024. https://power.mhi.com/news/231130.html.

National Energy Technology Laboratory. 2007. *Carbon Dioxide Capture from Existing Coal-Fired Power Plants*. DOE/NETL-401/110907. https://www.osti.gov/biblio/1499969/.

National Energy Technology Laboratory. 2010. *Cost and Performance Baseline for Fossil Energy Plants Volume 1: Bituminous Coal and Natural Gas to Electricity*. DOE/NETL-2010/1397. https://www.nrc.gov/docs/ML1217/ML12170A423.pdf.

National Energy Technology Laboratory. n.d.-a. "9.2 Carbon Dioxide Capture Approaches." Accessed September 5, 2024. https://netl.doe.gov/research/carbon-management/energy-systems/gasification/gasifipedia/capture-approaches.

National Energy Technology Laboratory. n.d.-b. "Black Liquor Gasification." Accessed September 5, 2024. https://netl.doe.gov/research/Coal/energy-systems/gasification/gasifipedia/blackliquor.

National Renewable Energy Laboratory. 2002. *Steam System Opportunity Assessment for the Pulp and Paper, Chemical Manufacturing, and Petroleum Refining Industries*. DOE/GO-102002-1639, NREL/BK-840-32806. https://www.nrel.gov/docs/fy03osti/32806.pdf.

National Renewable Energy Laboratory. 2024. "Annual Technology Baseline." Accessed September 5, 2024. https://atb.nrel.gov/electricity/2024/data.

Nitzsche, R., M. Budzinski, and A. Grongroft. 2016. "Techno-Economic Assessment of a Wood-Based Biorefinery Concept for the Production of Polymer-Grade Ethylene, Organosolv Lignin and Fuel." *Bioresource Technology* 200 (December): 928-939. https://doi.org/10.1016/j.biortech.2015.11.008. Accessed September 5, 2024. https://www.ncbi.nlm.nih.gov/pubmed/26609950.

Noram. 2014. "LignoForce™ Process a Breakthrough for Canada." Accessed September 5, 2024. https://www.noram-eng.com/lignoforce-process-a-breakthrough-for-canada/.

Noritake. n.d. "Indirect-Heating Continuous Rotary Kiln." Accessed September 5, 2024. https://www.noritake.co.jp/eng/products/eeg/parts/detail/145/.

Novotny, Vaclav, Kathleen P. Sweeney, Elizabeth K. Worsham, Eliezer A. Reyes Molina, Sam J. Root, Frederick Joseck, Byung-Hee Choi, Nipun Popli, Junyung Kim, Todd Knighton, and Rami M. Saeed. 2024. *Thermal Integration of Advanced Nuclear Reactors with a Reference Refinery, Methanol Synthesis, and a Wood Pulp Plant*. INL/RPT 24-76435: Idaho National Laboratory.

Nwaoha, C., and P. Tontiwachwuthikul. 2019. "Carbon Dioxide Capture from Pulp Mill Using 2-Amino-2-Methyl-1-Propanol and Monoethanolamine Blend: Techno-Economic Assessment of Advanced Process Configuration." *Applied Energy* 250 (April): 1202-1216. https://doi.org/10.1016/j.apenergy.2019.05.097.

OCI Global. 2023. "OCI Global to Double Its Green Methanol Capacity in the US." Accessed September 5, 2024. https://oci-global.com/news-stories/press-releases/oci-global-to-double-its-green-methanol-capacity-in-the-us/.

Office of Nuclear Energy. 2022. "3 Nuclear Power Plants Gearing Up for Clean Hydrogen Production." Accessed September 5, 2024. https://www.energy.gov/ne/articles/3-nuclear-power-plants-gearing-clean-hydrogen-production.

Oliveira, R. C. P., M. M. Mateus, and D. M. F. Santos. 2019. "Editors' Choice—On the Oxidation of Kraft Black Liquor for Lignin Recovery: A Voltammetric Study." *Journal of The Electrochemical Society* 166, no. 16: E547–E553. https://doi.org/10.1149/2.0131916jes.

Onarheim, K., S. Santos, P. Kangas, and V. Hankalin. 2017. "Performance and Costs of CCS in the Pulp and Paper Industry Part 1: Performance of Amine-Based Post-Combustion $CO_2$ Capture." *International Journal of Greenhouse Gas Control* 59 (August): 58-73. https://doi.org/10.1016/j.ijggc.2017.02.008.

Park, S., and E. Carrejo. 2024. "Modeling Results for Oxy-Fuel Combustion in a Black Liquor Boiler." Personal communication.

Parkhi, A., S. Cremaschi, and Z. H. Jiang. 2022. "Techno-Economic Analysis of $CO_2$ Capture from Pulp and Paper Mill Limekiln." *IFAC-PapersOnLine* 55, no. 7 (July): 284-291. https://doi.org/10.1016/j.ifacol.2022.07.458.

Parra, S. Q., and M. C. Romano. 2023. "Decarbonization of Cement Production by Electrification." *Journal of Cleaner Production* 425 (August): 138913. https://doi.org/10.1016/j.jclepro.2023.138913.

Parrish, David. 1998. "Black Liquor Recovery Boilers - An Introduction." *The National Board of Boiler and Pressure Vessel Inspectors.* Accessed September 5, 2024. https://www.nationalboard.org/index.aspx?pageID=164&ID=231.

Pisciotta, M., H. Pilorge, J. Feldmann, R. Jacobson, J. Davids, S. Swett, and Z. Sasso. 2022. "Current State of Industrial Heating and Opportunities for Decarbonization." *Progress in Energy and Combustion Science* 91 (December): 100982. https://doi.org/10.1016/j.pecs.2021.100982.

Pringer, Hannes. n.d. *Sustainable Lime Burning Technology for Steel Plants*. Accessed September 5, 2024. https://www.gifa.com/cgi-bin/md_gmtn/lib/all/lob/return_download.cgi/thinksteel_02_2023_02.pdf?ticket=g_u_e_s_t&bid=6353&no_mime_type=0.

Rao, Prakash, and Michael Muller. 2007. "Industrial Oxygen: Its Generation and Use." *ACEEE Summer Study on Energy Efficiency in Industry*. Accessed September 5, 2024. https://www.aceee.org/files/proceedings/2007/data/papers/78_6_080.pdf.

RI.SE. 2020. "Oxyfuel Combustion of Black Liquor in Swedish Recovery Boilers." Accessed September 5, 2024. https://www.ri.se/en/what-we-do/projects/oxyfuel-combustion-of-black-liquor-in-swedish-recovery-boilers.

S&P Global. 2023. "Feature: New US Producers Plan 4.4 Million mt/year Green Methanol for Shipping." Accessed September 5, 2024. https://www.spglobal.com/commodityinsights/en/market-insights/latest-news/shipping/091523-new-us-producers-plan-44-million-mtyear-green-methanol-for-shipping.

Sagues, W. J., H. Jameel, D. L. Sanchez, and S. Park. 2020. "Prospects for Bioenergy with Carbon Capture & Storage (BECCS) in the United States Pulp and Paper Industry." *Energy & Environmental Science* 13, no. 8 (August): 2243-2261. https://doi.org/10.1039/d0ee01107j.

Sher, F., A. Yaqoob, F. Saeed, S. F. Zhang, Z. Jahan, and J. J. Klemes. 2020. "Torrefied Biomass Fuels as a Renewable Alternative to Coal in Co-Firing for Power Generation." *Energy* 209 (December): 118444. https://doi.org/10.1016/j.energy.2020.118444.

Silva, W. L., J. C. T. Ribeiro, E. F. da Costa, and A. O. S. da Costa. 2008. "Reduction Efficiency Prediction of CENIBRA's Recovery Boiler by Direct Minimization of Gibbs Free Energy." *Brazilian Journal of Chemical Engineering* 25, no. 3: 603–11. https://doi.org/10.1590/S0104-66322008000300017.

Southards, W. T., J. D. Blue, J. A. Dickinson, R. A. McIlroy, and C. L. Verrill. 1997. *High-Solids Black Liquor Firing in Pulp and Paper Industry Kraft Recovery Boilers*. The Babcock and Wilcox Company. Accessed September 5, 2024. https://digital.library.unt.edu/ark:/67531/metadc696443/m2/1/high_res_d/607516.pdf.

Strömberg, L., G. Lindgren, J. Jacoby, R. Giering, M. Anheden, U. Burchhardt, H. Altmann, F. Kluger, and G. N. Stamatelopoulos. 2009. "Update on Vattenfall's 30 MWth Oxyfuel Pilot Plant in Schwarze Pumpe." *Greenhouse Gas Control Technologies* 9, no. 1 (January): 581-589. https://doi.org/10.1016/j.egypro.2009.01.077.

Suhr, Michael, Gabriele Klein, Ioanna Kourti, Miguel Rodrigo Gonzalo, Germán Giner Santonja, Serge Roudier, and Luis Delgado Sancho. 2015. *Best Available Techniques (BAT) Reference Document*

*for the Production of Pulp, Paper and Board*. JRC Science and Policy Reports. Accessed September 5, 2024. https://eippcb.jrc.ec.europa.eu/sites/default/files/2019-11/PP_revised_BREF_2015.pdf.

Summers, William Morgan, Steve E. Herron, and Alex Zoelle. 2014. *Cost of Capturing $CO_2$ from Industrial Sources*. DOE/NETL-2013/1602. United States. https://www.osti.gov/biblio/1480985.

Svensson, Elin, Holger Wiertzema, and Simon Harvey. 2021. "Potential for Negative Emissions by Carbon Capture and Storage From a Novel Electric Plasma Calcination Process for Pulp and Paper Mills." *Frontiers in Climate* 3. https://doi.org/10.3389/fclim.2021.705032.

Tardy, Blaise L., Erlantz Lizundia, Chamseddine Guizani, Minna Hakkarainen, and Mika H. Sipponen. 2023. "Prospects for the Integration of Lignin Materials into the Circular Economy." *Materials Today* 65 (April): 122-132. https://doi.org/10.1016/j.mattod.2023.04.001.

Theis, Joel. 2021. *Quality Guidelines for Energy Systems Studies: Cost Estimation Methodology for NETL Assessments of Power Plant Performance*. NETL-PUB-22580. National Energy Technology Laboratory. https://www.osti.gov/biblio/1567736/.

Thimsen, D., J. Wheeldon, and D. Dillon. 2011. "Economic Comparison of Oxy-Coal Carbon Dioxide ($CO_2$) Capture and Storage (CCS) with Pre- and Post-Combustion CCS." In *Oxy-Fuel Combustion for Power Generation and Carbon Dioxide ($CO_2$) Capture*, 17-34. Accessed September 5, 2024. https://www.sciencedirect.com/science/article/abs/pii/B9781845696719500028#t0010.

Tokheim, Lars-André, Anette Mathisen, Lars Erik Øi, Chameera Jayarathna, Nils Eldrup, and Tor Gautestad. 2019. "Combined Calcination and $CO_2$ Capture in Cement Clinker Production by Use of Electrical Energy." Trondheim CCS Conference – $CO_2$ Capture, Transport and Storage, Trondheim, Norway.

Tomani, P. 2010. "The Lignoboost Process." *Cellulose Chemistry and Technology* 44, no. 1-3 (January-March): 53-58.

Topolski, Kevin, Evan P. Reznicek, Burcin Cakir Erdener, Chris W. San Marchi, Joseph A. Ronevich, Lisa Fring, Kevin Simmons, Omar Jose Guerra Fernandez, Bri-Mathias Hodge, and Mark Chung. 2022. *Hydrogen Blending into Natural Gas Pipeline Infrastructure: Review of the State of Technology*. Accessed September 5, 2024. https://www.nrel.gov/docs/fy23osti/81704.pdf.

Towler, Gavin, and Ray Sinnott. 2012. *Chemical Engineering Design*. 2nd ed.

Tran, H., and E. K. Vakkilainen. 2012. "The Kraft Chemical Recovery Process." In *Increasing Energy and Chemical Recovery Efficiency in the Kraft Process*, Natural Sciences and Engineering Research Council of Canada. Accessed September 5, 2024. https://www.tappi.org/content/events/08kros/manuscripts/1-1.pdf.

Traubert, T.D. 2022. "Black Liquor Recovery Boiler." *Engineering Design and Testing Corp*. Accessed September 5, 2024. https://www.edtengineers.com/blog-post/black-liquor-recovery-boiler.

U.S. Congress. *H.R. 5376 - Inflation Reduction Act of 2022*. 117th Congress, 2nd session. Washington, D.C., 2022. https://www.congress.gov/bill/117th-congress/house-bill/5376.

U.S. Energy Information Administration. 2019. "New Methanol Plants Expected to Increase Industrial Natural Gas Use through 2020." *Today in Energy*. Accessed September 5, 2024. https://www.eia.gov/todayinenergy/detail.php?id=38412.

U.S. Energy Information Administration. 2021. *Annual Energy Outlook 2021 with Projections for 2050*. Accessed September 5, 2024. https://www.eia.gov/outlooks/archive/aeo21/.

U.S. Energy Information Administration. 2024. "Natural Gas: Henry Hub Natural Gas Spot Price." Accessed September 27, 2024. https://www.eia.gov/dnav/ng/hist/rngwhhdM.htm.

U.S. Energy Information Administration. n.d. "Table 2.10. Average Price of Electricity to Ultimate Customers by End Use Sector." *Electricity*. Accessed September 5, 2024. https://www.eia.gov/electricity/annual/html/epa_02_10.html.

U.S. Environmental Protection Agency. 2021. "Sources of Greenhouse Gas Emissions." Accessed September 27, 2024. https://www.epa.gov/ghgemissions/inventory-us-greenhouse-gas-emissions-and-sinks.

U.S. Environmental Protection Agency. 2022. *2011-2021 Greenhouse Gas Reporting Program Sector Profile: Pulp and Paper*. Accessed September 5, 2024. https://www.epa.gov/ghgreporting/ghgrp-2021-pulp-and-paper.

U.S. Environmental Protection Agency. 2023. "Inventory of U.S. Greenhouse Gas Emissions and Sinks: 1990-2022." Accessed September 27, 2024. https://www.epa.gov/ghgemissions/inventory-us-greenhouse-gas-emissions-and-sinks-1990-2022.

U.S. Environmental Protection Agency. *FLIGHT*. Edited by Greenhouse Gas Reporting Program (GHGRP). Accessed September 12, 2024. www.epa.gov/ghgreporting.

United States Department of Energy. 2022. *Industrial Decarbonization Roadmap*. DOE/EE-2635. https://www.energy.gov/sites/default/files/2022-09/Industrial%20Decarbonization%20Roadmap.pdf.

United States Department of Energy. 2023. "DOE Awards $22.1 Million to Advance Promising Nuclear Technologies." *Office of Nuclear Energy*. Accessed September 5, 2024. https://www.energy.gov/ne/articles/doe-awards-221-million-advance-promising-nuclear-technologies.

Vakkilainen, Esa K. 2005. *Kraft Recovery Boilers: Principles and Practice*. Suomen Soodakattilayhdistys r.y. https://lutpub.lut.fi/bitstream/handle/10024/111915/KRBFull.pdf;jsessionid=DF8DA7F6200F6B6BBC0C579E0376469D?sequence=2

Valmet. 2015. "LignoBoost Plants Produce Large Volumes of Lignin, Case Studies." Accessed September 5, 2024. https://www.valmet.com/media/articles/technology/lignoboost/.

Valmet. n.d. "Lignin Production with LignoBoost." Accessed September 5, 2024. https://www.valmet.com/pulp/other-value-adding-processes/lignin-extraction/.

Vural Gursel, Iris, Jan W. Dijkstra, Wouter J. J. Huijgen, and Andrea Ramirez. 2019. "Techno-Economic Comparative Assessment of Novel Lignin Depolymerization Routes to Bio-Based Aromatics." *Biofuels, Bioproducts and Biorefining* 13, no. 4: 1068-1084. https://doi.org/10.1002/bbb.1999.

Wendt, Daniel, and Lane Knighton. 2022. "High Temperature Steam Electrolysis Process Performance and Cost Estimates." *DOE Hydrogen Program AMR*. Accessed September 5, 2024. https://inldigitallibrary.inl.gov/sites/sti/sti/Sort_61222.pdf.

Wenger, J., and T. Stern. 2019. "Reflection on the Research on and Implementation of Biorefinery Systems - A Systematic Literature Review with a Focus on Feedstock." *Biofuels Bioproducts & Biorefining* 13, no. 5: 1347-1364. https://doi.org/10.1002/bbb.2021.

Wenger, Julia, Verena Haas, and Tobias Stern. 2020. “Why Can We Make Anything from Lignin Except Money? Towards a Broader Economic Perspective in Lignin Research.” *Current Forestry Reports* 6, no. 4: 294-308. https://doi.org/10.1007/s40725-020-00126-3.

Werner, Sven. 2017. “District Heating and Cooling in Sweden.” *Energy* 126: 419-429. https://doi.org/10.1016/j.energy.2017.03.052.

Wernet, Gregor, Christian Bauer, Bernhard Steubing, Jürgen Reinhard, Emilia Moreno-Ruiz, and Bo Weidema. 2016. “The ecoinvent Database Version 3 (Part I): Overview and Methodology.” *The International Journal of Life Cycle Assessment* 21, no. 9: 1218-1230. https://doi.org/10.1007/s11367-016-1087-8.

WestRock. 2023. *2023 Sustainability Report*. Accessed September 5, 2024. https://eippcb.jrc.ec.europa.eu/sites/default/files/2019-11/PP_revised_BREF_2015.pdf.

Wilhelmsson, Bodil, Claes Kollberg, Johan Larsson, Jan Eriksson, and Magnus Eriksson. 2018. *CemZero: A Feasibility Study Evaluating Ways to Reach Sustainable Cement Production via the Use of Electricity*. Accessed September 5, 2024. https://www.cement.heidelbergmaterials.se/sites/default/files/assets/document/65/de/final_cemzero_2018_public_version_2.0.pdf.pdf.

Wintoko, Joko, Suryo Purwono, Mohammad Fahrurrozi, and Bambang Soehendro. 2020. “Analysis Method of Black Liquor Pyrolysis and Gasification Using Deconvolution Technique to Obtain the Real-Time Gas Production Profile.” *Jurnal Rekayasa Proses* 14, no. 1. https://doi.org/10.22146/jrekpros.56152.

Worsham, E.K., and S.D. Terry. 2022. “Static and Dynamic Modeling of Steam Integration for a NuScale Small Modular Reactor and Pulp and Paper Mill Coupling for Carbon-Neutral Manufacturing.” *Applied Energy* 325. https://doi.org/10.1016/j.apenergy.2022.119613.

Yadav, S., and S.S. Mondal. 2022. “A Review on the Progress and Prospects of Oxy-Fuel Carbon Capture and Sequestration (CCS) Technology.” *Fuel* 308. https://doi.org/10.1016/j.fuel.2021.122057.

Zang, G., P. Sun, E. Yoo, A. Elgowainy, A. Bafana, U. Lee, M. Wang, and S. Supekar. 2021. "Synthetic Methanol/Fischer-Tropsch Fuel Production Capacity, Cost, and Carbon Intensity Utilizing $CO_2$ from Industrial and Power Plants in the United States." *Environmental Science & Technology* 55 (11): 7595-7604. https://doi.org/10.1021/acs.est.0c08674.

Zhang, Y., H. Chen, C.C. Chen, J.M. Plaza, R. Dugas, and G.T. Rochelle. 2009. “Rate-Based Process Modeling Study of $CO_2$ Capture with Aqueous Monoethanolamine Solution.” *Industrial & Engineering Chemistry Research* 48, no. 20: 9233-9246. https://doi.org/10.1021/ie900068k.

# Appendix A

# BLRB and Lime Kiln Oxy-Fuel Combustion- Aspen Plus Process Model Simulation, Heat and Mass Balances and Modeling Validation

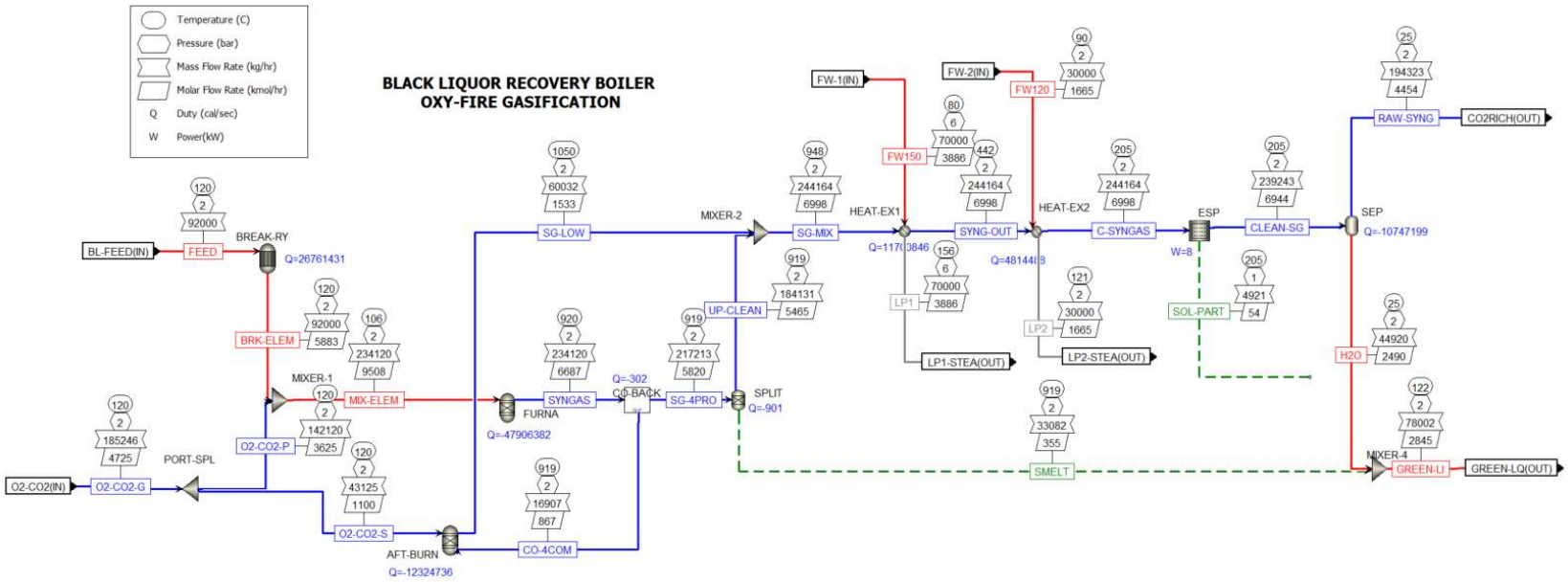


Figure 21. Black liquor recovery boiler oxy-fuel combustion – Aspen Plus Model.

Table 25. BLRB oxy-fuel combustion - streams heat and mass balance.

| Description | Units | BRK-ELEM | C-SYNGAS | CLEAN-SG | CO-4COM | FEED | FW120 | FW150 | GREEN-LI | H2O | LP1 | LP2 | MIX-ELEM | O2-CO2-G | O2-CO2-P | O2-CO2-S | RAW-SYNG | SG-4PRO | SG-LOW | SG-MIX | SMELT | SOL-PART | SYNG-OUT | SYNGAS | UP-CLEAN |
|---|---|---|---|---|---|---|---|---|---|---|---|---|---|---|---|---|---|---|---|---|---|---|---|---|---|
| From | | BREAK-RY | HEAT-EX2 | ESP | CO-BACK | | | | MIXER-4 | SEP | HEAT-EX1 | HEAT-EX2 | MIXER-1 | | PORT-SPL | PORT-SPL | SEP | CO-BACK | AFT-BURN | MIXER-2 | SPLIT | ESP | HEAT-EX1 | FURNA | SPLIT |
| To | | MIXER-1 | ESP | SEP | AFT-BURN | BREAK-RY | HEAT-EX2 | HEAT-EX1 | | MIXER-4 | | | FURNA | PORT-SPL | MIXER-1 | AFT-BURN | | SPLIT | MIXER-2 | HEAT-EX1 | MIXER-4 | | HEAT-EX2 | CO-BACK | MIXER-2 |
| Stream Class | | MCINCPSD | MCINCPSD | MCINCPSD | MCINCPSD | MCINCPSD | MCINCPSD | MCINCPSD | MCINCPSD | MCINCPSD | MCINCPSD | MCINCPSD | MCINCPSD | MCINCPSD | MCINCPSD | MCINCPSD | MCINCPSD | MCINCPSD | MCINCPSD | MCINCPSD | MCINCPSD | MCINCPSD | MCINCPSD | MCINCPSD | MCINCPSD |
| Temperature | C | 120 | 204.926367 | 204.92637 | 918.543522 | 120 | 90 | 80 | 122.032514 | 25 | 155.9727 | 121.31678 | 105.670448 | 120 | 120 | 120 | 25 | 918.54352 | 1050 | 948.267919 | 918.54352 | 204.92637 | 441.711003 | 920 | 918.54352 |
| Pressure | bar | 1.82385 | 2 | 1.99993927 | 2 | 1.8 | 2 | 5.5 | 2 | 2 | 5.5 | 2 | 1.8 | 1.8 | 1.8 | 1.8 | 2 | 2 | 2 | 2 | 2 | 1.01325 | 2 | 2 | 2 |
| Mass Vapor Fraction | | 0.468752357 | 0.97953818 | 0.99968676 | 1 | 0 | 0 | 0 | 0.16182795 | 0 | 1 | 1 | 0.79862773 | 1 | 1 | 1 | 1 | 0.833072 | 1 | 0.97955334 | 0.0548707 | 6.83E-07 | 0.97955334 | 0 | 0.9728871 |
| Mass Liquid Fraction | | 0.292181546 | 1.52E-05 | 2.32E-07 | 0 | 0 | 1 | 1 | 0.43636598 | 0.9983329 | 0 | 0 | 0.10742879 | 0 | 0 | 0 | 0 | 0 | 0 | 0 | 0 | 0.0007403 | 0 | 0.84512684 | 0 |
| Mass Solid Fraction | | 0.239066097 | 0.02044666 | 0.00031301 | 0 | 1 | 0 | 0 | 0.40180607 | 0.0016671 | 0 | 0 | 0.09394348 | 0 | 0 | 0 | 0 | 0.166928 | 0 | 0.02044666 | 0.9451293 | 0.999259 | 0.02044666 | 0.15487316 | 0.0271129 |
| Mass Enthalpy | cal/gm | -859.672007 | -2281.86944 | -2290.9971 | -572.300944 | -1906.8584 | -3742.265 | -3753.069 | -2974.54846 | -3809.1634 | -3151.311 | -3164.527 | -1198.60894 | -1418.016 | -1418.016 | -1418.0162 | -2139.158 | -2041.344 | -1918.9179 | -2038.3639 | -1841.278 | -1838.1225 | -2210.8836 | -1935.2513 | -2077.307 |
| Mass Density | gm/cc | 0.001785879 | 0.00177589 | 0.00174007 | 0.00039348 | 1.5341983 | 0.8078724 | 0.814877 | 0.00684341 | 0.8495384 | 0.0028718 | 0.0011152 | 0.00203174 | 0.0021633 | 0.0021633 | 0.0021633 | 0.0035596 | 0.0008033 | 0.00071143 | 0.00069234 | 0.0145763 | 2.1482484 | 0.00118392 | 0.29932373 | 0.0006868 |
| Enthalpy Flow | cal/sec | -21969395.7 | -154763779 | -152251119 | -2687786.92 | -48730827 | -31185545 | -72976344 | -64449864.5 | -47529619 | -61275496 | -26371058 | -77949654.1 | -72966983 | -55980270 | -16986714 | -1.15E+08 | -1.23E+08 | -31999237 | -138248443 | -16920246 | -2512659.2 | -149949291 | -125856036 | -1.06E+08 |
| Mass Flows | kg/hr | 92000 | 244163.664 | 239242.57 | 16907.2461 | 92000 | 30000 | 70000 | 78001.5911 | 44919.74 | 70000 | 30000 | 234120.359 | 185245.52 | 142120.36 | 43125.156 | 194322.83 | 217213.11 | 60032.402 | 244163.664 | 33081.851 | 4921.0936 | 244163.664 | 234120.359 | 184131.26 |
| C | kg/hr | 21994.08092 | 0 | 0 | 0 | 0 | 0 | 0 | 0 | 0 | 0 | 0 | 21994.0809 | 0 | 0 | 0 | 0 | 0 | 0 | 0 | 0 | 0 | 0 | 0 | 0 |
| S | kg/hr | 2632.02892 | 0 | 0 | 0 | 0 | 0 | 0 | 0.00920933 | 0 | 0 | 0 | 2632.02892 | 0 | 0 | 0 | 0 | 0.0092093 | 0 | 0 | 0.0092093 | 0 | 0 | 0.00920933 | 0 |
| K | kg/hr | 1815.192384 | 0 | 0 | 0 | 0 | 0 | 0 | 1815.19238 | 0 | 0 | 0 | 1815.19238 | 0 | 0 | 0 | 0 | 1815.1924 | 0 | 0 | 1815.1924 | 0 | 0 | 1815.19238 | 0 |
| SODIUM | kg/hr | 16725.70111 | 0 | 0 | 0 | 0 | 0 | 0 | 6.15E-05 | 0 | 0 | 0 | 16725.7011 | 0 | 0 | 0 | 0 | 6.15E-05 | 0 | 0 | 6.15E-05 | 0 | 0 | 6.15E-05 | 0 |
| O2 | kg/hr | 20602.43345 | 208.47801 | 208.478009 | 0 | 0 | 0 | 0 | 0.0004575 | 0.0004575 | 0 | 0 | 67000.9494 | 60477.732 | 46398.516 | 14079.216 | 208.47755 | 0 | 208.47801 | 208.47801 | 0 | 7.58E-07 | 208.47801 | 9.95E-13 | 0 |
| N2 | kg/hr | 60.506376 | 60.506376 | 60.5063759 | 0 | 0 | 0 | 0 | 4.77E-06 | 4.77E-06 | 0 | 0 | 60.506376 | 0 | 0 | 0 | 60.506371 | 60.506376 | 0 | 60.506376 | 0 | 1.14E-07 | 60.506376 | 60.506376 | 60.506376 |
| H2 | kg/hr | 2238.737292 | 0.00081044 | 0.00081044 | 572.054709 | 0 | 0 | 0 | 2.19E-10 | 2.19E-10 | 0 | 0 | 2238.73729 | 0 | 0 | 0 | 0.0008104 | 0 | 0.00081044 | 0.00081044 | 0 | 1.88E-12 | 0.00081044 | 572.054709 | 0 |
| CO2 | kg/hr | 0 | 192959.906 | 192959.904 | 0 | 0 | 0 | 0 | 2.78886755 | 2.7888675 | 0 | 0 | 95721.8431 | 124767.78 | 95721.843 | 29045.94 | 192957.11 | 138248.34 | 54711.5685 | 192959.906 | 0 | 0.002649 | 192959.906 | 138248.338 | 138248.34 |
| CO | kg/hr | 0 | 0.09053061 | 0.09053061 | 16335.1914 | 0 | 0 | 0 | 7.59E-09 | 7.59E-09 | 0 | 0 | 0 | 0 | 0 | 0 | 0.0905306 | 0 | 0.09053061 | 0.09053061 | 0 | 1.77E-10 | 0.09053061 | 16335.1914 | 0 |
| B-LIQUOR | kg/hr | 0 | 0 | 0 | 0 | 92000 | 0 | 0 | 0 | 0 | 0 | 0 | 0 | 0 | 0 | 0 | 0 | 0 | 0 | 0 | 0 | 0 | 0 | 0 | 0 |
| WATER | kg/hr | 25931.31955 | 45938.1925 | 45938.1784 | 0 | 0 | 30000 | 70000 | 44842.0659 | 44842.066 | 70000 | 30000 | 25931.3195 | 0 | 0 | 0 | 1096.1125 | 40825.928 | 5112.2642 | 45938.1925 | 0 | 0.0140139 | 45938.1925 | 40825.9283 | 40825.928 |
| NA2S | kg/hr | 0 | 2305.36683 | 34.5803104 | 0 | 0 | 0 | 0 | 4133.01023 | 34.58031 | 0 | 0 | 0 | 0 | 0 | 0 | 0 | 6403.7967 | 0 | 2305.36683 | 4098.4299 | 2270.7866 | 2305.36683 | 6403.79674 | 2305.3668 |
| NA2CO3 | kg/hr | 0 | 2686.96469 | 40.3042465 | 0 | 0 | 0 | 0 | 27208.5027 | 40.304247 | 0 | 0 | 0 | 0 | 0 | 0 | 0 | 29855.163 | 0 | 2686.96469 | 27168.198 | 2646.6605 | 2686.96469 | 29855.1632 | 2686.9647 |
| NA2SO4 | kg/hr | 0 | 4.15771341 | 0.52777128 | 0 | 0 | 0 | 0 | 3.09E-05 | 3.09E-05 | 0 | 0 | 0 | 0 | 0 | 0 | 0.5277404 | 4.1577134 | 0 | 4.15771341 | 0 | 3.6299421 | 4.15771341 | 4.15771341 | 4.1577134 |
| NAOH | kg/hr | 0 | 0 | 0 | 0 | 0 | 0 | 0 | 0.02114608 | 0 | 0 | 0 | 0 | 0 | 0 | 0 | 0 | 0.0211461 | 0 | 0 | 0.0211461 | 0 | 0 | 0.02114608 | 0 |
| Mass Fractions | | | | | | | | | | | | | | | | | | | | | | | | | |
| C | | 0.239066097 | 0 | 0 | 0 | 0 | 0 | 0 | 0 | 0 | 0 | 0 | 0.09394348 | 0 | 0 | 0 | 0 | 0 | 0 | 0 | 0 | 0 | 0 | 0 | 0 |
| S | | 0.02860901 | 0 | 0 | 0 | 0 | 0 | 0 | 1.18E-07 | 0 | 0 | 0 | 0.0112422 | 0 | 0 | 0 | 0 | 4.24E-08 | 0 | 0 | 2.78E-07 | 0 | 0 | 3.93E-08 | 0 |
| K | | 0.019730352 | 0 | 0 | 0 | 0 | 0 | 0 | 0.02327122 | 0 | 0 | 0 | 0.00775324 | 0 | 0 | 0 | 0 | 0.0083567 | 0 | 0 | 0.0548697 | 0 | 0 | 0.00775324 | 0 |
| SODIUM | | 0.181801099 | 0 | 0 | 0 | 0 | 0 | 0 | 7.88E-10 | 0 | 0 | 0 | 0.07144061 | 0 | 0 | 0 | 0 | 2.83E-10 | 0 | 0 | 1.86E-09 | 0 | 0 | 2.63E-10 | 0 |
| O2 | | 0.223939494 | 0.00085385 | 0.00087141 | 0 | 0 | 0 | 0 | 5.87E-09 | 1.02E-08 | 0 | 0 | 0.28618164 | 0.3264734 | 0.3264734 | 0.3264734 | 0.0010728 | 0 | 0.00347276 | 0.00085385 | 0 | 1.54E-10 | 0.00085385 | 4.25E-18 | 0 |
| N2 | | 0.000657678 | 0.00024781 | 0.00025291 | 0 | 0 | 0 | 0 | 6.12E-11 | 1.06E-10 | 0 | 0 | 0.00025844 | 0 | 0 | 0 | 0.0003114 | 0.0002786 | 0 | 0.00024781 | 0 | 2.31E-11 | 0.00024781 | 0.00025844 | 0.0003286 |
| H2 | | 0.024334101 | 3.32E-09 | 3.39E-09 | 0.03383488 | 0 | 0 | 0 | 2.81E-15 | 4.87E-15 | 0 | 0 | 0.00956233 | 0 | 0 | 0 | 4.17E-09 | 0 | 1.35E-08 | 3.32E-09 | 0 | 3.83E-16 | 3.32E-09 | 0.00244342 | 0 |
| CO2 | | 0 | 0.7902892 | 0.80654502 | 0 | 0 | 0 | 0 | 3.58E-05 | 6.21E-05 | 0 | 0 | 0.40885741 | 0.6735266 | 0.6735266 | 0.6735266 | 0.9929719 | 0.6364641 | 0.91136731 | 0.7902892 | 0 | 5.38E-07 | 0.7902892 | 0.59050114 | 0.750814 |
| CO | | 0 | 3.71E-07 | 3.78E-07 | 0.96616512 | 0 | 0 | 0 | 9.74E-14 | 1.69E-13 | 0 | 0 | 0 | 0 | 0 | 0 | 4.66E-07 | 0 | 1.51E-06 | 3.71E-07 | 0 | 3.60E-14 | 3.71E-07 | 0.06977262 | 0 |
| B-LIQUOR | | 0 | 0 | 0 | 0 | 1 | 0 | 0 | 0 | 0 | 0 | 0 | 0 | 0 | 0 | 0 | 0 | 0 | 0 | 0 | 0 | 0 | 0 | 0 | 0 |
| WATER | | 0.281862169 | 0.18814508 | 0.19201507 | 0 | 0 | 1 | 1 | 0.57488655 | 0.9982708 | 1 | 1 | 0.11076063 | 0 | 0 | 0 | 0.0056407 | 0.1879533 | 0.08515842 | 0.18814508 | 0 | 2.85E-06 | 0.18814508 | 0.17438009 | 0.2217219 |
| NA2S | | 0 | 0.00944189 | 0.00014454 | 0 | 0 | 0 | 0 | 0.05298623 | 0.0007698 | 0 | 0 | 0 | 0 | 0 | 0 | 0 | 0.0294816 | 0 | 0.00944189 | 0.1238876 | 0.4614394 | 0.00944189 | 0.02735258 | 0.0125202 |
| NA2CO3 | | 0 | 0.01100477 | 0.00016847 | 0 | 0 | 0 | 0 | 0.34881984 | 0.0008973 | 0 | 0 | 0 | 0 | 0 | 0 | 0 | 0.1374464 | 0 | 0.01100477 | 0.8212418 | 0.5378196 | 0.01100477 | 0.12752058 | 0.0145927 |
| NA2SO4 | | 0 | 1.70E-05 | 2.21E-06 | 0 | 0 | 0 | 0 | 3.96E-10 | 6.87E-10 | 0 | 0 | 0 | 0 | 0 | 0 | 2.72E-06 | 1.91E-05 | 0 | 1.70E-05 | 0 | 0.0007376 | 1.70E-05 | 1.78E-05 | 2.26E-05 |
| NAOH | | 0 | 0 | 0 | 0 | 0 | 0 | 0 | 2.71E-07 | 0 | 0 | 0 | 0 | 0 | 0 | 0 | 0 | 9.74E-08 | 0 | 0 | 6.39E-07 | 0 | 0 | 9.03E-08 | 0 |
| Volume Flow | l/min | 858587.4605 | 2291472.89 | 2291504.64 | 716139.525 | 999.43618 | 618.90962 | 1431.7089 | 189967.535 | 881.25776 | 406253.32 | 448365.72 | 1920525.91 | 1427154.4 | 1094912.9 | 332241.55 | 909857.56 | 4506488.2 | 1406385.55 | 5877777.99 | 37826.093 | 38.179117 | 3437215.26 | 13036.073 | 4468016.2 |

Table 26. BLRB Aspen Plus modeling validation.

| | Source | | | | | | |
|---|---|---|---|---|---|---|---|
| **Parameter** | ***(Damasceno et al. 2020)*** | ***(Silva et al. 2008)*** | ***(Wintoko et al. 2020)*** | ***(Hupa n.d.)*** | ***(Hruška et al. 2020)*** | ***(Park 2024)*** | ***This work*** |
| **Ultimate Analysis (wt.%)** | | | | | | | |
| C | 34.53 | 34.4 | 36.3 | 39 | 33.8 | 37.6 | 36.35 |
| H | 3.4 | 3.7 | 3.1 | 3.8 | 3.6 | 3.5 | 3.7 |
| O | 28.08 | 31.6 | 35.3 | 33 | 35.1 | 32.9 | 34.05 |
| N | - | - | 0.1 | 0.1 | 0.1 | - | 0.1 |
| Cl | 1.54 | 1.5 | 0.3 | - | - | 0.2 | 21.5 (ash) |
| K | - | 2 | 2.5 | 2 | 2.2 | 1 | |
| Na | 14.25 | 21.4 | 19.7 | 18.6 | 20.1 | 19.9 | |
| S | 2.73 | 5.4 | 2.8 | 3.6 | 5.1 | 4.8 | 4.3 |
| $Na_2CO_3$ | 9.44 | — | — | — | — | — | no recycle |
| $Na_2SO_4$ | 6.03 | — | — | — | — | * | no recycle |
| **BLRB Operating Conditions** | | | | | | | |
| Black liquor flow rate (kg/s) | 22.37 | — | — | — | — | — | 25.56 |
| Solids Content (wt.%) | 70 | — | — | — | 75 | 70-75 | 70 |
| **Smelt Variables** | | | | | | | |
| Production (kg/s) | 6.92 | — | — | — | — | | 9.19 |
| $Na_2CO_3$ (mol %) | 0.76 | — | — | — | — | 0.80-0.85 | 0.82 |
| $Na_2S$ (mol%) | 0.22 | — | — | — | — | 0.10-0.15 | 0.16 |
| $Na_2SO_4$ (mol %) | 0.02 | — | — | — | — | - | 0.02 |
| Reduction Efficiency (%) | 91.34 | — | — | — | — | 95-97 | 94.3 |
| **Others** | | | | | | | |
| Steam production (1000 metric tons/yr) | 8448 | — | — | — | — | — | 8400 |
| Air emissions, ESP efficiency (%) | 99.5 | — | — | — | — | — | 99 |

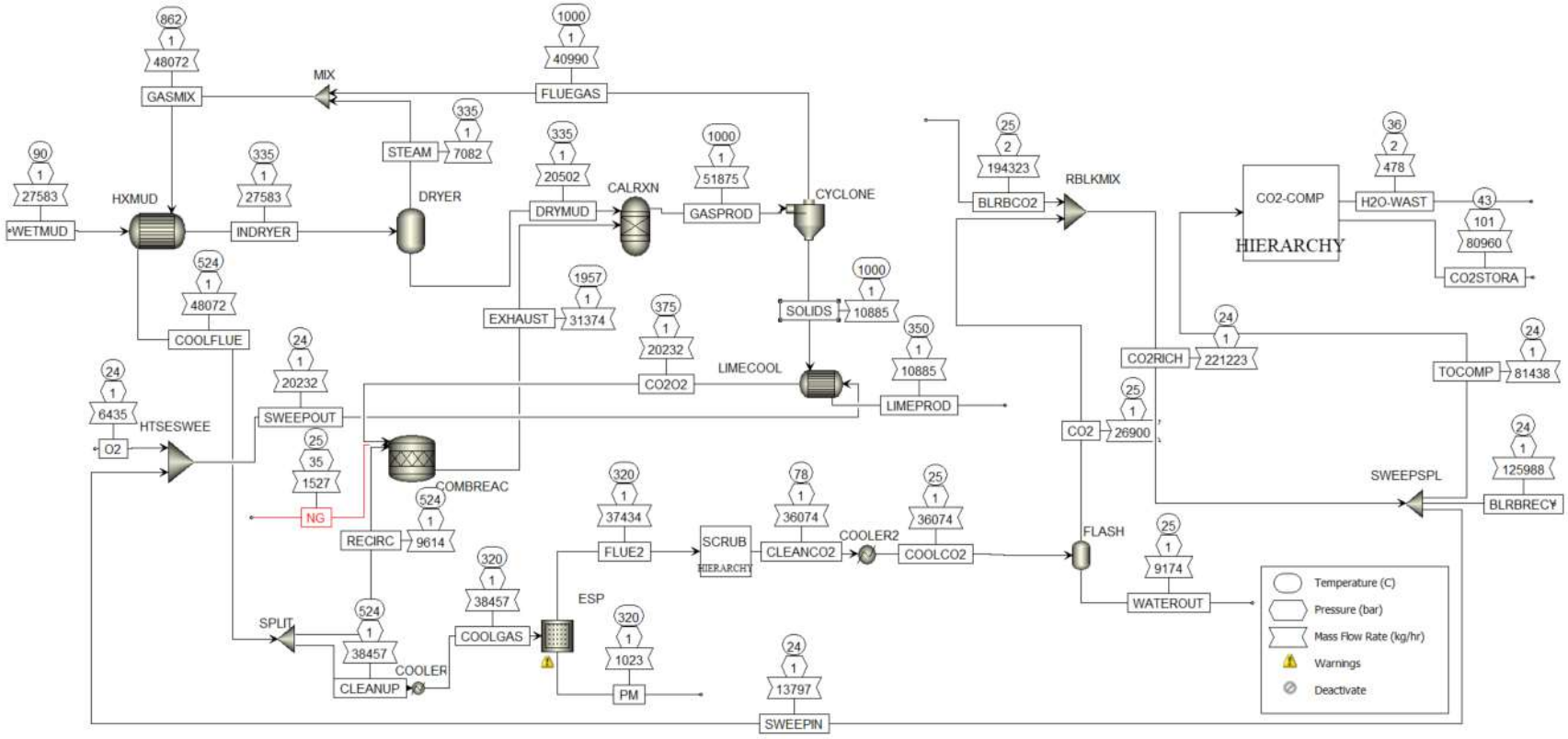


Figure 22. Lime Kiln Oxy-Fire Combustion (Gasification) – Aspen Plus model.

Table 27. Lime Kiln Oxy-Fire Combustion (Gasification) – Streams heat and mass balance

| Stream Name | Units | WETMUD | SWEEPOUT | PM | LIMEPROD | CO2RICH | BLRBCO2 | CO2RICH | CO2STORA | H2O-WAST |
|---|---|---|---|---|---|---|---|---|---|---|
| From | | | HTSESWEE | ESP | LIMECOOL | RBLKMIX | | RBLKMIX | CO2-COMP | CO2-COMP |
| To | | HXMUD | LIMECOOL | | | SWEEPSPL | RBLKMIX | SWEEPSPL | | |
| Stream Class | | MIXCIPSD | MIXCIPSD | MIXCIPSD | MIXCIPSD | MIXCIPSD | MIXCIPSD | MIXCIPSD | MIXCIPSD | MIXCIPSD |
| Temperature | C | 90 | 23.939696 | 320 | 350 | 24.01828103 | 25 | 24.01828103 | 43 | 43.365541 |
| Pressure | bar | 1 | 1 | 1.01325 | 0.997707 | 1 | 2 | 1 | 101 | 2 |
| Mass Vapor Fraction | | 0.0047483 | 0.9999984 | 0 | 0 | 0.999997614 | 0.999997279 | 0.999997614 | 1 | 0 |
| Mass Liquid Fraction | | 0.2557517 | 0 | 0.0640832 | 0 | 0 | 5.42E-09 | 0 | 0 | 0.999531 |
| Mass Solid Fraction | | 0.7395 | 1.63E-06 | 0.9359168 | 1 | 2.39E-06 | 2.72E-06 | 2.39E-06 | 0 | 0.000469 |
| Mass Enthalpy | cal/gm | -3069.447 | -1457.353 | -2607.308 | -2646.649 | -2136.91251 | -2139.158417 | -2136.91251 | -2170.485 | -3794.178 |
| Mass Entropy | cal/gm-K | -0.936031 | 0.0441605 | -0.322271 | -0.307623 | 0.016010939 | -0.015777033 | 0.016010939 | -0.291139 | -2.161536 |
| Mass Density | gm/cc | 0.2390298 | 0.0015871 | 2.4353769 | 3.2573034 | 0.001773121 | 0.003559586 | 0.001773121 | 0.5090944 | 0.9763681 |
| Enthalpy Flow | cal/sec | -23518220 | -8190386 | -737490.4 | -8002382 | -131314875.9 | -115468742.1 | -131314875.9 | -48849619 | -436552.9 |
| Average MW | | 46.364322 | 39.07278 | 55.53871 | 57.06438 | 43.56449379 | 43.62943867 | 43.56449379 | 43.882404 | 18.023499 |
| Mole Fractions | | | | | | | | | | |
| Mass Flows | kg/hr | 27583.333 | 20232.147 | 1018.2784 | 10884.923 | 221222.6992 | 194322.9021 | 221222.6992 | 81022.724 | 414.21108 |
| H2O | kg/hr | 6895.8333 | 87.298819 | 0.0732942 | 0 | 1399.734237 | 1096.112921 | 1399.734237 | 101.28844 | 413.98447 |
| CO2 | kg/hr | 0 | 13671.705 | 0.0001451 | 0 | 219209.7635 | 192957.1861 | 219209.7635 | 80695.898 | 0.0313855 |
| CAO | kg/hr | 0 | 0 | 890.98526 | 10176.352 | 0 | 0 | 0 | 0 | 0 |
| CACO3 | kg/hr | 19777.25 | 0 | 0 | 0 | 0 | 0 | 0 | 0 | 0 |
| N2 | kg/hr | 0 | 4.0230448 | 1.35E-09 | 0 | 64.50480691 | 60.50639198 | 64.50480691 | 23.745636 | 1.84E-09 |
| O2 | kg/hr | 0 | 6469.0273 | 8.33E-07 | 0 | 547.2016603 | 208.4776271 | 547.2016603 | 201.43695 | 6.04E-06 |
| CO | kg/hr | 0 | 0.0064872 | 4.34E-12 | 0 | 0.10401467 | 0.090530637 | 0.10401467 | 0.0382901 | 1.89E-12 |
| CH4 | kg/hr | 0 | 0 | 9.05E-27 | 0 | 0 | 0 | 0 | 0 | 0 |
| C2H6 | kg/hr | 0 | 0 | 7.51E-32 | 0 | 0 | 0 | 0 | 0 | 0 |
| NO | kg/hr | 0 | 0.0020581 | 2.28E-11 | 0 | 0.032999207 | 0 | 0.032999207 | 0.0121477 | 9.83E-11 |
| NO2 | kg/hr | 0 | 6.13E-06 | 2.83E-12 | 0 | 9.83E-05 | 0 | 9.83E-05 | 3.59E-05 | 2.82E-07 |
| S | kg/hr | 0 | 0 | 9.21E-21 | 0 | 0 | 0 | 0 | 0 | 0 |
| SO3 | kg/hr | 186.1875 | 0.0517109 | 4.48E-06 | 0 | 0.829124449 | 0 | 0.829124449 | 0.3042759 | 0.000943 |
| H2S | kg/hr | 0 | 0 | 1.08E-20 | 0 | 0 | 0 | 0 | 0 | 0 |
| H2 | kg/hr | 0 | 6.70E-05 | 8.20E-13 | 0 | 0.001073792 | 0.000810437 | 0.001073792 | 0.0003953 | 7.73E-14 |
| C | kg/hr | 0 | 0 | 0 | 0 | 0 | 0 | 0 | 0 | 0 |
| MGO | kg/hr | 206.875 | 0 | 16.634253 | 189.98743 | 0 | 0 | 0 | 0 | 0 |
| SIO2 | kg/hr | 103.4375 | 0 | 8.3171264 | 94.993717 | 0 | 0 | 0 | 0 | 0 |
| P2O5 | kg/hr | 206.875 | 0 | 16.634253 | 189.98743 | 0 | 0 | 0 | 0 | 0 |
| NAOH | kg/hr | 103.4375 | 0 | 65.181099 | 0 | 0 | 0 | 0 | 0 | 0 |
| NA2S | kg/hr | 103.4375 | 0 | 0 | 0 | 0 | 0 | 0 | 0 | 0 |
| NA2SO4 | kg/hr | 0 | 0.0329142 | 20.453004 | 233.60314 | 0.527740583 | 0.527740583 | 0.527740583 | 0 | 0.1942729 |
| NA2CO3 | kg/hr | 0 | 0 | 9.58E-27 | 0 | 0 | 0 | 0 | 0 | 0 |
| SO2 | kg/hr | 0 | 6.74E-09 | 2.41E-13 | 0 | 1.08E-07 | 0 | 1.08E-07 | 3.98E-08 | 0 |
| CASO3 | kg/hr | 0 | 0 | 3.85E-26 | 0 | 0 | 0 | 0 | 0 | 0 |
| H2SO4 | kg/hr | 0 | 0 | 4.39E-11 | 0 | 0 | 0 | 0 | 0 | 0 |
| CASO4 | kg/hr | 0 | 0 | 5.56E-30 | 0 | 0 | 0 | 0 | 0 | 0 |
| C3H8 | kg/hr | 0 | 0 | 8.69E-45 | 0 | 0 | 0 | 0 | 0 | 0 |
| Mass Fractions | | | | | | | | | | |
| Volume Flow | l/min | 1923.2844 | 212460.26 | 6.9686575 | 55.694961 | 2079409.345 | 909857.2902 | 2079409.345 | 2652.5116 | 7.0706103 |

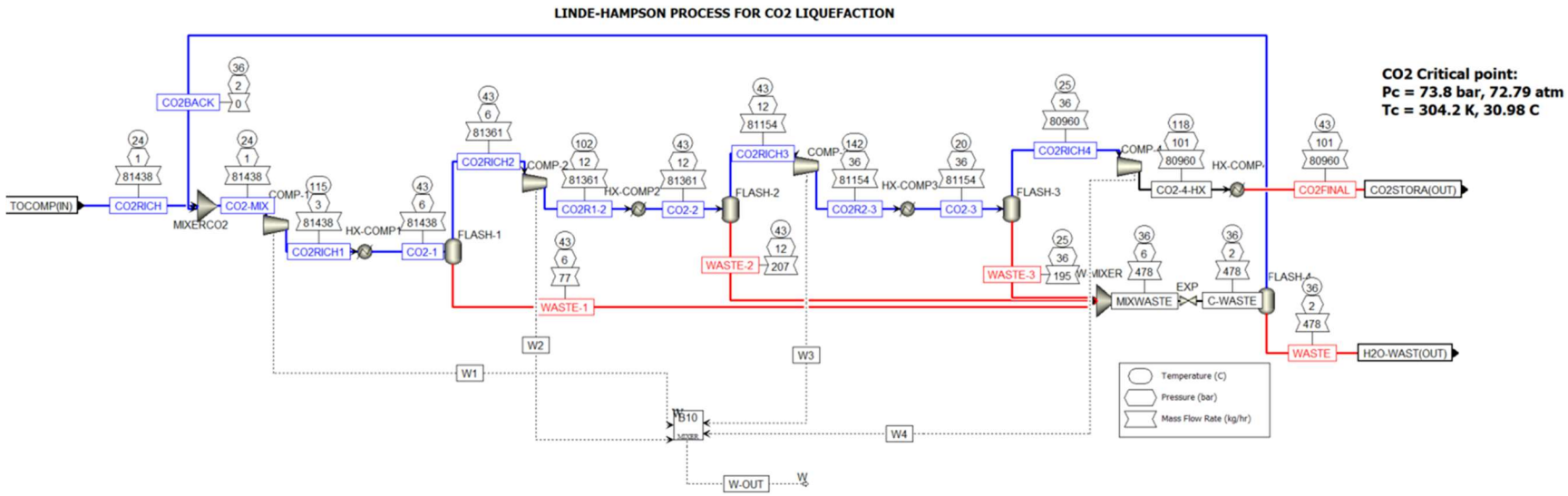


Figure 23. Lime kiln & BLRB $CO_2$ liquefaction – Aspen Plus model

Table 28. Carbon storage model validation (IEAGHG 2011).

| Component | $CO_2$ Quality Recommendation | $CO_2$ Expected Compositions EIA | $CO_2$ to Storage |
|---|---|---|---|
| H20 | 500 ppm | 100 ppm | 464 ppm |
| H2S | 200 ppm | 0 ppm | 0 ppm |
| CO | 2000 ppm | 50 ppm | 0 ppm |
| O2 | Aquifer <4 vol%, EOR 100-1000 ppm | 0.01 vol% | 0% vol, 3574 ppm |
| CH4 | Aquifer <4% vol%, EOR <2 vol% | 0 vol% | 0 ppm |
| N2 | < 4 vol% (all non-condensable gases) | 0.01 vol% | 0 vol% |
| Ar | < 4 vol% (all non-condensable gases) | 0.01 vol% | 0 vol% |
| H2 | < 4 vol% (all non-condensable gases) | 0 vol% | 0 vol% |
| SOX | 100 ppm | 50 ppm ($SO_2$), 20 ppm ($SO_3$) | 4 ppm |
| NOx | 100 ppm | 100 | 0 ppm |
| $CO_2$ | >95.5% | 99.94 | 99.67% |

Table 29. Lime kiln & BLRB $CO_2$ liquefaction – stream mole and heat summary.

| | Units | LK & BLRB Mixed $CO_2$ | $CO_2$ to Storage |
|---|---|---|---|
| Temperature | C | 24.01828369 | 43 |
| Pressure | bar | 1 | 101 |
| Molar Vapor Fraction | | 0.999999268 | 1 |
| Molar Liquid Fraction | | 0 | 0 |
| Molar Solid Fraction | | 7.32E-07 | 0 |
| Mass Vapor Fraction | | 0.999997614 | 1 |
| Mass Liquid Fraction | | 0 | 0 |
| Mass Solid Fraction | | 2.39E-06 | 0 |
| Molar Enthalpy | cal/mol | -93092.28662 | -95293.69682 |
| Mass Enthalpy | cal/gm | -2136.892133 | -2169.122789 |
| Molar Entropy | cal/mol-K | 0.697646209 | -12.7196547 |
| Mass Entropy | cal/gm-K | 0.016014159 | -0.289531142 |
| Molar Density | mol/cc | 4.07E-05 | 0.011455306 |
| Mass Density | gm/cc | 0.001773115 | 0.50325343 |
| Enthalpy Flow | cal/sec | -48339990.81 | -48781114.58 |
| Average MW | | 43.56433588 | 43.93190525 |
| Mole Flows | kmol/hr | 1869.37042 | 1842.850245 |
| Mole Fractions | | | |
| H2O | | 0.015300633 | 0.001131133 |
| $CO_2$ | | 0.980861516 | 0.994976539 |
| CAO | | 0 | 0 |
| CACO3 | | 0 | 0 |
| N2 | | 0.000453446 | 0.000459971 |
| O2 | | 0.003380582 | 0.003429231 |
| CO | | 7.30E-07 | 7.41E-07 |
| CH4 | | 0 | 0 |
| C2H6 | | 0 | 0 |

| | Units | LK & BLRB Mixed $CO_2$ | $CO_2$ to Storage |
|---|---|---|---|
| NO | | 2.17E-07 | 2.20E-07 |
| NO2 | | 4.23E-10 | 4.22E-10 |
| S | | 0 | 0 |
| SO3 | | 2.04E-06 | 2.06E-06 |
| H2S | | 0 | 0 |
| H2 | | 1.05E-07 | 1.06E-07 |
| C | | 0 | 0 |
| MGO | | 0 | 0 |
| SIO2 | | 0 | 0 |
| P2O5 | | 0 | 0 |
| NAOH | | 0 | 0 |
| NA2S | | 0 | 0 |
| NA2SO4 | | 7.32E-07 | 0 |
| NA2CO3 | | 0 | 0 |
| SO2 | | 3.23E-13 | 3.28E-13 |
| CASO3 | | 0 | 0 |
| H2SO4 | | 0 | 0 |
| CASO4 | | 0 | 0 |
| C3H8 | | 0 | 0 |
| Mass Flows | kg/hr | 81437.88085 | 80959.92233 |

# Appendix B

# Tax Credit Information

The Inflation reduction Act (IRA), enacted in 2022 provides a vast set of financial supporting mechanisms for existent nuclear power plants, new advanced nuclear power plants and carbon capture and storage, A summary of the mechanisms that could benefit the coupling of nuclear reactors with the pulp and paper industry is provided below.

## Production Tax Credit, Section 45U, for existent nuclear power plants

Section 45U establishes a tax credit for existent nuclear power plants, providing a credit amount depending on the requirements the taxpayer met for each megawatt hour (MWh) of electricity sold from a qualified nuclear power facility to unrelated parties. A qualified nuclear power facility, meeting specific criteria, includes those utilizing nuclear energy for electricity production and in operation before the enactment date (2023).

The PTC can be increased if the labor requirements, the domestic content bonus, and energy community requirements are met. A description is included in the Table 30.

Table 30. Rates for Production Tax Credits, Section 45U.

| | |
|---|---|
| Benefit | PTC |
| Section | 45U |
| Base Rate Without Labor Requirements | $3/MWh |
| Base Rate with Labor Requirements | $15/MWh |
| Description | Not for advanced nuclear power facilities |
| Credit Start Date | Nuclear Reactors in service before IRA.<br>Electricity produced and sold after Dec-2023 |
| Duration | 9 years |
| End Date | Dec-32 |

There is a reduction amount of the PTC 45U that a stakeholder can claim that depends on the gross receipt of the nuclear plant owner. The amount reduction of the PTC is determined as the lesser of:

- The corresponding tax credit rate received or
- 0.3*kWh - 0.16 * (GR - 2.5kWh)
  - Where kWh is the total quantity of kilowatts of electricity sold.
  - GR is Gross receipts.

  Figure 24 shows how the PTC decreases when the gross receipts increase.

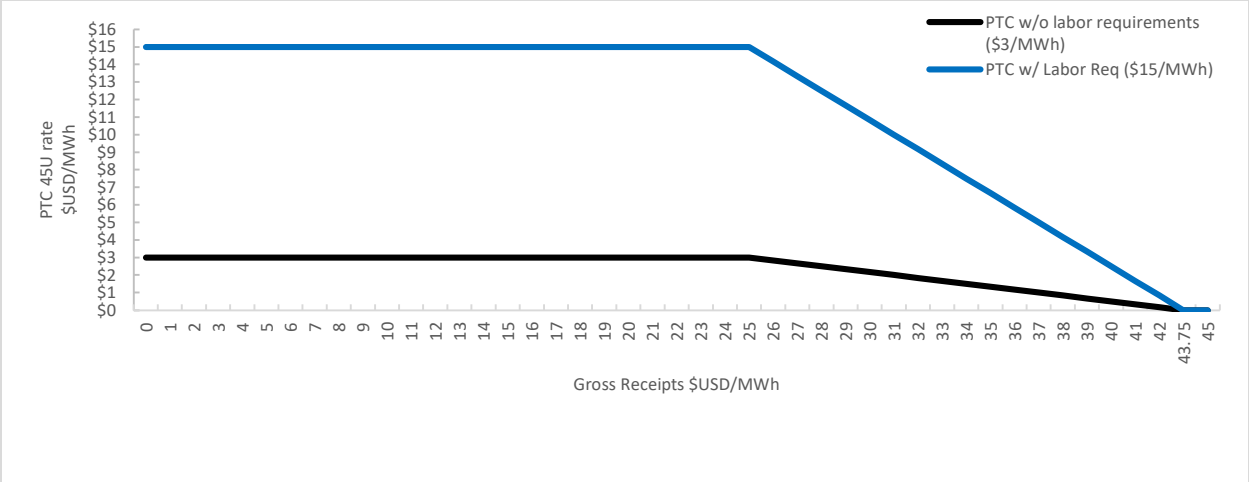


Figure 24. PTC 45U rates.

For a better understanding of the rules regarding inflation adjustment, wage requirements, termination, and the Secretary's regulatory authority are outlined to ensure proper implementation and compliance, the IRA lecture is recommended (U.S. House 2022)

## Production Tax Credit, Section 45Y, for new nuclear power plants

The Clean Electricity Production Credit, outlined in section 45Y of the Internal Revenue Code, offers incentives for the generation of clean energy based on the kilowatt hours of electricity produced by the taxpayer at a qualified facility. Facilities that were placed in service after December 31, 2024, can claim the tax credit. The credit amount is calculated by multiplying the electricity produced and sold to unrelated parties during the taxable year by the applicable rate, which varies depending on the characteristics of the qualified facility and requirements met such as labor, domestic content, and energy requirements.

Qualified facilities under section 45Y are those used for electricity generation with greenhouse gas emissions rates not greater than zero. The credit duration spans over a 10-year period beginning from when the facility is originally placed in service. Note that there are provisions for the phase-out of the credit overtime, particularly depending on the reduction of greenhouse gas emissions. Additionally, there are bonus incentives available, such as the labor requirements, which are based on the wage levels the facility is paying and in apprenticeships. The Domestic Content Bonus Credit, which increases the credit by 10 percent for facilities using domestically produced steel, iron, or manufactured products. Finally, the bonus of energy requirements which depends on the area the facility is built. A summary of the base rate and bonus are described on Table 31.

Table 31. Rates for Production Tax Credit, Section 45Y.

| | | |
|---|---|---|
| **Base Rate Without Labor Requirements** | | $5.5/MWh |
| **Base Rate with Labor Requirements** | | $27.5/MWh |
| **Bonus Domestic Content** | It doesn't meet Labor req. | 10% |
| | It meets Labor req. | |
| **Bonus Energy Communities** | It doesn't meet Labor req. | 10% |

| | | |
|---|---|---|
| | It meets labor req. | |
| **Description** | | Technology-neutral production tax credit/ Start Construction before January 2025 |
| **Credit Start Date** | | 2025 |
| **Duration** | | 10-year technology neutral PTC |
| **End Date** | | The annual GHG emissions from production of electricity is equal or less than 25% of GHG emissions in 2022, or (2) 2032 |

## Tax Credit, Section 45Q for Carbon Capture of $CO_2$

The IRA, Section 45Q, provides a tax Credit for Carbon Sequestration. The credit aims to incentivize investments in carbon capture and sequestration (CCS) technologies, primarily focusing on emissions from fossil fuel-fired power plants and large industrial sources (Clean Air Task Force 2017). Carbon sequestration involves injecting carbon oxides, predominantly carbon dioxide ($CO_2$), into underground geological formations, where they are either permanently trapped or transformed, thereby reducing net emissions of greenhouse gases (GHG). This process can involve capturing $CO_2$ emitted from anthropogenic sources like power plants or industrial facilities and injecting it underground for permanent sequestration or as part of enhanced oil recovery (EOR) operations. The Section 45Q provides a tax credit, computed per metric ton of qualified carbon oxide captured and sequestered (Congressional Research Service 2023). To qualify for the credit, the equipment should be placed in service before January 2033 and the taxpayer must repay the tax credit if the carbon oxide ceases to be captured, disposed of, or if it escapes into the atmosphere.

The carbon oxide emissions are measured both at the point of capture and at the point of disposal, injection, or other use. Geological sequestration, which includes storage in deep saline formations, oil and gas reservoirs, and unmineable coal seams, qualifies for the credit. Additionally, the tax credit extends to emerging technologies like direct air capture (DAC), which captures $CO_2$ directly from the atmosphere. Finally, note that to qualify for the credit, the entity must own the capture equipment and manage the disposal, utilization, or use of the $CO_2$ either directly or through a contractual agreement. Certain tax-exempt entities have the option to claim the tax credit directly, while others can transfer it to another entity once (Congressional Research Service 2023).

Table 32. Carbon Capture Tax Credit, Section 45Q.

| Credit Amount (per Metric Ton of $CO_2$) | | | | | | | |
|---|---|---|---|---|---|---|---|
| Geologically Sequestered/Other Qualified Use of $CO_2$ with EOR - Base Rate | Geologically Sequestered $CO_2$ - Base Rate | DAC sequestered carbon oxide - Base rate | DAC used carbon oxide - base rate | Other Qualified Use of $CO_2$ with labor requirements | Geologically Sequestered $CO_2$ with Labor requirements | DAC sequestered with labor req. | DAC used with Labor requirements |
| $12.00 | $17.00 | $26.00 | $36.00 | $60.00 | $85.00 | $130.00 | $180.00 |

## Production Tax Credit, Section 45V for hydrogen production

The IRA Clean Hydrogen Production Credit, section 45V, offers different financial incentives for hydrogen production based on lifecycle greenhouse gas emissions (lifecycle GHG emissions)-carbon dioxide equivalent. It provides credits ranging from $.12 to $.60 per kilogram of hydrogen produced, contingent upon emissions levels. Note that the base rate can be increased by five if the labor requirements are met. Finally, the PTC lasts for 10 years after a facility begins operation, extending to projects initiated before 2033. Eligibility is determined by the Clean Air Act's greenhouse gas emissions definition, which means that the indirect emissions are counted. In other words, the emissions are considered from the well to gate using the latest GREET model from Argonne National Laboratory (Congress 2022). Finally, the PTC requires that a third-party verifies the clean hydrogen production (Internal Revenue Service 2023).

It is important to mention the December 26th proposed rules notice from IRS. The IRS proposed Energy Attribute Certificates (EACs) to demonstrate the purchase of clean power by the hydrogen facility. The criteria for EACs include ensuring incrementality, which means sourcing clean power from the same region as the hydrogen producer, and eventually matching power generation with hydrogen production on an hourly basis. The December Notice also clarifies that a nuclear power plant that wants to sell electricity for a hydrogen plant could only claim 10% of the PTC 45U in conjunction with the 45V but the final definition form IRS is still pending (Internal Revenue Service 2023). A summary of the PTC 45V levels can be found in Table 33.

Table 33. Rates for Hydrogen Production Tax Credit (45V)

| PTC (45V) | | | | | | |
|---|---|---|---|---|---|---|
| Period | Base Rate | 2.5KG<$CO_2$<4KG | 1.5KG<$CO_2$<2.5KG | 0.45KG<$CO_2$<1.5KG | $CO_2$<0.45KG | Bonus if met labor requirements |
| 2023 - 2032 | $0.6/Kg H2 | 20% of Base Rate | 25% of Base Rate | 33% of Base Rate | 100% of Base Rate | x5 |

## Investment Tax Credit, Section 48E for New Nuclear Power Plants

The investment tax credit, section 48E of the Inflation Reduction Act encompasses qualified renewable energy facilities and energy storage technology. It provides a percentage of the capital expenditure for qualified facilities. The base rate for qualified facilities and energy storage technology is 6 percent.

An alternative rate of 30 percent is available for smaller facilities or technologies meeting the labor requirements. Note that depending on that, additional increases of 2 or 10 percentage points apply for investments in energy communities or those meeting the domestic content. The credit applies to property placed in service after December 31, 2024, and extends until the later of 2032, or the annual GHG emissions from production of electricity is equal or less than 25% of GHG emissions in 2022. The total credit percentage decreases over time after 2032. Furthermore in 2033 and 2034, 75 and 50% of the total qualified amount respectively can be claimed. It is important to note that qualified property refers to tangible personal property or other tangible property integral to the facility subject to depreciation or amortization. Facilities must meet greenhouse gas emissions criteria, with certain exclusions for facilities receiving other energy-related credits such as 45, 45J, 45Q, 45U, 45Y, 48, coal project under 48A, or 38 (Congress 2022). A summary of PTC 48E levels can be found in Table 34.

Table 34, Rates for Investment Tax Credit, Section 48E.

| Base Rate Without Labor Requirements | Base Rate with Labor Requirements | Bonus Domestic Content | | Bonus Energy Communities | |
|---|---|---|---|---|---|
| | | It doesn't meet Labor req. | It meets Labor req. | It doesn't meet Labor req. | It meets labor req. |
| 6% | 30% | +2% | +10% | +2% | +10% |

For a more detailed description of how to adjust nuclear cost data according to tax credits, see (Guaita and Hansen 2024).

# Appendix C

# TEA Results and ACC for A Project Life of 20 Years Using Same Advanced Nuclear Reactor Cost

Table 35. Summary of key data outputs for high CAPEX ($8,000/kWe) at 20 years project lifetime.

| 20 years Project Lifetime | | | | | | | |
|---|---|---|---|---|---|---|---|
| CAPEX HTGR = $8,000/kWe | | Case 1 | Case 2 | Case 3a | Case 3b | Case 4 | Case 5 |
| IRA Benefits | Tax Credits | — | TC 45Q | ITC 48E + TC 45Q | ITC 48E + TC 45Q | ITC 48E + PTC 45V + TC 45Q | ITC 48E + PTC 45V + TC 45Q |
| Finance | NPV Cash Flow | $2763M | $2989M | $2542M | $2677M | $635M | $1219M |
| | Delta NPV of Total Costs (Relative to BAU) | — | $227M | -$220M | -$85M | -$2128M | -$1544M |
| | Avoided Cost of Carbon ($/metric-ton-CO2) | — | $16.9 | $69.0 | $35.3 | $240.0 | $195.5 |
| | Avoided Net Cost of Carbon ($/metric-ton-CO2) w/ tax credits | — | -$16.1 | $22.7 | -$1.8 | $59.9 | $41.1 |
| | IRR | — | 960.0% | 71.0% | 121.0% | 17.0% | 27.0% |

Table 36. Summary of key data outputs for high CAPEX ($5,500/kWe) at 20 years project lifetime.

| 20 years Project Lifetime | | | | | | | |
|---|---|---|---|---|---|---|---|
| CAPEX HTGR = $5,500/KWe | | Case 1 | Case 2 | Case 3a | Case 3b | Case 4 | Case 5 |
| IRA Benefits | Tax Credits | — | TC 45Q | ITC 48E + TC 45Q | ITC 48E + TC 45Q | ITC 48E + PTC 45V + TC 45Q | ITC 48E + PTC 45V + TC 45Q |
| Finance | NPV Cash Flow | $2763M | $2989M | $2863M | $2839M | $2216M | $2268M |
| | Delta NPV of Total Costs (Relative to BAU) | — | $227M | $100M | $77M | -$547M | -$495M |
| | Avoided Cost of Carbon ($/metric-ton-CO2) | — | $16.9 | $48.1 | $24.8 | $182.7 | $147.7 |
| | Avoided Net Cost of Carbon ($/metric-ton-CO2) w/ tax credits | — | -$16.1 | $9.2 | -$8.6 | $22.6 | $10.0 |
| | IRR | — | 960.0% | 101.0% | 166.0% | 41.0% | 47.0% |

Table 37. Summary of key data outputs for high CAPEX ($3,000/kWe) at 20 years project lifetime.

| 20 years Project Lifetime | | | | | | | |
|---|---|---|---|---|---|---|---|
| CAPEX HTGR = $3,000/kWe | | Case 1 | Case 2 | Case 3a | Case 3b | Case 4 | Case 5 |
| IRA Benefits | Tax Credits | — | TC 45Q | ITC 48E + TC 45Q | ITC 48E + TC 45Q | ITC 48E + PTC 45V + TC 45Q | ITC 48E + PTC 45V + TC 45Q |
| Finance | NPV Cash Flow | $2763M | $2989M | $3121M | $2839M | $2216M | $2268M |
| | Delta NPV of Total Costs (Relative to BAU) | — | $226M | $358M | $231M | $80M | $102M |
| | Avoided Cost of Carbon ($/metric-ton-CO2) | — | $16.9 | $29.0 | $13.9 | $130.2 | $105.4 |
| | Avoided Net Cost of Carbon ($/metric-ton-CO2) w/ tax credits | — | -$16.1 | -$8.7 | -$15.8 | -$9.8 | -$15.6 |
| | IRR | — | 958.0% | 168.0% | 324.0% | 66.0% | 74.0% |

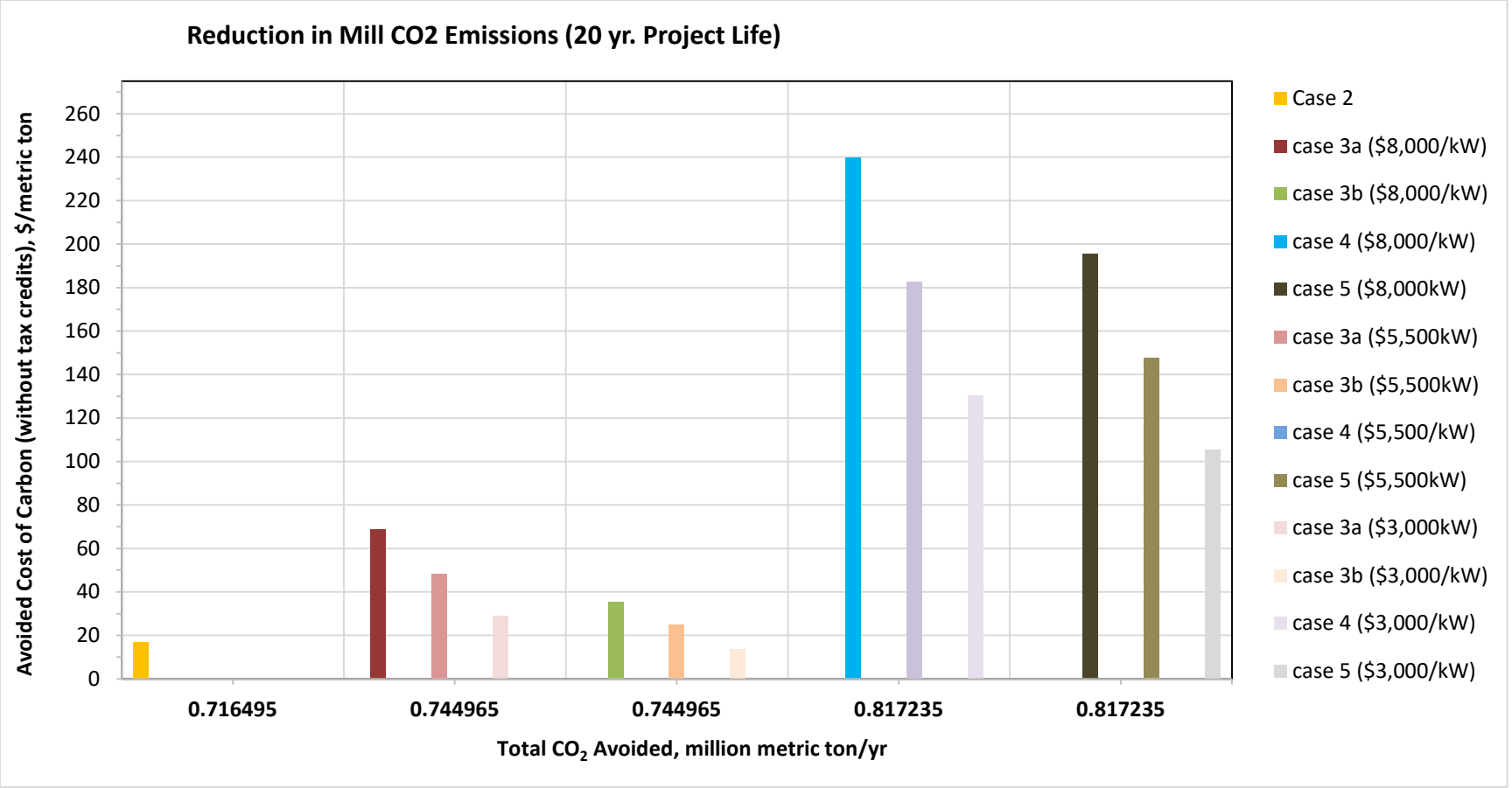


Figure 25. HTGR-type SMNR Pulp and Paper synthesis plant decarbonization total onsite CO2 avoidance and annual cost by case without IRA ITCs and PTCs.

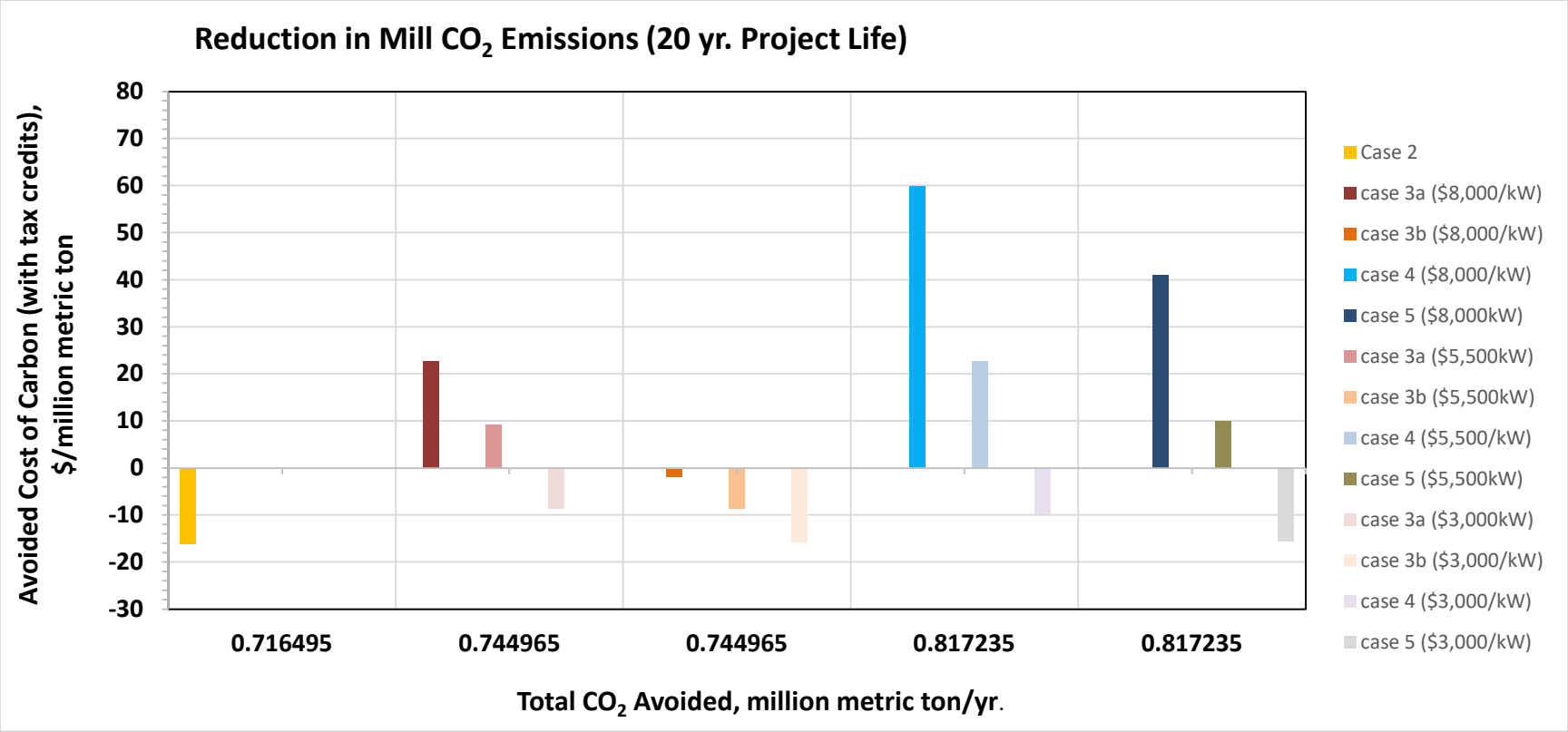


Figure 26. HTGR-type SMNR Pulp and Paper plant decarbonization total onsite CO2 avoidance and annual cost by case with IRA ITCs and PTCs.

# Appendix D

# MEA Carbon Capture Cost Estimation

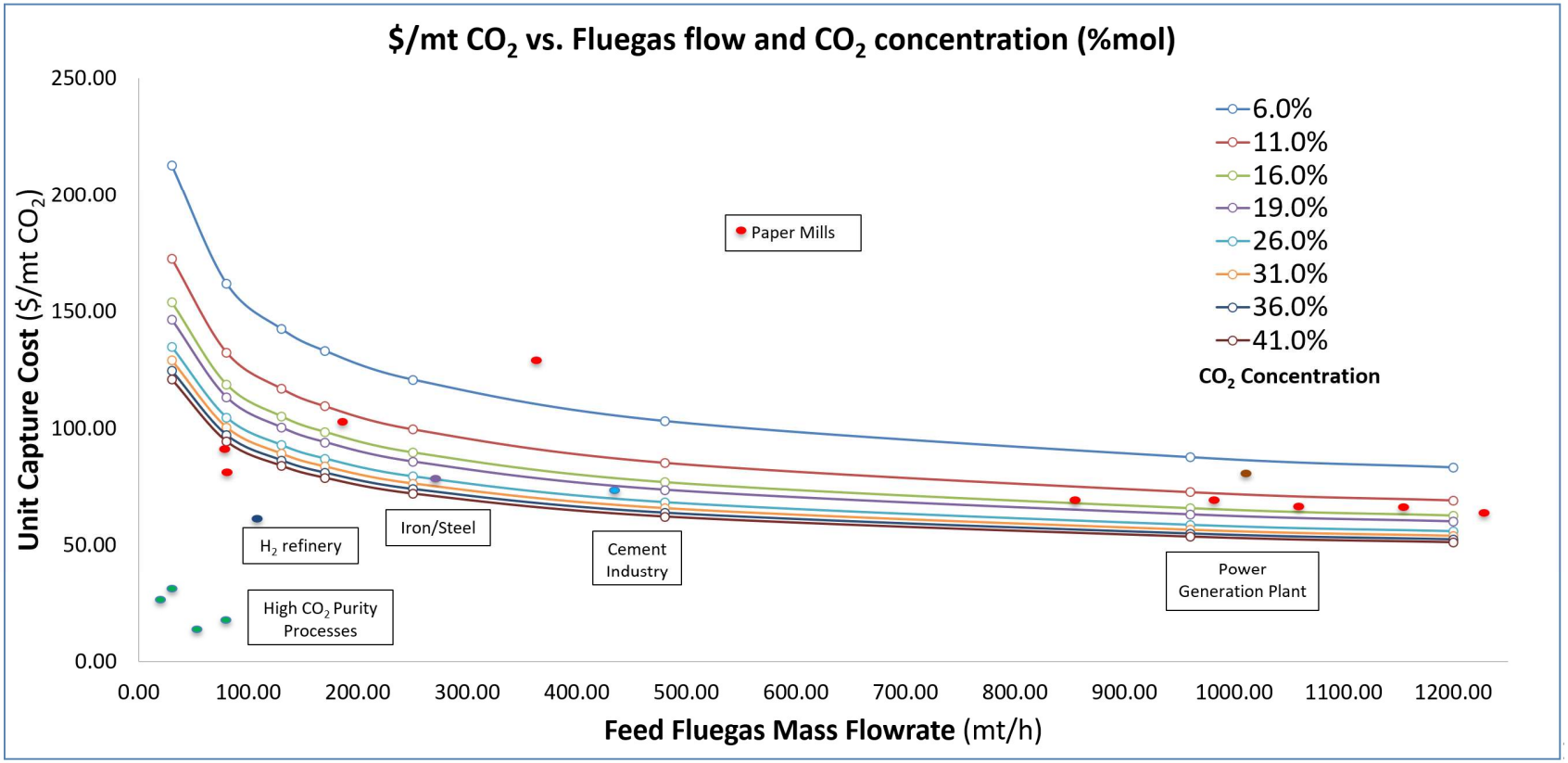


Figure 27. Cost of $CO_2$ capture using MEA system in function of total flue gas flow (metric-tons/h) and $CO_2$ concentration (mol%).

Table 38.$CO_2$ capture cost based on amine system reported in the literature.

| Source | Total flue gas flow (metric-ton/h) | $CO_2$ concentration (mol%) | Capture cost ($/metric-ton-$CO_2$) | Reference |
|---|---|---|---|---|
| Duke Energy Gibson 3 Plant | 1005.8 | 9.51 | 88.2 | (Jones 2019) |
| Duke Energy Buck NGCC Plant | 1770.4 | 3.85 | 122.7 | (Jones 2019) |
| Ammonia Plant | 56.2 | 99 | 19 | (Hughes 2022) |
| Ethylene Oxide Plant | 13.87 | 100 | 26 | (Hughes 2022) |
| Ethanol Plant | 16.33 | 100 | 32 | (Hughes 2022) |
| Natural Gas Processing | 74.42 | 99 | 16.1 | (Hughes 2022) |
| Hydrogen Refinery | 11.4 | 12.7 | 59.9 | (Hughes 2022) |
| Cement | 433.95 | 22.4 | 78 | (Hughes 2022) (Hughes et. al) |
| Iron/Steel | 269.1 | 27 | 65.9 | Hughes 2022) |
| Canadian Paper Mill (NBSK) | 361.9 | 10.9 | 137.65 | (Nwaoha and Tontiwachwuthikul 2019) |
| European Market Pulp Mill (BSKP) | 967.6 | 13 | 71.5 | (Onarheim et al. 2017) |
| | 179.01 | 12.1 | 100.1 | (Onarheim et al. 2017) |
| | 81.2 | 20.4 | 91.3 | (Onarheim et al. 2017) |
| | 1146.61 | 12.9 | 68.2 | (Onarheim et al. 2017) |
| | 1048.8 | 13.6 | 68.2 | (Onarheim et al. 2017) |
| | 1227.81 | 13.4 | 69.3 | (Onarheim et al. 2017) |
| Pulp Mill (Recovery Boiler) | 846.8 | 13 | 61.8 | (Gardarsdóttir et al. 2018) |
| Pulp Mill (Lime Kiln) | 81.43 | 20.4 | 76 | (Parkhi, Cremaschi, and Jiang 2022) |
| Coal-Fired Power Plant | 4392.6 | 12.8 | 95.2 | (Massood et al. 2007) |

# Appendix E

# $CO_2$ Compression Cost Estimation

Table 39. Detailed Cost estimations for $CO_2$ compression. Sourced from: (Hughes 2022; Summers, Herron, and Zoelle 2014; Theis 2021; National Energy Technology Laboratory 2010; Towler and Sinnott 2012; Zang et al. 2021; Chemical Engineering n.d.; Davis et al. 2015)

| Item/Description | Bare Erected Cost ($) | Eng'g CM H.O. & Fee | Contingencies | Total Plant Cost ($/1000) | Total Retrofit Cost ($/1000) | $/1000/metric-ton per year |
|---|---|---|---|---|---|---|
| $CO_2$ REMOVAL AND COMPRESSION | | | | | | |
| Duct work/piping | 1,000 | 100 | 220 | 1,320 | | |
| $CO_2$ compression (including intercoolers) | 19,905 | 1,99 | 4,379 | 26,275 | | |
| Cooling Water Chiller Unit | 2,323 | 232 | 511 | 3,066 | | |
| Balance of Plant (Instrument, site, buildings, etc.) | 2,091 | 209 | 460 | 2,760 | | |
| **Total Capital Expenses ($/1000)** | 25,319 | 2,532 | 5,570 | **33,422** | **33,756** | **0.021** |
| O&M Costs | | | | | | |
| Annual Operating Labor Cost | — | — | — | 323 | | |
| Maintenance Labor | — | — | — | 97 | | |
| Labor Cost, Administrative and Support Labor | — | — | — | 105 | | |
| Property Taxes and Insurance | — | — | — | 668 | | |
| **Total Fixed O&M ($/year/1000)** | — | — | — | **1,194** | **1,206** | **0.00075** |
| Variable O&M (Maintenance Material Cost) | — | — | — | 1,003 | | |
| Consumables (Cooling Water) | — | — | — | 463 | | |
| Purchased Power | — | — | — | **Not Included** | | |
| **Total Variable O&M ($/year/1000)** | — | — | — | **2,660** | **2,686** | **0.0017** |
| Owners Cost | — | — | — | 7,132 | | |
| Total Overnight Costs (TOC) | — | — | — | 40,554 | 40,959 | 0.025 |
| TASC Multiplier | — | — | — | 1.022 | | |
| Total As-Spent Cost (TASC) | — | — | — | **41,446** | **41,860** | **0.026** |

Table 40. Financial assumptions for $CO_2$ compression cost analysis

| Financial Parameter | Value |
|---|---|
| Capital Charge Factor | 15.20% |
| Debt/Equity ratio | 50/50 |
| Payback Period | 30 years |
| Interest on Debt | 8.00% |
| Return on Equity | 20% |
| Capital Expenditure Period | 1 year |
| Capital Distribution | 1st year-100% |
| Source | 1 |

Table 41. Summary of costs for $CO_2$ compression.

| | $ | $/metric-ton$CO_2$ |
|---|---|---|
| Total Capital Expenses | $33.8 MM | $21 |
| Total Fixed O&M (annual) | $1.21 MM | $0.75 |
| Total Variable O&M (annual)) | $2.69 MM | $1.7 |
| Total Overnight Costs (TOC) | $41.0 MM | $25 |
| Total As-Spent Cost (TASC) | $41.9 MM | $26 |

# Appendix F

# Sensitivity Analysis

Table 42. Net Present Value of Cashflows, 40-year period, with and without tax credits when the price of natural gas is set to $2.3/MBTU.

| | Low Capital Costs ($3,000/kWe) | | Medium Capital Costs ($5,500/kWe) | | High Capital Costs ($/8,000/kWe) | |
|---|---|---|---|---|---|---|
| | W/ Tax Credits | W/o Tax Credits | W/ Tax Credits | W/o Tax Credits | W/ Tax Credits | W/o Tax Credits |
| Case 1 - BAU | $ 2,830 M | $ 2,830 M | $ 2,830 M | $ 2,830 M | $ 2,830 M | $ 2,830 M |
| Case 2 | $ 3,144 M | $ 2,670 M | $ 3,144 M | $ 2,670 M | $ 3,144 M | $ 2,670 M |
| Case 3a | $ 3,252 M | $ 2,782 M | $ 3,067 M | $ 2,488 M | $ 2,884 M | $ 2,195 M |
| Case 3b | $ 3,069 M | $ 2,625 M | $ 2,976 M | $ 2,478 M | $ 2,884 M | $ 2,332 M |
| Case 4 | $ 3,135 M | $ 846 M | $ 2,518 M | -$ 98 M | $ 1,728 M | -$ 1,215 M |
| Case 5 | $ 3,136 M | $ 1,157 M | $ 2,669 M | $ 417 M | $ 2,086 M | -$ 439 M |

# Appendix G

# HTGR Cogeneration Cycle Meeting Reference Mill Steam Requirements without NG Auxiliary Boiler or Hog Boiler

The cogeneration cycle shown in Figure 28 was designed to supply the reference mill with the required amount of main steam while also generating as much electricity as possible. This is based off BAU operation with the natural gas auxiliary boiler and hog boiler decommissioned. Table 43 displays the thermodynamic properties of the mill steam system.

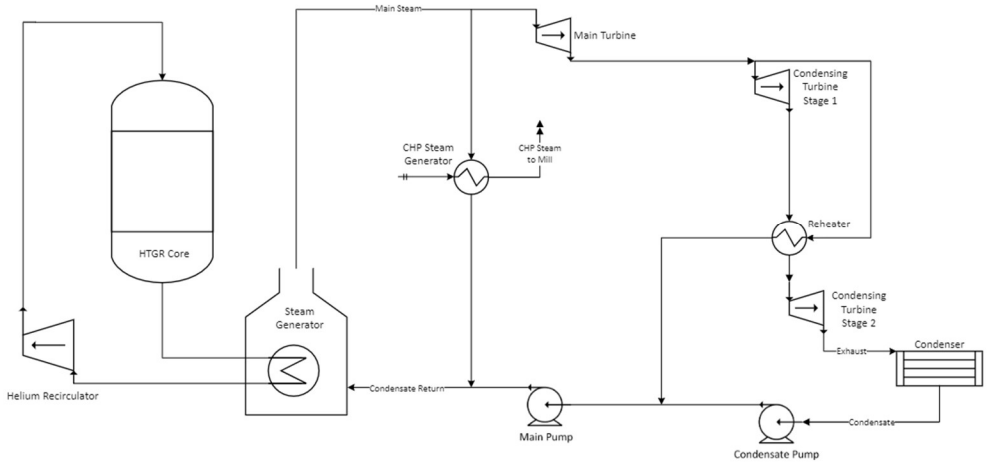


Figure 28. Schematic of the HTGR cogeneration-cycle.

Table 43. Thermodynamic properties of reference mill main steam.

| Stream | Temperature (°C) | Pressure (bar) | Phase | Flow Rate (kg/s) | Duty (MWth) |
|---|---|---|---|---|---|
| Main Steam to Mill | 500 | 90 | Gas | 6.01 | 63 |
| Feedwater | 304.8 | 91.8 | Saturated liquid | | |

The model was based on the following assumptions:

- Nominal pressure drop in all heat exchangers is 2%
- Isentropic turbine efficiency is 90%
- Isentropic pump efficiency is 75%
- Roughly 42% of the main power cycle steam bypasses the turbine to generate the 500°C steam sent to the reference mill
- Approximately 90% of the steam exiting the main turbine is reheated and enters the vacuum turbine
- The condenser and process steam generator provides condensate with 4°C of subcooling.

Table 44 contains the energy balance for the mill-specific cogeneration cycle, which produces 51.4 MWe for thermal efficiency of 25.7%, and 63 MW of total process heating. The thermodynamic properties for the cogeneration cycle steam streams are listed in Table 45.

Table 44. HTGR CHP-cycle energy balance.

| Equipment | Heat/Work (MW) |
|---|---|
| Core | 200 |
| Primary Helium Recirculator | 4.9 |
| Main Turbine | 23.4 |
| Condensing Turbine Stage 1 | 8.8 |
| Condensing Turbine Stage 2 | 25.1 |
| Mill Steam Generation | 63 |
| Condenser Duty | 85.6 |
| Main Pump | 0.948 |
| Condenser Pump | 0.132 |
| Process Steam Gen Pump | 0.050 |

Table 45. Thermodynamic properties of cogeneration cycle steam.

| Unit | Stream | Temperature (°C) | Pressure (bar) | Phase | Flow (kg/s) |
|---|---|---|---|---|---|
| Main Steam Generator | Feedwater | 220 | 168.4 | Sub-cooled liquid | 81.1 |
| | Main Steam | 565 | 165 | Gas | |
| Process Steam Generator | Steam | 565 | 165 | Gas | 34.0 |
| | Condensate | 344.3 | 161.7 | Subcooled liquid | |
| Main Turbine | Inlet | 565 | 165 | Gas | 47.1 |
| | Outlet | 285.6 | 23.7 | Superheated vapor | |
| Reheater | Inlet | 285.6 | 23.7 | Superheated vapor | 4.7 |
| | Outlet | 220 | 23.2 | Saturated vapor | |
| Condensing Turbine | Stage 1 Inlet | 285.6 | 23.7 | Superheated vapor | 42.4 |
| | Stage 1 Outlet | 170.2 | 8.0 | Saturated vapor | |
| | Stage 2 Inlet | 177.6 | 7.8 | Superheated vapor | |
| | Stage 2 Outlet | 46.2 | 0.1 | Two Phase (0.84) | |
| Condenser | Exhaust | 46.2 | 0.1 | Two Phase (0.84) | 42.4 |
| | Condensate | 41.8 | 0.1 | Subcooled liquid | |